FINAL PROJECT SUMMARY REPORT

PROJECT IDENTIFICATION INFORMATION

1. BUSINESS FIRM AND ADDRESS
Midé Technology Corporation
200 Boston Avenue
Suite 1000
Medford, MA 02155

2. DOT SBIR PROGRAM
2003 PHASE I

3. DOT CONTRACT NUMBER
DTRS57-04-C-10016

4. PERIOD OF PERFORMANCE
From December 17, 2003
To June 17, 2004

5. PROJECT TITLE
PIEZO STRUCTURAL ACOUSTIC PIPELINE LEAK DETECTION SYSTEM

SUMMARY OF COMPLETED PROJECT

The data in this final report shall not be released outside the Government without permission of the contractor for a period of four years form the completion date, June 17, 2004, of this project from which the data were generated.

The ability to detect in real-time leaks in pipelines will eliminate supply disruption costs and the cost of finding the location of the leak. Furthermore, catastrophic events that have claimed 66 lives and cost the US more than $200 M in the last six years could have been prevented. Historically, mechanical damage is the single largest cause of leaks that develop into failures on pipelines. Mechanical damage usually occurs after a pipeline is constructed and is caused by excavation equipment, which deforms the shape of the pipe, scrapes away metal and coating, and changes the mechanical properties of the pipe. These changes in the structural integrity of the pipe often do not cause immediate rupturing of the pipe, but rather initiates a chain of events that eventually cause leaks in pipe systems.

Midé proposed to develop a structural-acoustic sensing and alert system that will continuously monitor a pipeline without the need of an external power source. This system is based on Midé's patented PowerAct™ conformable packaged piezoelectric actuator and sensor. This sensor produces voltage in response to strain induced in its active material. When bonded to a structure such a pipe, any disturbances in the pipe will show up as a voltage trace over the poles of the sensor. These sensors are extremely sensitive with very high gain and can detect the most minute and high frequency strains. Since leaks in high-pressure gas pipes fit this description, there is currently no better sensor to apply to the specific problem.

The sensor generates voltage upon detection of leaks and impacts, thus no auxiliary power is required to keep the sensor continuously active. By merely capturing the electrical energy produced by the disturbance, a chain of events that report the location and magnitude of the leak can be initiated.

A comprehensive set of prototype tests was completed to assess the feasibility of the concept. A scaled pipe was constructed and instrumented. The pipe was pressurized with air and a leak was induced by means of a valve. The sensors produced measurable signals that were used to identify the magnitude and location of the leak. The sensors also demonstrated the ability to sense the location of hammer impacts on the scaled pipe.

The results of this effort led to the design of a system that could sense, locate and report leaks and impacts in a buried pipeline system. This system is estimated to cost less than $400 / km of pipe.

In conclusion, the results from this project were encouraging and indicate that it is feasible to use the PowerAct™ sensors in a cost effective system to locate impacts and leaks in pipelines.

APPROVAL SIGNATURES

1. PRINCIPAL INVESTIGATOR (Typed)	2. PRINCIPAL INVESTIGATOR (Signature)	3. DATE
Dr. Marthinus van Schoor		6/16/04

1. Executive Summary

1.1. Background

The ability to detect in real-time leaks in pipelines will eliminate supply disruption costs and the cost of finding the location of the leak. Furthermore, catastrophic events that have claimed 66 lives and cost the US more than $200 M in the last six years could have been prevented. Historically, mechanical damage is the single largest cause of leaks that develop into failures on pipelines. Mechanical damage usually occurs after a pipeline is constructed and is caused by excavation equipment, which deforms the shape of the pipe, scrapes away metal and coating, and changes the mechanical properties of the pipe. These changes in the structural integrity of the pipe often do not cause immediate rupturing of the pipe, but rather initiates a chain of events that eventually cause leaks in pipe systems.

Midé proposed to develop a structural-acoustic sensing and alert system that will continuously monitor a pipeline without the need of an external power source. This system is based on Midé's patented PowerAct™ conformable packaged piezoelectric actuator and sensor. This sensor produces voltage in response to strain induced in its active material. When bonded to a structure such a pipe, any disturbances in the pipe will show up as a voltage trace over the poles of the sensor. These sensors are extremely sensitive with very high gain and can detect the most minute and high frequency strains. Since leaks in high-pressure gas pipes fit this description, there is currently no better sensor to apply to the specific problem.

The sensor generates voltage upon detection of leaks and impacts, thus no auxiliary power is required to keep the sensor continuously active. By merely capturing the electrical energy produced by the disturbance, a chain of events that report the location and magnitude of the leak can be initiated.

A comprehensive set of prototype tests was completed to assess the feasibility of the concept. A scaled pipe was constructed and instrumented. The pipe was pressurized with air and a leak was induced by means of a valve. The sensors produced measurable signals that were used to identify the magnitude and location of the leak. The sensors also demonstrated the ability to sense the location of hammer impacts on the scaled pipe.

The results of this effort led to the design of a system that could sense, locate and report leaks and impacts in a buried pipeline system. This system is estimated to cost less than $400 / km of pipe.

In conclusion, the results from this project were encouraging and indicate that it is feasible to use the PowerAct™ sensors in a cost effective system to locate impacts and leaks in pipelines.

1.2. Summary of Work Completed in Phase I

This section is a short summary of the main tasks and highlights that were completed in the program. The work breakdown structure form the Phase I proposal will serve as an outline to summarize the progress that was made. *(If you are viewing the document in Word or Adobe, please follow the hyperlinks (in brackets) from the summary to the detailed sections in the document)*

1.2.1. Review of current leaks

Midé researched the literature on current leak detection mechanisms and standards for implementing such systems. A study into major pipeline accidents and their causes was also performed. Midé completed an evaluation of current leak detection systems. The systems' advantages and shortcomings as well as their performance against metrics identified through the literature search are noted herein. The following metrics were used for the evaluation: (Section 2.1)

- Complete Pipeline Coverage
- Frequency of Inspection
- Ability to Predict Future Leaks
- Automatic Detection
- Accuracy of Detection
- Ability to Precisely Locate Leak
- Ability to Assess Nature/Magnitude of Leak
- Cost

1.2.2. Requirements

Literature searches, consulting with individuals having experience in the industry and having intimate knowledge of pipeline systems, as well as sound engineering system design principles were used to set the requirements for a pipeline leak detection system. An initial analysis of acoustic wave propagation through a representative pipe system was completed. Midé also prepared a proposed test setup for evaluating the new leak detecting mechanism. The technical monitor evaluated and approved this test setup. (Section 2.2)

1.2.3. Laboratory Tests

The laboratory test setup was designed and built. The pipe section was instrumented with Midé's PowerAct™ conformable piezoelectric actuator and sensor (Section 2.3.1). This actuator / sensor was deemed the best product, offered commercially off-the-shelf, for this application. Preliminary tests indicated that good signal to noise ratios were produced by the sensors when leaks were introduced into the pipe. The following specific progress was made with regard to testing:

- The sensors illustrated the ability to pick up vibrations in the pipe. Specifically, shocks introduced into the pipe were sequentially observed with the sensors. (Section 2.3.2)
- Leaks were detected. The sensor signals show a measurable difference when a small valve is fully closed, half open and fully open. (Section 2.3.2)
- Sine waves were generated by one of the actuators and picked up by the others. The waveforms were characterized and proved that it was indeed acoustic waves traveling through the pipe and not RF noise. This indicated that acoustic data transfer was possible through the pipe. (Section 2.3.2)
- Data was captured from a desktop signal-conditioning device. (Section 2.3.3)
- FFT analysis on the captured data illustrated that the location and intensity of the leak can be observed while employing the sensors. The figures below illustrate the frequencies that are picked up by the sensors when there is no leak (left) and when a ball valve is 2/3 open with 60 psi of air in the pipe. (Section 2.3.3).

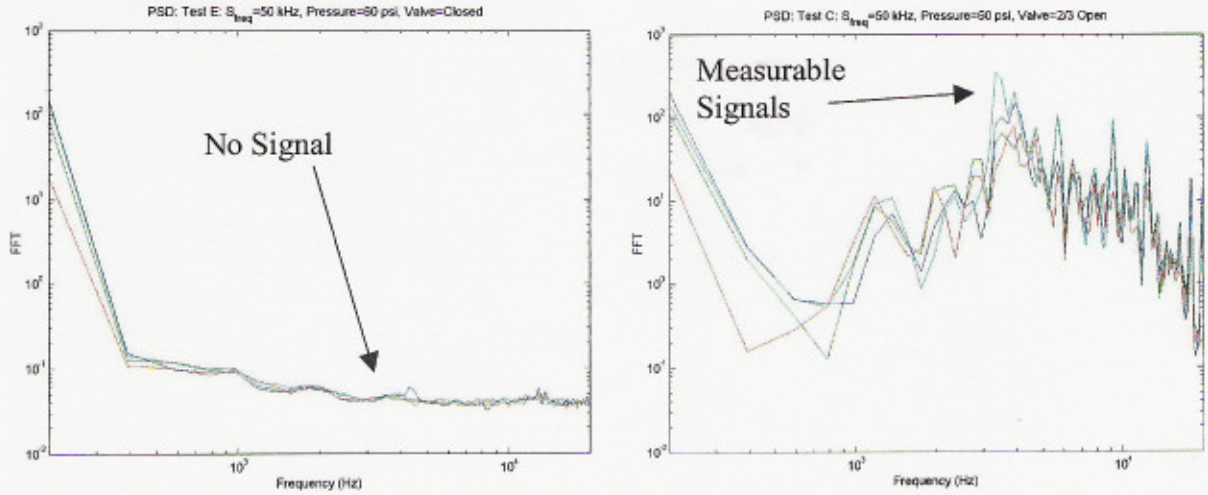

This figure illustrates the difference in Midé's PowerAct™ sensor' output when there is no leak in the pipe(left) and when a leak is present (right)

- Results indicate that the location and magnitude of the leak can be determined by integrating the energy output from the sensors at specific frequencies. (Section 2.3.3)
- An FEA model of the test setup was constructed. (Section 2.3.4)
- The FEA model was validated with the experimental results. (Section 2.3.4)
- The FEA model indicates that the pipe's higher natural frequencies are only marginally affected by boundary conditions. It easily follows that experimental results in air (above ground) may reasonably approximate system performance below ground. (Section 2.3.4)

1.2.4. Protocol Development

The risks and tradeoffs associated with developing a reporting protocol were identified. Based on these, a communications protocol for reporting the leaks, once identified by the sensors, was developed. This protocol is flexible enough that it can accommodate many different pipe sizes, locations and setups. (Section 2.4)

1.2.5. System Design and Costing

The system that was designed in the previous section was costed based on Midé's experience of producing high volume piezoelectric sensors and electronics. The total cost of the system per kilometer of pipeline is $320 (Table 6). Midé also performed a comparison of commercially available packaged piezoelectric materials on the basis of performance, reliability, cost and manufacturability. (Section 2.5).

2. Description of work completed

This section details the progress that Midé made under each of the WBS tasks from the Phase I proposal. The proposed tasks are given in *italics* at the beginning of each task.

2.1. Review of current leaks

Develop and understanding of current pipeline leaks, the structural vibrations excited by the leaks and their acoustic signatures.

This section details Midé's effort to gain knowledge of current, state of the art, pipeline leak detection methods and systems. An attempt was made to highlight requirements for the proposed piezoelectric system. The analysis of current techniques highlights their performance and shortcomings and serve as design metrics for the proposed system.

2.1.1. Background

To best assess the effectiveness of a pipeline leak detection system, an evaluation of pipeline failures was undertaken in order to determine the cost of pipeline failures both in terms of dollars and lives. The details of several accidents between 1994 and 2000 were examined to understand how pipeline failure started, but also how leak detection equipment could have reduced the severity of the leak. This will create criteria to evaluate the efficacy of commercially available pipeline leak detection systems and compare it to Midé's proposed solution. It will also serve as design guidelines for the new system.

2.1.2. Pipeline accidents

Data was collected from formal reports from the National Transportation Safety Board (NTSB) that were published on its website (www.ntsb.gov). Information from the reports is tabulated in Table 1. The list of accidents is by no means exhaustive, but it is believed to be a representative cross-section of the worst pipeline accidents from between 1994 and 2000. Furthermore, the data was collected as accident reports by the NTSB, and information should be reported impartially and fairly consistently.

Table 1 Pipeline Accident Synopsis, 1994-2000 (from www.ntsb.gov)

Date	Location	Leaked Fluid	Cost (Damage + Cleanup)	Fatalities	Summary
10/1999	Bellingham, WA	Gasoline	$45,000,000	3	237,000 gallons of gasoline leak into a creek and ignite. Excavation likely to blame. In-line inspection data was misinterpreted or ignored. Construction was poorly managed. SCADA system not functioning properly on day of accident.

8/2000	Carlsbad, NM	Nat. Gas	$1,000,000	12	Pipeline ruptures and ignites. Pipeline design and corrosion control program are questioned.
4/2000	Chalk Point, MD	Fuel Oil	$71,000,000	0	140,400 gallons released into wetlands and riverways. Probable cause: A fracture in a buckle that was incorrectly interpreted as a T-Piece by Ultrasonic Tool Data. Also lacked monitoring equipment to detect loss of fuel.
7/1998	South Ridding, VA	Nat. Gas	?	1	Explosion in newly constructed home. Corrosion and overheating in Electrical Service are probable cause.
3/2000	Greenville, TX	Gasoline	$18,000,000	0	546,000 gallon released in ruptured buried pipeline. Corrosion fatigue cracking at weld seam is the probable cause. Three years prior, system was inspected with smart pig and no damage detected
1/2000	Winchester, KY	Crude Oil	$7,100,000	0	489,000 gallons released into golf course and creek. In 1997 a 'dent' was located in failure location by magnetic flux standard inline inspection tools but was deemed too small (<2% of OD). Severity of accident increase due to failure of controller to recognize rupture
2/1999	Knoxville, TE	Diesel Fuel	$7,000,000	0	A 53,500 gallon leak due to cracking in an area of pipe coating failure. Pipe also had low fracture toughness. Pressure drop in pipe not immediately detected as a leak and system started and restarted, increasing amount of released diesel fuel.
1/1999	Bridgeport, AL	Nat. Gas	$1,400,000	3	Backhoe fractures natural gas pipe in one location, and separates a pipe joint nearby, releasing gas and exploding 3 buildings. Problem exacerbated because gas flow was not stopped, even though gas was clearly leaking – workers at location did not know all of the information about leak, and poor

					emergency response.
12/1998	St. Cloud, MN	Nat. Gas	$399,000	4	Network Installation Crew ruptures plastic natural gas pipeline. Explosion occurs 39 minutes later. While emergency personnel were present, only preliminary discussions had begun regarding the proper response.
11/1996	Murfreesboro, TN	Diesel Fuel	$5,700,000	0	During planned maintenance, proper procedures were not followed – Rupture caused by overpressure, overpressure not initially reduced, and later was not countered because of erroneous information in SCADA system. Problem worsened due to delay in recognizing leak.
7/1997	Indianapolis, IN	Nat. gas	$2,000,000	1	Directional drilling operation damages existing pipe, which ruptures and ignites
3/1998	Sandy Springs, GA	Gasoline	$3,200,000	0	Leak was undetected until someone detected odor, and found gasoline leaking up through ground. No alarms in control center had been tripped. Cracks due to buckling caused by pipeline being inadequately supported by trash and settling soil
8/1996	Lively, TX	Liquid Butane	$217,000	2	Pipeline not adequately protected from and inspected for corrosion.
6/1996	Fork Shoals, SC	Fuel Oil	$20,500,000	0	Corroded pipeline ruptures over Reedy River, releasing 957,600 gallons. Data indicated a problem, but controller did not respond, increasing amount of leakage. Pipeline also being operated above recommended pressure levels, and pre-accident measurement of pipe failed to correctly measure extent of pipe corrosion
10/1996	Tiger Pass, LA	Nat. Gas	?	0	Pipeline Ruptured during dredging operation in channel. Released gas ignites and destroys dredge and tug. A delay in recognition of the rupture increased the magnitude of

					the problem.
5/1996	Gramercy, LA	Gasoline and Diesel	$7,000,000	0	Pipeline ruptured during excavation activities. Rupture not reported to pipeline company. SCADA alarms functioned properly to indicate the problem, but controller incorrectly interpreted the alarms as being due to activity at Garyville refinery.
10/1994	Waterloo, IA	Nat. gas	$250,000	6	Soil settlement at a connection between a polyethylene pipe and a steel main causes cracking due to pipe brittleness. Leak ignites causing explosion
11/1996	San Juan, PR	There are two categories of these criteria: Pre-leak criteria, and post-leak criteria. Propane	?	33	Soil compaction 4 years prior causes stresses on plastic pipe, eventually cracking and leaking. When leaks reported, gas company didn't give proper warnings, and also failed to properly test for and locate the leak, and therefore, the leak was not repaired. Leak persisted for one week before igniting and destroying building.
6/1994	Allentown, PA	Nat. Gas	$5,000,000	1	A compression coupling became separated during an excavation. Gas flowed through foundation of building and explodes.

Over the six-year span in question, the total of the cost (damage plus cleanup) of the accidents presented was over $200,000,000 and claimed sixty-six lives. While Midé's leak detection system would not necessarily have prevented the accidents listed, estimates will be attempted at the amount the cost of the accidents could have been reduced (both in dollars and fatalities) with Midé's leak detection system. This will provide the ability to properly analyze the cost-benefit relationship of the system.

Several trends became evident when examining the list of accidents. The first observation is that there is a distinction between the destruction caused by damage to liquid pipelines (Gasoline, Diesel, Fuel Oil, Crude Oil) and gaseous pipelines (Natural Gas, Propane, etc.). The damage caused by leaks in liquid pipelines tended to be much more costly in terms of destruction of personal property and cleanup. Especially evident is the cost of such spills in terms of environmental impact. When gaseous pipelines are damaged, the property damage and cleanup costs are generally lower, but fatalities are far higher – these gases can ignite and deadly explosions are a common result.

Another distinction between the systems is in the usual method of leak detection. In most of the liquid pipeline leaks, the leak was detected by observing changes in pipeline pressure (usually drops) by the pipeline controllers using a Supervisory Control and Data Acquisition (SCADA). Frequently leaks in gaseous pipelines were detected by persons sensing the odor from the leak. Many leaks in both the liquid and gaseous pipelines were caused during excavation activity, so both types of leaks can also be 'detected' by excavation companies who realize they have damaged or ruptured a pipeline.

Based on the aforementioned accidents, some criteria become evident which a viable leak detection system must possess. There are two categories of these criteria: Pre-leak criteria, and post-leak criteria. A system with the proper traits can minimize the damage caused by a pipeline rupture by predicting a problem ahead of time, rapidly identifying the leak after it occurs, and pinpointing the location of the problem to emergency response personnel. Clearly, also adding a component of the system to automatically shut down appropriate sections of the pipeline to further minimize damage due to the leak would also be valuable, but is beyond the scope of this present project.

2.1.2.1. Pre-Leak Criteria

Many of the accidents in question were caused by direct contact with excavation equipment such as backhoes and drills. While the prevention of such excavation accidents is clearly of paramount importance, a system must be able to sense such trauma, as the damage may go unnoticed by excavation crews. However, sometimes damage to the pipeline is not catastrophic in the short term, but may lead to a pipe rupture at a later time (see Winchester, Kentucky).

Smart pigs can sometimes, but not always predict the presence of likely failure points (see Greenville, Texas). Other drawback with smart pigs is their inability to go through pipes of certain cross-sections or geometries. Another problem with smart pigs is that often they are only used to inspect sections of the pipeline once every several years. Two important criteria then for an improved leak detection system is a system that has *Complete Coverage* of the pipeline network and that monitors for leaks or potential leaks with a *Frequency* that makes monitoring close to constant.

Finally, leaks may be sufficiently small to be undetected as pressure drops in SCADA systems. Such leaks may eventually cause significant damage if the leak becomes a rupture. SCADA system also cannot generally predict regions of corrosion or pipe dents. A final pre-leak performance criterion of an ideal leak detection system will be able to *Predict* areas in the pipe that have become susceptible to leaks though corrosion, trauma, or sediment shifting.

2.1.2.2. Post-Leak Criteria

One of the common problems with pipeline operators using SCADA systems is the reliance on humans to interpret the data. In the accidents reported, one of the common themes is user error. Like in the Fork Shoals, South Carolina case, pipeline control operators simply missed alarms. Another problem is misinterpretation of alarms. In some accidents pressure drops were assumed to be caused by activity elsewhere in the pipeline system. For example, in the Gramercy, Louisiana accident, the operator assumed that the SCADA alarms indicating a pressure drop was activated by actions at the Garyville refinery. The reality is that these pipeline networks are very complex, and the changing pressures could be caused by a variety of dynamics in the system. The way to reduce the complexity of the system dynamics is to increase the number of controller operation points, but that may be impractical and will not prevent missed operator

cues. From this, two criteria for an improved system emerge: It must *Automatically* (i.e. with a minimum of human interaction) and *Accurately* (i.e. able to distinguish between a leak and a change in the operating parameters of the pipeline system). It should be noted that gaseous leaks often go undetected until an odor is sensed. Clearly, damage from these gaseous pipeline leaks could be reduced by an automatic and accurate leak detection system.

Another area that is subject to Human Operator error is in the response of emergency personnel. Due to the ambiguous nature of some of the clues, operators didn't respond as rapidly to some of the clues. Some of this is a lack of following procedures (like in San Juan, Puerto Rico) that will continue to be problematic, though it will be mitigated by an *Accurate* and *Automatic* system, as expressed in the previous paragraph. However, sometimes the response of the emergency response team was affected by a lack of quality of information about the location and nature of the leak. While damage that is caused instantaneously by excavation activity, generally the location and nature of the leak is well known. However, leaks from excavation activities may not present themselves until well after the excavation equipment has contacted the pipe. Also, many leaks can occur underground, which can make ascertaining the location of the leak a difficult and frustrating problem. Two more criteria that arise from this are the ability of a system to *Locate* a leak. Furthermore, it would be useful if a system could identify the *Nature* of a leak (size of rupture, amount of leakage, etc.), to better prepare emergency personnel when arriving to the scene or controlling emergency valving systems of the proper response. Again, this could ultimately be automated but is beyond the scope of this project.

2.1.2.3. Overall Criteria

Since these criteria have been developed for a cost-benefit analysis of various leak detection systems, it is important to evaluate the *Cost* associated with the proposed leak detection systems. Cost includes material costs, installation costs and maintenance costs. Based on all of the above analysis the following performance criteria will be used to rate the efficacy of a leak detection system:

- Complete Pipeline Coverage
- Frequency of Inspection
- Ability to Predict Future Leaks
- Automatic Detection
- Accuracy of Detection
- Ability to Precisely Locate Leak
- Ability to Assess Nature/Magnitude of Leak
- Cost

2.1.3. Competing Technologies

There are many techniques currently used to inspect pipelines and fewer to detect for leaks. Several industries were examined to investigate competing technologies. In addition to the Petroleum and Natural Gas industries, water transport, nuclear plants, and other systems were investigated. Some representative commercially available systems are indicated. These are not the only companies who sell products using the technology in question - they are merely examples of how the given technology has been applied.

Smart Pigs have been used to inspect pipes. As stated previously, these pigs are limited by being unable to go through pipes of certain cross-sections or geometries, and the fact that they cannot continuously monitor

the pipeline. A smart pig is often moved through the pipe via the flow of the liquid inside the pipe, though some are self-propelled. There can be several types of inspection equipment present on a smart pig. Examples include 1) a Magnetic Flux Leakage Tool where the pipeline is saturated with Magnetic Flux and anomalies are detected by changes in the magnetic return (Vectra – BJ Inspection Service), 2) Digital Calipers, 3) Nonlinear Hamonics where outside forces are applied and the resultant reactions are measured (Southwest Research Institute), and 4) Ultrasonic detection with compression waves measuring corrosion in pipes and 45 degree shear waves measuring cracks (Ultrascan CD - Pipetronix).

Pressure Evaluation Systems like the SCADA systems discussed above are widely used to monitor pressure fluctuations in pipeline systems and sound alarms based on behavior associated with leaks. (Avistar is one of the companies who make such systems). Some of the shortcomings were outlined above and include inability to accurately pinpoint the leak as well as susceptibility to operator error. Pressure testing is also done by pressurizing a closed-circuit pipeline system and studying to see if the pressure is maintained. A serious drawback of this approach is that the pressurization sometimes weakens existing pipe deficiencies or actually causes the pipe to rupture.

Mass Balance Calculations on inlet and outlet flows is another way to detect the presence of a leak. The mass of fluid is measured at both the inlet and outlet port of the flow. If the mass of the liquid is less at the outlet port, then there is a leak. While conceptually this should be a very effective tool, it cannot pinpoint the location of a leak, and also small leaks may not be detectable due to limits in the accuracy of mass flow measurement systems. (Accusonic makes an acoustic based mass flowmeter).

Acoustic Systems are perhaps the earliest leak detection system. In fact, a listening stick, a steel rod with a wooden earpiece that is placed against a pipe to listen for and locate leaks still finds use today. More sophisticated and modern equipment include microphones that listen outside the pipe for leaks. Some measurements of underground have successfully been made above the ground. Signal processing is done to correlate the frequency of a measured leakage sound to the size of the leak, as well as processing to distinguish between leakage noises and other burst-type noises. Leak Noise Correlators are a common trade name for these type devices, and are available from many companies (Subsurface Leak Detection, Radcom-USA, and others). Some of this acoustic equipment is called Ultrasonic Leak Detectors. These Acoustic Devices have most commonly been used as periodic diagnostic equipment rather than permanent installations.

Vibration Systems are similar to acoustic systems in that they are attempting to measure the high-frequency signals associated with a leak. They differ from the microphone systems in their sensor. Most solutions involve accelerometers or microphonic solutions.

Tracer Systems is another method that is popular. A tracer gas or liquid is released into the pipeline system. This gas is usually inert, but easily sensed from outside the pipe in case of a leak. Sensor can either be permanently installed, or temporarily installed. Companies like Tracer, Inc. have products that use Tracer Technology. One of the big drawback of this type of system is the fact that it often requires the system to have some shutdown time to be implemented, and cannot always pinpoint the location of the leak.

Fiber Optic Systems have been explored for use in new pipeline installations. While these systems may be effective for assessing leaks throughout the system, they may not be able to pinpoint the location of the leak. Furthermore, they can be costly, as well is susceptible to damage through excavation activities, etc.

Remote Sensing Systems attempt to assess the performance of the pipeline by taking a more macroscopic view of the system. These systems look at the pipeline from a great distance, in some case by satellite. Among the sensors used are Satellite imaging to predict sub-centimeter ground movements (C-Core) and which may cause pipe damage, and infrared systems (EnTech) which can sense the presence of an underground leak by observing temperature changes in the ground caused by the leaking gas or liquid.

Non Destructive Pipe Assessment can be used to determine the state of repair of pipeline systems. Among the technologies that are used in this kind of analysis are ultrasonic systems to measure wall thickness and X-Ray systems (Profiler, Lixi, Inc.).

Midé System is a combination Acoustic System and Vibration System. Midé's solution uses piezoelectrics as a sensor and transmitter. A key feature is that it is easily integrated in plurality along a pipeline system and they can better continuously monitor for and locate leaks. Another benefit is that they can also act as a data transmission system eliminating the need for supplementary data transmission systems (telemetry, RF, etc.). The system can theoretically monitor the structural integrity of the pipe through continuous monitoring. The response of the pipeline structure may change as cracks, corrosion, dents, etc. become present. While this is fairly theoretical, the proposed solution offers some exciting benefits over existing commercial technology.

2.1.4. Benefit Analysis

Table 2 shows how the various systems compare to each other based on the criteria previously presented. The systems were rated on a scale of 1 to 5, 1 being poor, and 5 being excellent. It is important to note, that other solutions include hybrids of different systems. For example, it is currently quite common for Smart Pig Systems to be used along with Pressure Evaluation Systems.

Table 2 Benefit Analysis of Various systems

Solution	Pre-Leak			Post-Leak					Pros	Cons
	Coverage	Inspection Frequency	Predict Leaks	Automatic	Accurate	Locate	Leak Nature	Cost		
Smart Pigs	3	2	4	1	1	1	1	5	Already accepted by industry, can be effective in locating and predicting leaks	Cannot fit all pipes and geometries, and may get stuck. Monitor pipeline systems only periodically

Pressure Evaluation Systems	1	1	1	3	3	1	3	3	Accepted by industry, Pressure is reasonably easy to monitor	Relies on human interaction. May not correctly identify problems due to complexity of pipeline dynamics.
Mass Balance Calculations	2	1	1	4	3	1	2	2	Works well for large leaks	Cannot determine location of leak. May not work effectively on small leaks.
Acoustic Systems	1	1	1	2	4	3	5	4	Excellent at assessing presence nature of leak. Many systems available, so refinements have been made in technology	Limited coverage. Presently only used for periodic measurements, possibly due to system cost. May not always be able to do underground sensing
Vibration Systems	1	1	1	2	4	3	5	3	Good at assessing size of leak	Difficult to implement systems. Most systems are not currently permanently installed, and system needs direct contact with pipe, reducing efficacy of underground measurements.
Tracer Systems	2	1	1	2	3	2	2	3	Straight forward system, can be implemented fairly easily without major cost	System may need to be shutdown. Permanent sensor installation required for more continuous monitoring
Fiber Optic Systems	4	1	1	3	3	1	1	1	Response should be quick to a leak.	Not robust, expensive, can not easily locate leak, requires

										maintenance
Remote Sensing Systems	4	4	2	3	3	3	1	1	Entire pipeline easily evaluated.	Extremely high cost
Nondestructive Pipe Assessment	3	2	4	1	1	1	1	2	Good at predicting leaks	Poor at detecting leaks. Not continuous monitoring.
Midé System	5	5	1	5	5	5	4	3	Robust, Low Maintenance, good at predicting nature of leak. System can cover entire pipeline network. Piezoelectric system acts as both a sensor and transmitter, reducing complexity and cost.	Unclear if pipe deficiencies can be predicted. Not currently commercially viable, though that is the point of this SBIR process

2.1.5. List of Pertinent Standards

The following ASTM standards were found to be relevant to pipe leak detection. These standards provide background as well as applicable information on leak detection using acoustic equipment.

Table 3: ASTM standards that are relevant to the PIPE project.

Standard	Description	Cost
E1002-96	Standard Test Method for Leaks Using Ultrasonics	$27
E650-97(2002)e1	Standard Guide for Mounting Piezoelectric Acoustic Emission Sensors	$27
E750-98	Standard Practice for Characterizing Acoustic Emission Instrumentation	$32
E432-91(1997)	Guide for Selection of a Leak Testing Method	$27
E494-95(2001)	Standard Practice for Measuring Ultrasonic Velocity in Materials	$38
E543-02	Standard Practice for Agencies Performing Nondestructive Testing	$38
E1211-02	Standard Practice for Leak Detection and Location Using Surface-Mounted Acoustic Emission Sensors	$32
E569-02	Standard Practice for Acoustic Emission Monitoring of Structures During Controlled Stimulation	$32
E1316-03	Standard Terminology for Nondestructive Examinations	$43
E1118-00	Standard Practice for Acoustic Emission Examination of Reinforced Thermosetting Resin Pipe (RTRP)	$38
E664-93(2000)	Practice for Measurement of the Apparent Attenuation of Longitudinal Ultrasonic Waves by Immersion Method	$27

2.1.6. Purchased ASTM Standards

After evaluating the abstracts of the different standards, it was decided to purchase the most pertinent standards. As short summary well as relevant information is provided below for purchased ASTM standards.

2.1.6.1. E1002-96: Standard Test Method for Leaks Using Ultrasonics

- Summary: Describes method for measuring pressurized gas leak from a distance with an ultrasonic transducer. Measures air pressure waves.

2.1.6.2. E650-97(2002)e1: Standard Guide for Mounting Piezoelectric Acoustic Emission Sensors

- The methods and procedures used in mounting acoustic emission (AE) sensors can have significant effects upon the performance of those sensors. Optimum and reproducible detection of AE requires both appropriate sensor-mounting fixtures and consistent sensor-mounting procedures.

- *Compression Mounts*—The compression mount holds the sensor in intimate contact with the surface of the structure through the use of force. This force is generally supplied by springs, torqued-screw threads, magnets, tape, or elastic bands. The use of a couplant, such as adhesive, is strongly advised with a compression mount to maximize the transmission of acoustic energy through the sensor-structure interface.

- *Bonding*—The sensor may be attached directly to the structure with a suitable adhesive. In this method, the adhesive acts as the couplant. The adhesive must be compatible with the structure, the sensor, the environment, and the examination procedure.

- If a couplant is impractical, a dry contact may be used, provided sufficient mechanical force is applied to hold the sensor against the structure. The necessary contact pressure must be determined experimentally. As a rough guide, this pressure should exceed 0.7 MPa (100 psi).

- The thickness of the couplant may alter the effective sensitivity of the sensor. The thinnest practical layer of continuous couplant is usually the best. Care should be taken that there are no entrapped voids in the couplant. Unevenness, such as a taper from one side of the sensor to the other, can also reduce sensitivity or produce an unwanted directionality in the sensor response.

Note: This standard confirms the methods that Midé recommend to bond its standard products to structures. Please see the application notes on our website (www.mide.com).

2.1.6.3. E1211-02: Standard Practice for Leak Detection and Location Using Surface-Mounted Acoustic Emission Sensors

- Summary: This practice describes a passive method for detecting and locating the steady state source of gas and liquid leaking out of a pressurized system. The method employs surface mounted acoustic emission sensors. *This practice is not intended to provide a quantitative measure of leak rates.*

- Leakage of gas or liquid from a pressurized system, whether through a crack, orifice, seal break, or other opening, may involve turbulent or cavitational flow, which generates acoustic energy in both the external atmosphere and the system pressure boundary. Acoustic energy transmitted through the pressure boundary can be detected at a distance by using a suitable acoustic emission sensor.

- With proper selection of frequency passband, sensitivity to leak signals can be maximized by eliminating background noise. At low frequencies, generally below 100 kHz, it is possible for a leak to excite mechanical resonances within the structure that may enhance the acoustic signals used to detect leakage. External or internal noise sources can affect the sensitivity of an acoustic emission leak detection system. Examples of interfering noise sources are:

    - Turbulent flow or cavitation of the internal fluid,
    - Noise from grinding or machining on the system,
    - Airborne acoustic noise, in the frequency range of the measuring system,
    - Metal impacts against, or loose parts frequently striking the pressure boundary, and
    - Electrical noise pick-up by the sensor channels.

- Stability or constancy of background noise can also affect the maximum allowable sensitivity, since fluctuation in background noise determines the smallest change in level that can be detected.

- The acoustic emission sensors must have stable characteristics over time and as a function of both the monitoring structure and the instrumentation system examination parameters, such as temperature.

- Improper sensor mounting, electronic signal conditioner noise, or improper amplifier gain levels can decrease sensitivity. When leak location calculations are to be performed, the acoustic attenuation between sensors should be characterized over the frequency band of interest, especially if the presence of discontinuities, such as pipe joints, may be suspected to affect the uniformity of attenuation. The measurements should then be factored into the source location algorithm.

2.1.6.4. E569-02: Standard Practice for Acoustic Emission Monitoring of Structures During Controlled Stimulation

- Summary: Acoustic emission (AE) examination of a structure usually requires application of a mechanical or thermal stimulus. Such stimulation produces changes in the stresses in the structure. During stimulation of a structure, AE from discontinuities (such as cracks and inclusions) and from other areas of stress concentration, or from other acoustic sources (such as leaks, loose parts, and structural motion) can be detected by an instrumentation system, using sensors which, when stimulated by stress waves, generate electrical signals.

- In addition to immediate evaluation of the emissions detected during the application of the stimulus, a permanent record of the number and location of emitting sources and the relative amount of AE detected from each source provides a basis for comparison with sources detected during the examination and during subsequent stimulation.

- The preferred technique for conducting a performance verification is a pencil lead break. Lead should be broken on the structure at a distance of 4 in. (100 to 102 mm) from the sensor centerline. 2H lead, 0.3 mm diameter, 0.1 in. (2 to 3 mm) long should be used.

- During application of the stimulus, the locations of acoustic sources are usually determined through analysis of the times of arrival of AE signals at multiple sensors. Example parameters are pressure, time, and stress. As the stimulus is applied, record the number and location of emitting sources and the amount of AE detected from each source.

- Continuous emission from any leak in a structure stimulated by pressure can mask acoustic emission from sources near the leak. Effects of leaks on acoustic emission measurements should be eliminated to adequately examine pressure boundaries.

- Knowledge of attenuation in the structure and the response of sensors affected by leak noise may help localize the leak.

- A source's acoustic activity is normally measured by event count or emission count. A source is considered to be active if its AE activity continues to increase with increasing or constant stimulus. A source is considered to be critically active if the rate of change of its AE activity with respect to the stimulus, consistently increases with increasing stimulation, or if the rate of change of its AE activity with respect to time, consistently increases with time under constant stimulus.

- Preferred intensity measures of a source are its: average detected energy per event, average emission count per hit, or average amplitude per hit. A source is considered to be intense if it is active and its intensity measure consistently exceeds, by a specified amount, the average intensity of active sources. The intensity of a source can be calculated for increments of the stimulus or of hits. It is noted that, if there is only one active source, the intensity measure of the source is the average intensity of all sources, and therefore the intrinsic comparison no longer is applicable. In this case, it is necessary to classify the source through comparison with results from similar examinations.

- When using source location algorithms, in addition to activity and intensity, another characteristic of each detected AE source that should be considered for source classification is the size of the "region" of the located source. The clustering of the located events from a sharp discontinuity, such as a crack, is usually dense, while regions of plastic deformation associated with, for example, corrosion pits, result in source areas that show more uncertainty in the definition of their size, the events being contained rather sparsely in the region. In most cases, a growing crack is considered to be the more serious defect. However, activity and intensity may not suffice for distinguishing between the two. Normally, there is subjective judgment on what size of location bundle or cluster constitutes an isolated source.

2.1.7. Case Study

Case studies are a welcome resource for information on the methods followed by others. One case study has pertinent relevance to this effort.

2.1.7.1. Acoustical Characteristics of Leak Signals in Plastic Water Distribution Pipes. (Reference 1)

Abstract: Acoustical characteristics of leak signals in plastic pipes were investigated in this study for several types of leaks simulated under controlled conditions at an experimental site. The investigation included the characterization of frequency content of sound or vibration signals as function of leak type, flow rate, pipe pressure and season, the determination of the attenuation rate, and the variation of propagation velocity

with frequency. The information presented in this paper for the acoustic characteristics of leak signals will help leak detection professionals in the selection of appropriate instrumentation, the design of appropriate measurement procedures, and in the case of propagation velocity, in accurately locating leaks using the cross-correlation method.

Summary: The characteristics of leak signals in a typical PVC water distribution pipe have been investigated under controlled conditions at an experimental leak detection facility. The main findings of the investigation can be summarized as follows:

- Most of the frequency content of leak signals measured with hydrophones was below 50 Hz. Signal amplitudes at higher frequencies were extremely small. Accelerometer measured leak signals had higher levels at high frequency than hydrophone measured leak signals.
- The amplitude of leak signals diminished rapidly with distance, at a rate of about 0.25dB/m. The winter's rate is significantly higher.
- Below 50Hz, there was no measurable attenuation across pipe joints.
- The propagation velocity of leak signals is identical for both hydrophone and accelerometer-measured signals. The propagation velocity was about 7% higher in winter.
- Below 50Hz, the propagation velocity is independent of frequency.

2.1.8. Preliminary FEA Analysis

The acoustic signature of a leaking pipe is actually a complex FSI, or Fluid-Structure Interaction problem. To avoid painstaking FSI FEA analyses, it is prudent to first investigate common pipe vibrations. Knowing the general resonant modes of a pipe would certainly help in detecting leaks in a pipe.

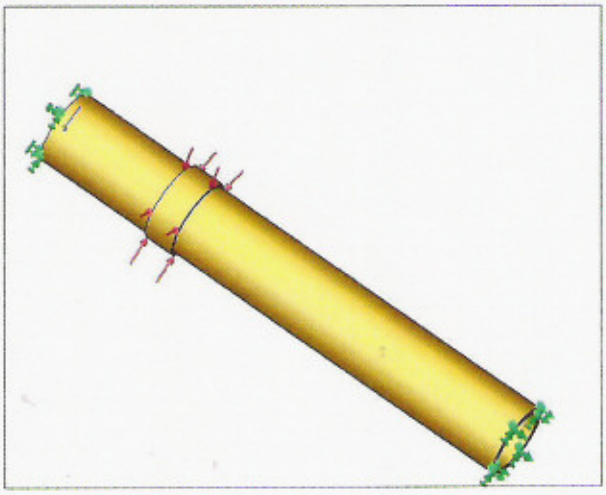

Figure 1: Model for initial pipe modal investigation.

A FEA frequency analysis was performed for a simple pipe being subjected to a radial pressure (Figure 1). Since the primary purpose of the exercise is to visualize the vibration modes that may be seen in a pipe, no dimensions or material properties will be given. The pipe is fixed at the ends, and the pressure is applied at some distance along the pipe. The first thirty modes are shown in Appendix A. Shown in Figure 2, is a typical result. Appendix A shows all thirty modes. As will be evident by the figures, there are many pairs of matching vibration modes. The modes, shown in increasing order, ranged from 1.5 to 12 kHz. As soon as a characteristic pipe is defined, this analysis will be performed again to match pipe dimensions and material properties with the resonant pipe frequencies.

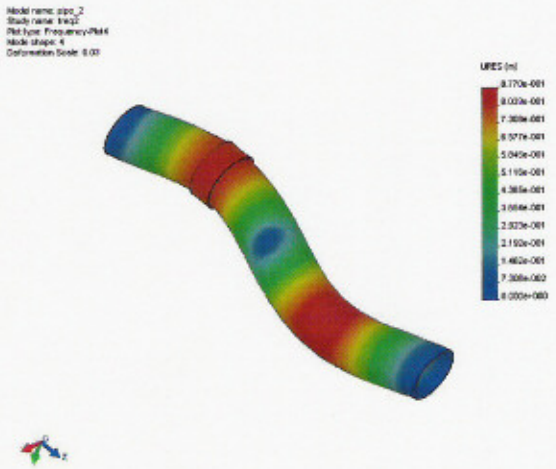

Figure 2: Example of preliminary FEA analysis results. For details, please see Appendix A.

2.2. Requirements

Develop a system requirements document that will drive the design.

2.2.1. Test Setup and Demonstration Model

A test and desktop demonstration concept was presented to the technical monitor for approval. The concept is shown in Figure 3. The system consists of the following:

- Variable Speed Pump
- Pipe
- Baffle for noise control
- Needle Valve
- Flow Rate Sensor
- Supports
- Piezoelectric Sensors
- Signal Conditioning Unit
- Laptop Computer with AD/DA capability

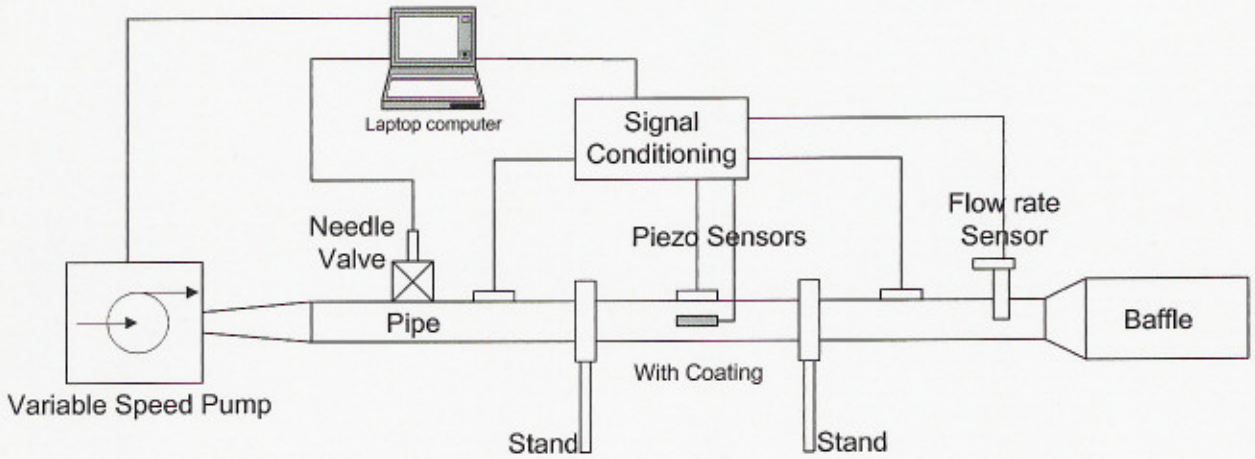

Figure 3: Concept for the desktop demonstrator.

The laptop computer will control the speed of the pump and the opening of the needle valve. These two variables will determine the rate of the leak. The piezoelectric elements will sense the leak, their output voltage determined by the intensity of the leak and their proximity to it. These signals, as well as a flow rate sensor signal, will be conditioned and transmitted to the laptop for visual display. The operator will be able to change the speed and the size of the orifice from the laptop and immediately see the effect on the sensors.

The related data transfer work can be implemented as an option. Midé proposed to use ultrasonic data transfer along the pipeline. With multiple sensors integrated on the desktop demonstrator, it will be possible to excite one piezo element and determine the effect of these vibrations on the others. The excitation waveform and accompanied signal generated by the other elements will also be displayed on the laptop.

As another option, Midé can integrate its multi event recorder with the piezo elements. This will allow the user to determine how many times in a given interval a certain level has been exceeded. This functionality can readily be integrated with the laptop computer.

Since the pipes that are used in the field have coatings, we will need to determine the effectiveness of the system through such coatings. Midé will add another set of sensors that are bonded to the pipe through a representative coating. Comparing the results from the coated and uncoated sensors will indicate the sensitivity to the system to the coating material.

In order to construct the desktop demonstration model, a number of parameters needed to be defined. Midé compiled a list as shown in Table 4. Midé's initial assumptions and the feedback from the technical monitor is also shown in Table 4

Table 4: Parameters for the demonstration setup.

Parameter	Midé's Assumption	Actual Value
Pipe Inside Diameter	4 – 6 inches	4″
Working Fluid	Air	Air
Valve diameter	0.05″ – 0.2″	TBD
Flow Rate	TBD	Pressurized System
Pipe Material	Stainless Steel	Representative Pipeline Material
Pipe Length	4-6 ft	6 ft
Pipe Coating	TBD	Representative Pipeline Material
Support	Stands / Underground	Stands
System	Portable	Portable

2.3. Laboratory Tests

Scaled pipeplines will be constructed. Leaks will be introduced in these scales lines at various pressures and flow rates and piezo sensors will be used to determine how far monitors must be spaced to detect these leaks. The same lines will be used to demonstrate the quality and the distance over which data can be transmitted using Midé structural acoustics data communications system.

This section will describe Midé's test setup, provide some preliminary tests results, and will then present actual test data. This data is reduced and presented in forms that will make it possible for electronic systems to identify leaks, categorize their magnitude and location. This section also presents an FEA model that corroborates the tests results. This FEA model can be used to design and optimize for different boundary conditions (i.e. in the ground, et al.), pipe geometries and sensor locations.

2.3.1. Laboratory test setup

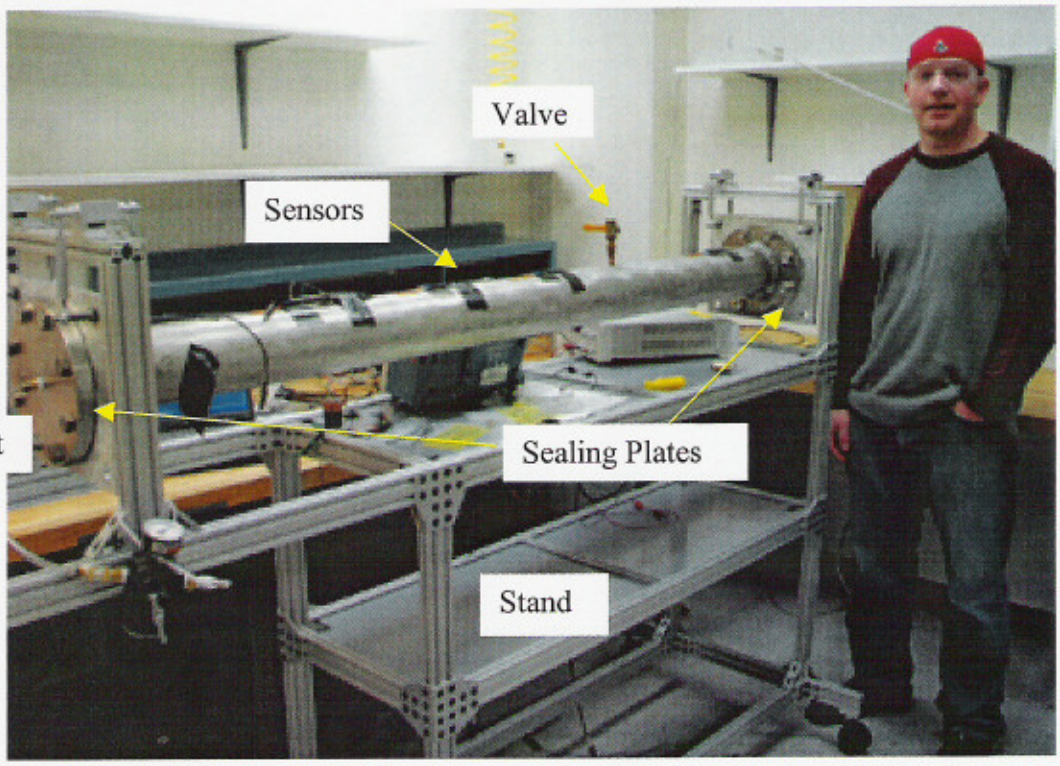

Figure 4: The test pipe section. The inlet tube connects the pipe to the regulated air while the sealing plates ensure that the outlet valve produces the only leak. The location of the sensors and the portable stand is also shown.

Figure 4 shows the laboratory test pipe section. The test setup consists of a 6′ stainless steel pipe section of 4″ ID. The pipe was sealed on both ends with sealing plates. One of the sealing plates has an inlet for air. A hole was drilled and taped and a valve placed 2 ft from the other sealing plate.

Four PowerAct™ actuators / sensors were vacuum bonded, equally spaced from the outlet. Figure 5 shows the PowerAct conforming to the pipe radius. Also shown in the Figure is the connection from the PowerAct

connector to a BNC cable. These BNC cables transfer the signal from the PowerAct to the sensing electronics.

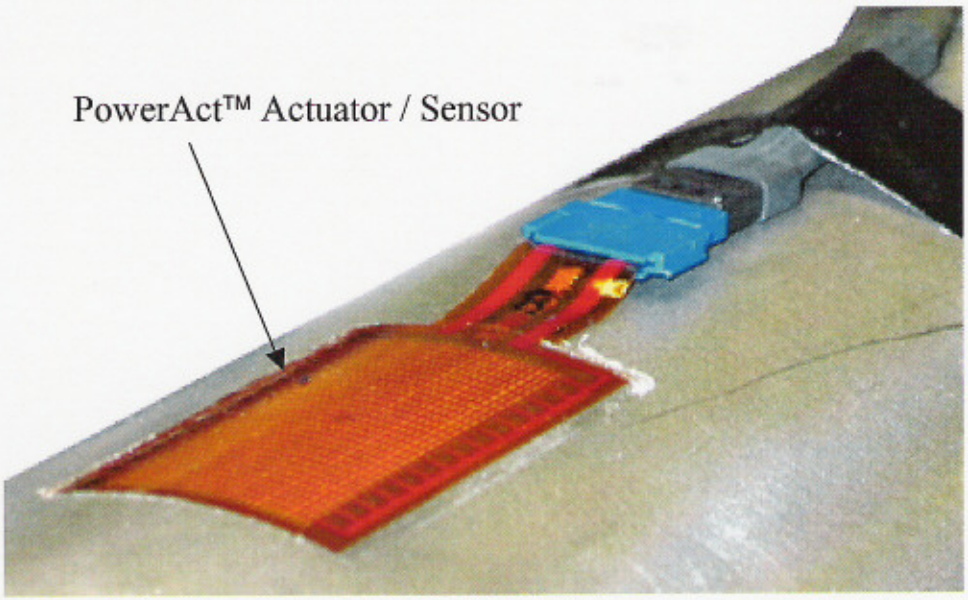

Figure 5: Close-up of PowerAct™ Actuator / Sensor as bonded on to the test pipe section.

The sensing electronics are an A/D card which is connected to a laptop computer. The signals from the sensors are read from the card by means of LabView™ software. Data traces were collected using an oscilloscope.

Figure 6 shows the sensor numbering scheme that will be used throughout the report. Sensor 1 is the furthest away from the valve, at the one end of the pipe. Sensor 2 is closer to the valve with Sensors 3 and 4 closest. Sensor 4 is at the other end of the pipe. All sensors and the valve are equally spaced in such a manner that the distance from the end of the pipe to sensor 1 equals the distance form Sensor 1 to 2, 2 to 3, 3 to the valve and the valve to Sensor 4.

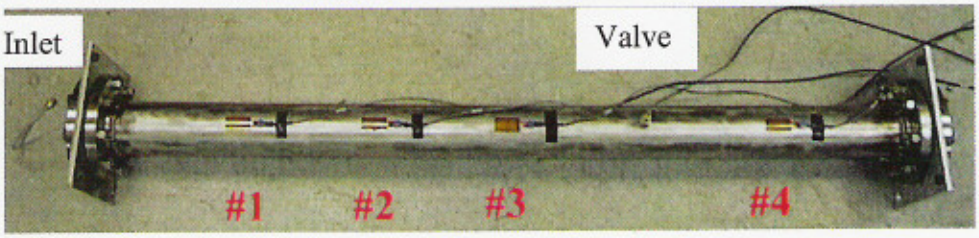

Figure 6: Sensor numbering scheme.

2.3.2. Initial Tests

Preliminary tests to measure the sensitivity and effectiveness of the PowerAct™ sensors were conducted. These tests include a traveling wave experiment, leak (flow) detection tests and pipeline communications tests. The traveling wave experiment showed that the sensors are able to locate the position of a mechanical

impact such as excavating equipment. The leak tests show that small leaks are identifiable. The communications test illustrates the ability of the sensors to transmit data between themselves.

2.3.2.1. Traveling Wave Test

To get an indication of the sensitivity of the sensors, the pipe was struck with a hammer on different locations and the response of the sensors recorded. Figure 7 is the result of the pipe being struck on the left end. For this illustration, a DC offset was added to sensors in order for clarity. 1.5 Volts were added to Sensor 1's signal, 1 Volt to Sensor 2's and 0.5 Volt to Sensor 3's. Sensor one, then two, three and four in succession, senses the wave traveling through the pipe. This indicates that the sensors work fine and that the sensors pick up the wave as expected. Another interesting feature of the plot is that the wave dissipates slightly as it travels down the pipe, away from the source of impact.

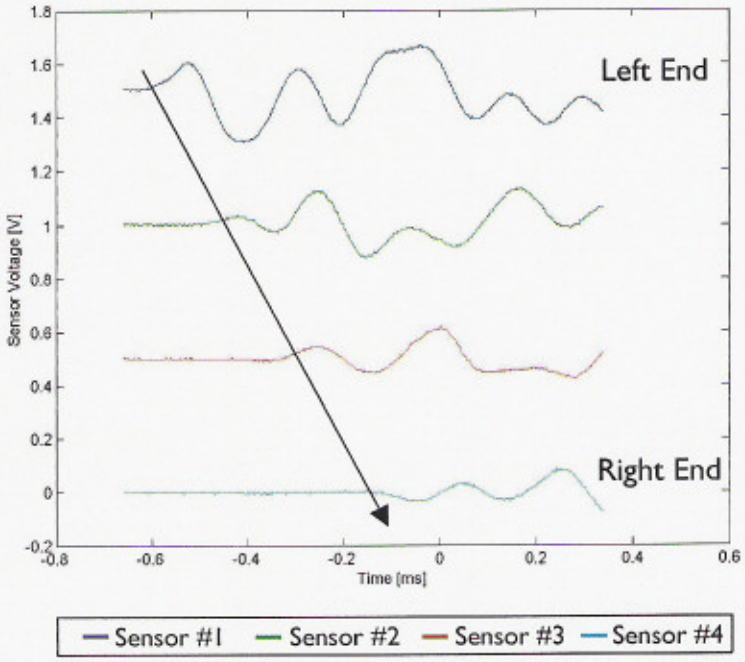

Figure 7: Test data depicting an acoustic wave traveling from left to right. The Sensor trace results are separated in this figure for clarity. 1.5 Volts were added to Sensor 1's signal, 1 Volt to Sensor 2's and 0.5 Volt to Sensor 3's.

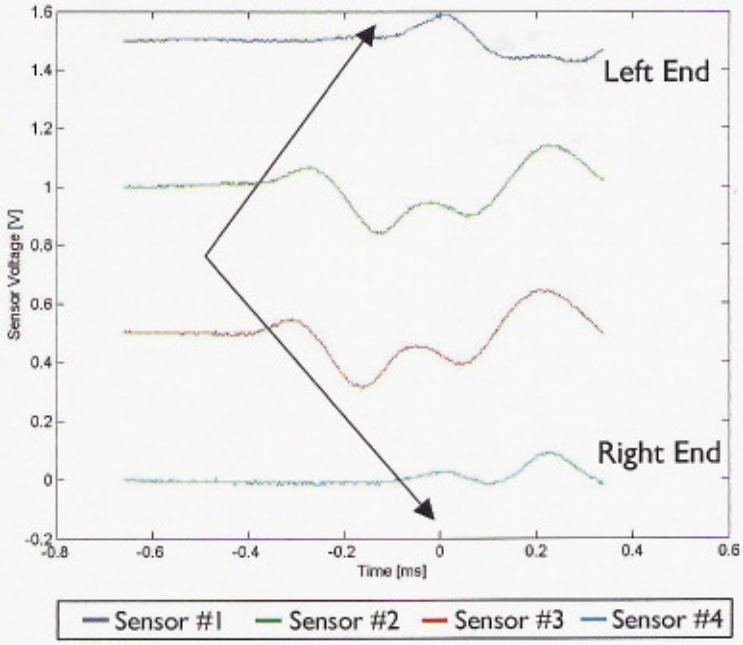

Figure 8: Test data depicting an acoustic wave traveling from between #2 and #3 sensors to sensors #1 and #4.

Figure 8 shows the result of striking the pipe in the middle, between sensors two and three. As expected, the wave arrives at sensors two and three at almost the same time and then arrives at one and four at a later time. Again the signal is diminishing as it is measured further from the event.

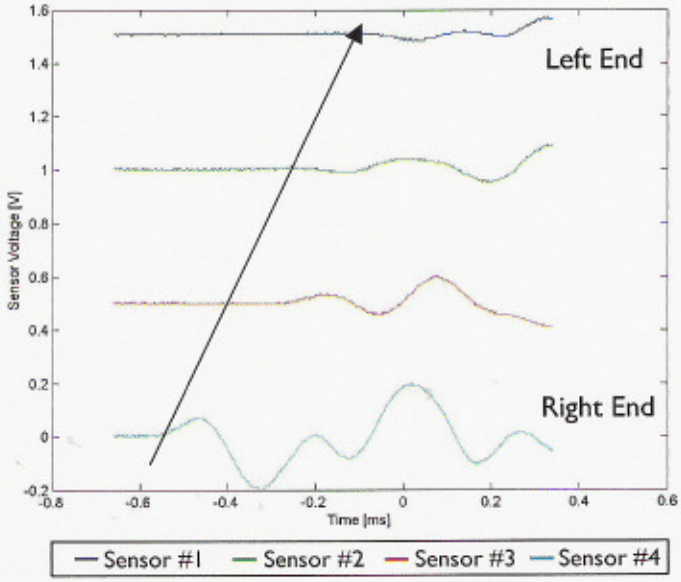

Figure 9: Test data depicting an acoustic wave traveling from right to left.

Figure 9 is the opposite of Figure 7 in the sense that the pipe was struck on the right side. Again the wave is shown traveling down the pipe, away from the event and dissipating as it moves.

The significance of these tests are twofold: the sensors work and an impact could be sensed. Furthermore, the sensors may be calibrated to detect impact above a known dangerous level and the location of the leak may be deduced using two or more sensors. This has significant potential since most pipe leaks originate from excavating equipment impacting the pipe. The tests indicate that such an event can firstly be sensed, and secondly, since the traveling and dissipation could be recorded, the impact can also be located.

2.3.2.2. Leak Tests

These tests were conducted in order to determine how the sensor's output correlated with various degrees of leakage. A manual needle valve was placed between PowerAct™ 3 and 4 and used to change the flow rate from the pressurized pipe. The sensor response to these events was recorded as before. The pipe was pressurized to 90 psi and three readings were taken: valve fully closed, half open and fully open. The results of these three tests are depicted in Figure 10 to Figure 12.

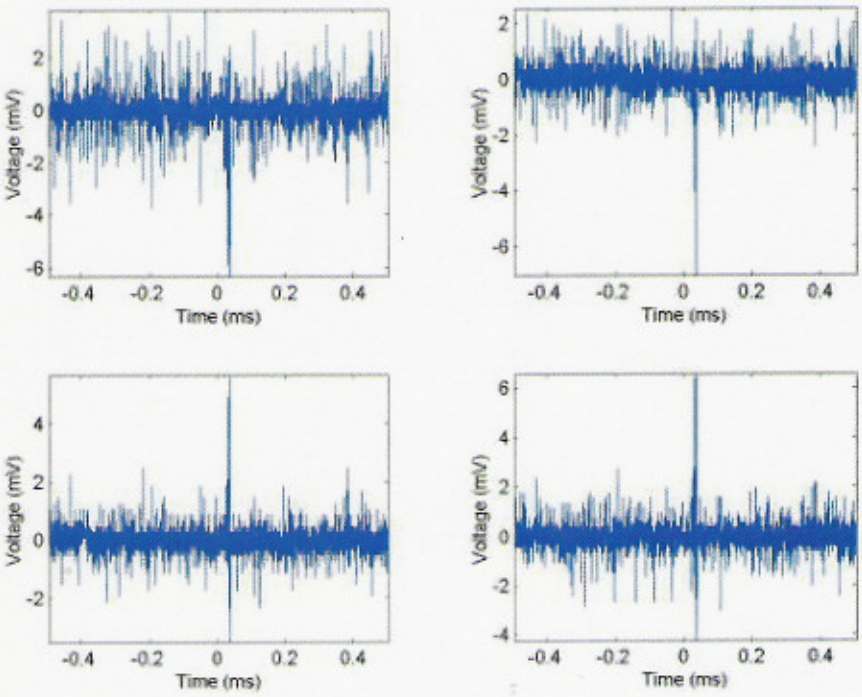

Figure 10: Data traces from the PowerAct™ sensors with 90 psi pressure and the pipe completely sealed. Traces are from left to right top to bottom, from sensor numbers 1,2,3,4.

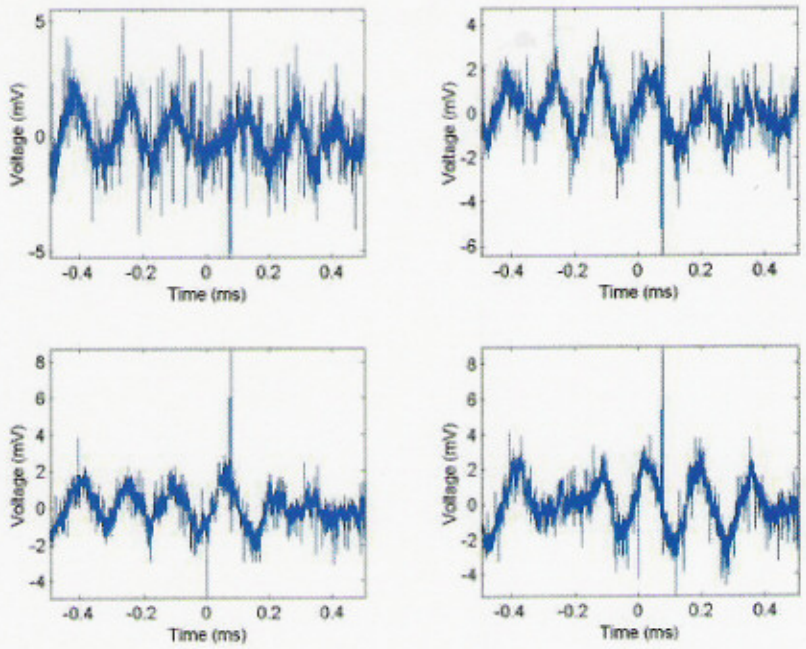

Figure 11: Data traces with 90 psi pipe pressure the needle valve half open. PowerAct™s 1,2,3,4 from left to right, top to bottom.

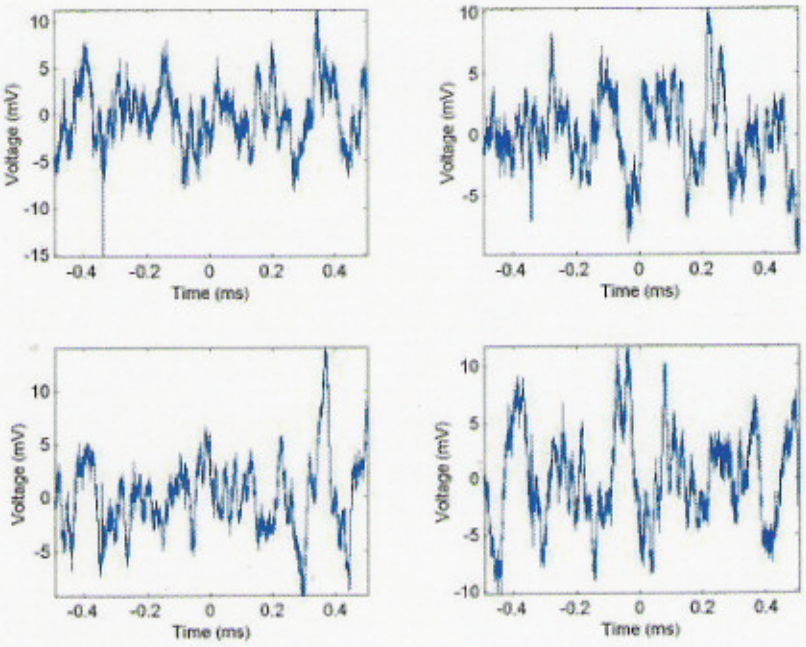

Figure 12: Data traces for pipe pressure at 90 psi and needle valve fully open. Traces are PowerAct™s 1,2,3 and 4 from left to right top to bottom.

When the valve is fully closed the sensors pick up random noise at 1mV p-p. The half open valve produces 2 mV p-p output at 7.5 kHz. When the valve is fully open, the sensors measure around 5 mV p-p at 6 kHz, with a significant high frequency element.

The sensors were able to differentiate between the different flow rates produced by the valve. These differences were seen in both frequency and amplitude. A systematic evaluation and characterization of these trends will follow.

2.3.2.3. Signal Transfer Tests

These tests aimed at proving feasibility of transferring data down the pipe, actuator to sensor, one to the next. Please note the dual functionality of the PowerAct™: sensing and actuation, is a significant cost saving tactic. The tests were performed by actuating the left (#1) PowerAct™ and measuring the response of the other PowerAct™s. The result of this test is shown in Figure 13

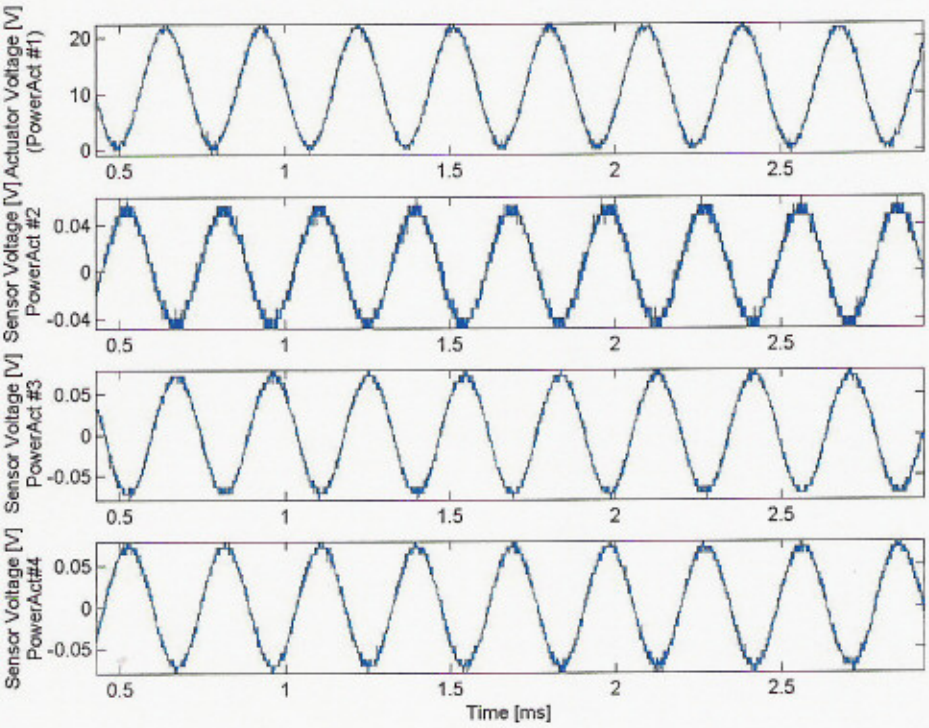

Figure 13: Result of the data transfer test. The trace on top is the input signal to the actuator, PowerAct™ #1. The following traces are the measured response from the other piezo actuators, used as sensors. All the Sensors produce the same signal amplitude, but with a phase shift.

The input signal is 10V p-p and the responses around 50 – 60 mV. It is interesting to note how "clean" the signal is. There is another high frequency mode on top of the approximately 3.5 kHz signal. This high frequency noise can be filtered with little effort and should not pose a problem for the data transfer.

Another interesting fact is that it takes about 0.4 ms for the signal to move from PowerAct#1 to PowerAct#4. Since the speed of sound in stainless steel is 5,000 m/s, it means the wave traveled

$$\lambda = v.\omega = 4.10^{-4} \times 5.10^{3} = 1.2\ m = 4\ ft$$

This distance is exactly the distance between PowerAct™#1 and PowerAct#4.

2.3.3. Leak Identification Testing

For the leak identification testing, it was decided to remove the needle valve of the preliminary tests and replace it with a ¼" ball valve. The ball valve resembles a leak closer since it can be set to have a small crack.

A LabView™ program was written that allowed an A/D card to read and collect the output from the PowerAct™ sensors. A number of tests were conducted at different pressures and valve openings. The output from the sensors were collected and stored with the LabView™ system.

In order to ensure that the data was statistically significant, a number of traces were recorded for the same test condition. Table 5 lists the experimental conditions and the number of data traces that were taken at each condition. All the results are listed in Appendix B. Since the results in Appendix B prove the repeatability of the tests, only the most relevant results will be discussed here.

Table 5: Number of tests performed at tests conditions

Number of Tests	Valve Opening		
Pressure in Pipe	**Closed**	**1/3**	**2/3**
30 psi	6	3	3
60 psi	6	3	3

A sample of the raw data traces collected by the LabView™ program had is shown in Figure 14. The leaking air exits multiple frequencies at different amplitudes in the pipe. The logical next step in the data collecting process was to convert these time domain traces into frequency domain traces by means of an FFT algorithm.

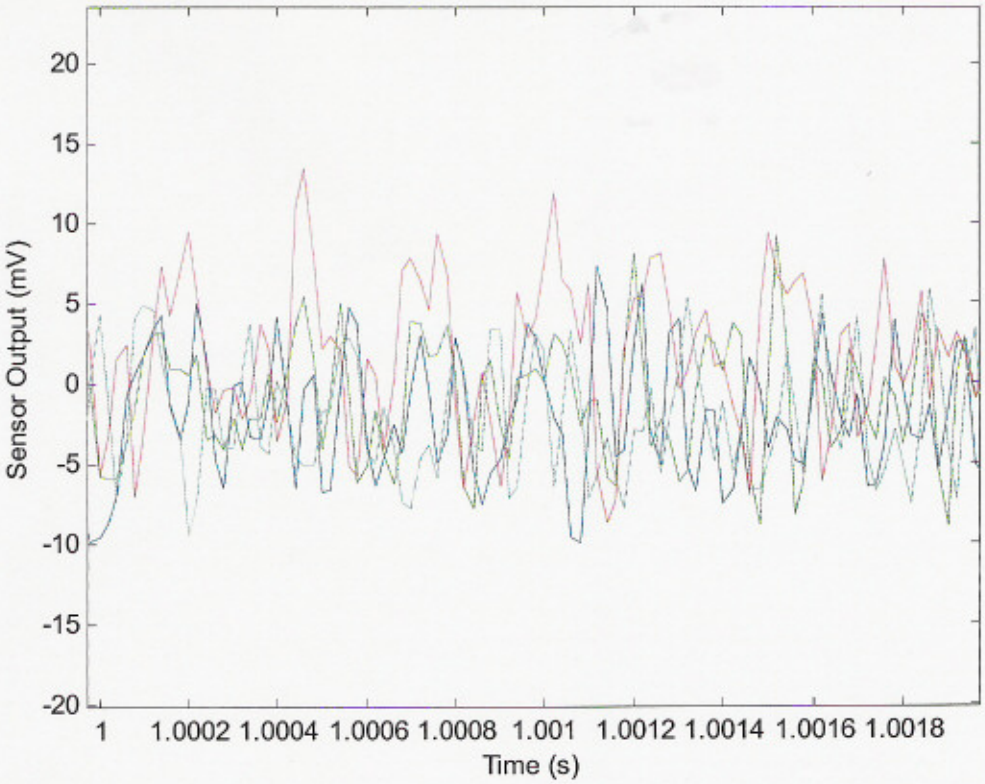

Figure 14: Sample of a LabView™ data trace for one of the tests. Senor 1 = blue, Sensor 2 = green, Sensor 3 = red, Sensor 4 = cyan.

2.3.3.1. Auto-Spectra and Power Spectral Density Results

This section presents the Auto-Spectra (FFT) and Power Spectral Densities (PSD) of the measured sensor outputs. When the "leak" and "no-leak" results are compared, it is clear that leaks are detectable. It is also clear that the sensor outputs increase with increased pressure and size of leak. These conclusions are also supported by the results presented in the next section.

A Fast Fourier Transform (FFT) is a computationally less expensive form of a Fourier Transform. These transforms are used to convert signals from the time domain to the frequency domain. When signals have multiple frequencies and amplitudes such as Figure 14, it is difficult to extract useful information when the data is viewed in the time domain. When such a signal is transformed to the frequency domain, a number of interesting results can be obtained. For instance, the natural frequencies of the structure of the pipe can be identified. By combining or integrating the results of the FFT in certain discreet frequency bands, the data is cleared up and results are apparent. This integration is referred to as power spectral density, because one effectively adds the power in a certain discreet frequency spectrum.

Typical results for no leak, i.e. the ball valve in the closed position is shown in Figure 15 for the Auto Spectrum and Figure 16 for the Power Spectral Density. The FFT in Figure 15 shows quite a bit of noise at very low power. The PSD of Figure 16, because of the integration of the FFT over every decade, smoothes

the FFT curve. The PSD clearly illustrates that there are almost no frequencies at which the sensors generate any significant power.

When we compare Figure 16, when the valve is shut, with Figure 18, when the valve is a third open, it is clear that energy is produced in the sensors by the leak. Not only are there multiple resonant frequencies, but also the amplitude of the signal had risen by two orders of magnitude. If we compare Figure 18 with Figure 20, we see the same resonant frequencies and that the magnitude of the sensor output has increased. This clearly illustrates the ability of the PowerAct™ sensors to detect the leak and its magnitude.

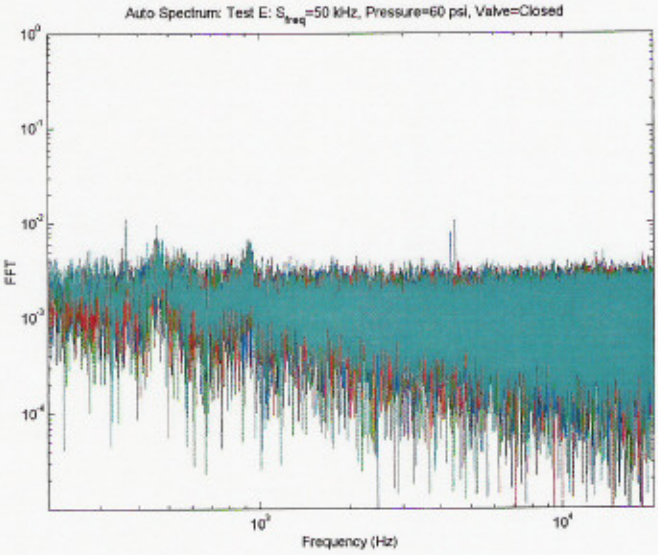

Figure 15: FFT (Auto Spectrum) of the sensor outputs when the pipe is at 60 psi and the valve is completely shut.

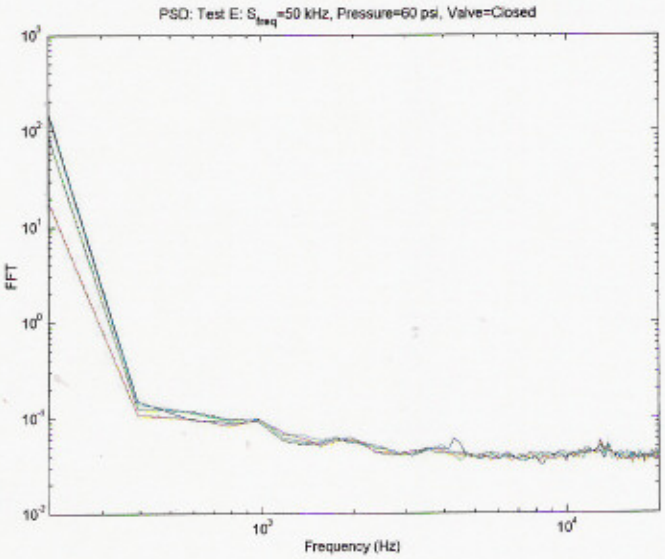

Figure 16: Power Spectral Density of the sensors when the pipe is at 60psi and the valve is completely shut.

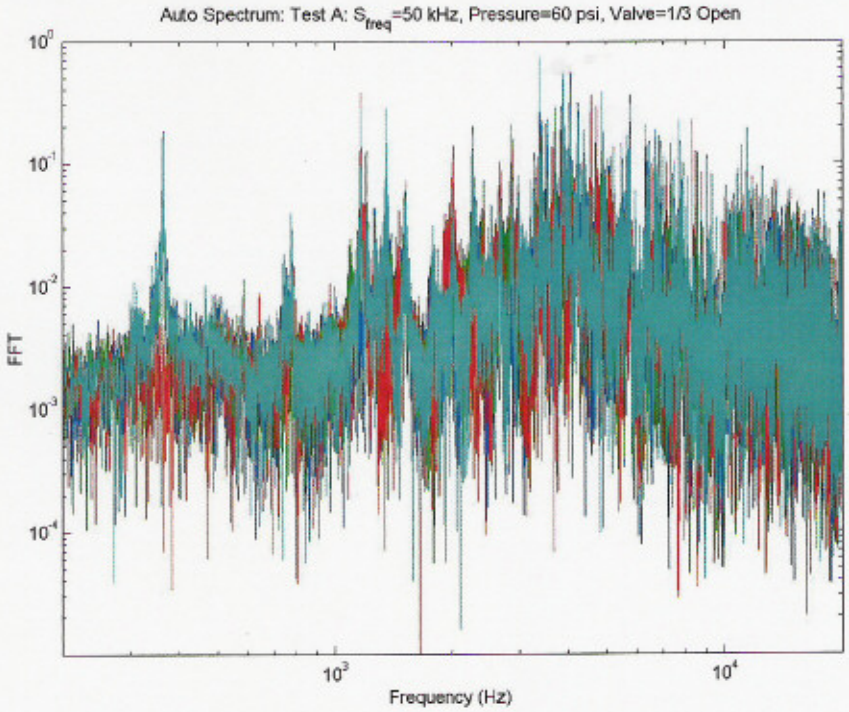

Figure 17: FFT (Auto Spectrum) of the sensor outputs when the pipe is at 60 psi and the valve is 1/3 open.

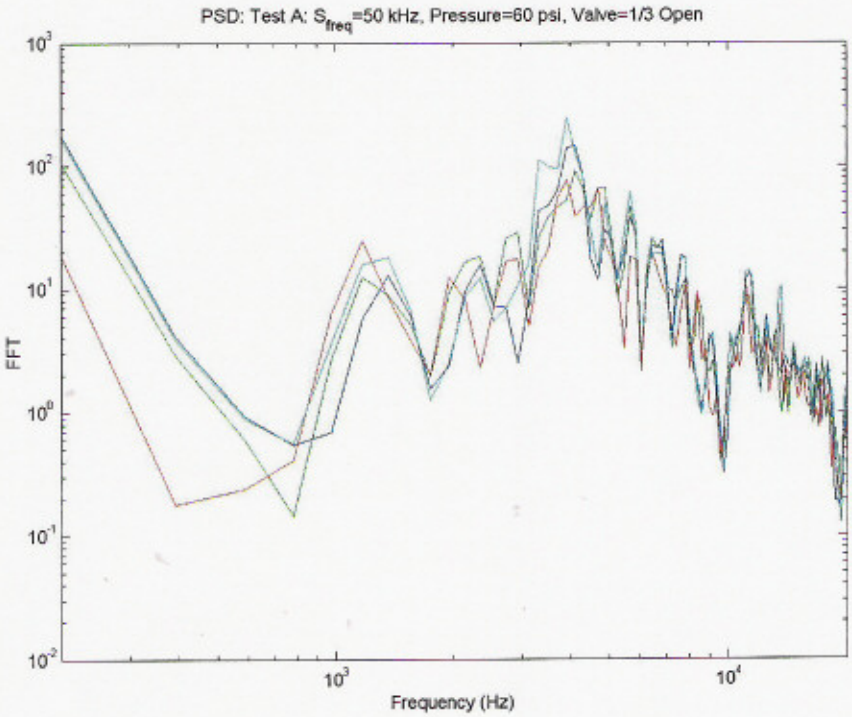

Figure 18: Power Spectral Density of the sensors when the pipe is at 60psi and the valve is 1/3 open.

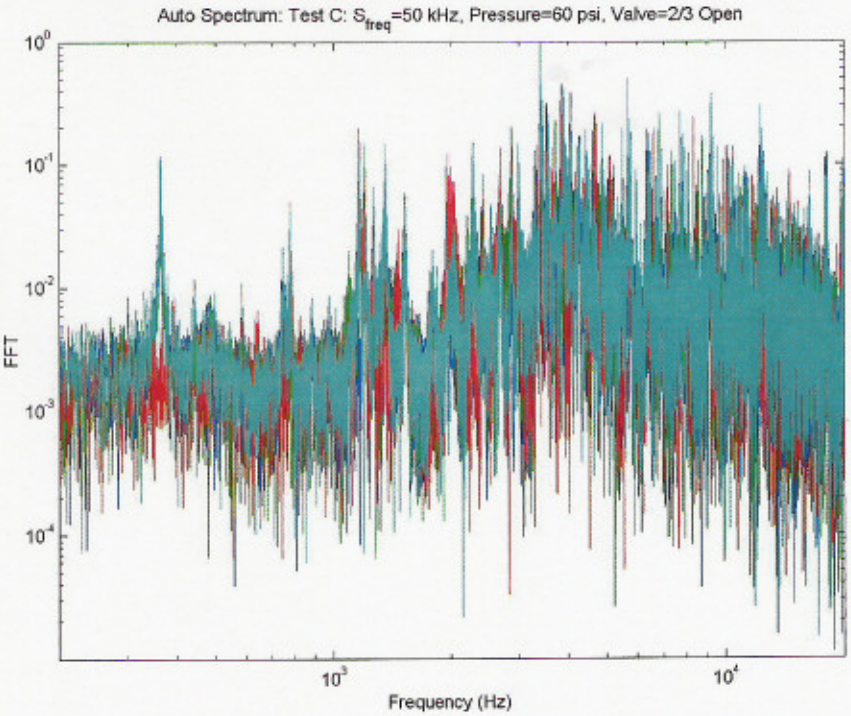

Figure 19: FFT (Auto Spectrum) of the sensor outputs when the pipe is at 60 psi and the valve is 2/3 open.

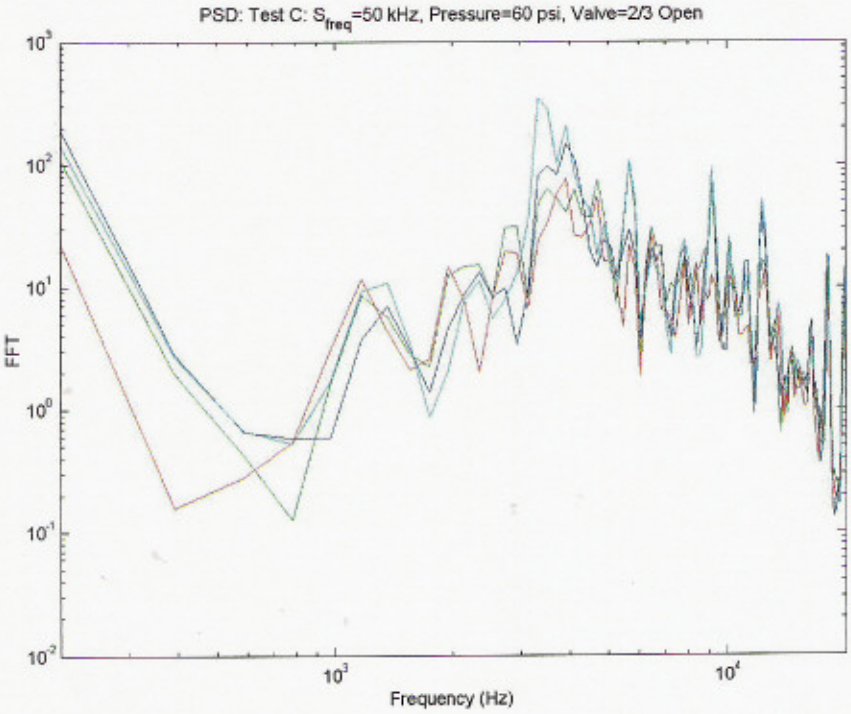

Figure 20: Power Spectral Density of the sensors when the pipe is at 60psi and the valve is 2/3 open.

2.3.3.2. Location and Magnitude of the Leak

In order to determine the location and the size of the leak, the phasing and amplitude of the measured disturbances were examined near the peak or resonant frequencies. Four "resonant" frequencies were identified, namely:

- 362.5 Hz
- 751.0 Hz
- 1168.5 Hz
- 4000.0 Hz

It is expected that these four frequencies are structural resonant frequencies and Midé has constructed a structural Finite Element Model to confirm this.

The data was examined by either looking at the phase and amplitude near the peak or at the peak. Preliminary results concluded that more accurate phasing information could be obtained when only the phasing and amplitude at the peak is used. The amplitude and phase was obtained by numerically integrating for the Fourier coefficients. These results are graphically summarized in the Figures below.

It should be noted that the data acquisition system used by Midé does not have a simultaneous sample and hold and that the phase must still be adjusted according to the following relation that takes the sampling frequency of the DAQ into account:

$$\bar{\phi}_i = \phi_i - 0.0018(i-1)f$$

Where f is the frequency in Hz, i is the sensor channel number, ϕ_i is the uncorrected phase of channel number i and $\bar{\phi}$ is the corrected phase. This work is scheduled for the next reporting period.

What follows are the preliminary results of integrating the FFT at 1,168.5 Hz and 4 kHz frequencies. These are preliminary results and are presented purely for interest. Midé is currently interpreting these results and more work will follow.

2.3.3.2.1 Sensor Signal Amplitudes and Phasing at 1168.5 Hz

For the case where there is no leak, the amplitudes are below .002 (Figure 21), about an order of magnitude lower than any one of the leak tests (Figure 22 and Figure 23.) In all these tests, the maximum amplitude was near Sensor 3. In most cases the next strongest output is from Sensor 4, indicating the leak is between these two sensors.

The phase results are more difficult to interpret. This can mainly be attributed to the fact that multiple frequencies are been picked up by the sensors. It is thus difficult to distinguish peaks on a specific frequency and this makes is mathematically complicated to calculate phase shifts. A fix for this problem will be to make a narrow band high and low pass filter that targets a specific resonance. By filtering all other frequencies, phase shifts will readily appear. The specific frequency will be a function of the geometry and boundary conditions of each individual pipe section. This work will be performed in Phase II.

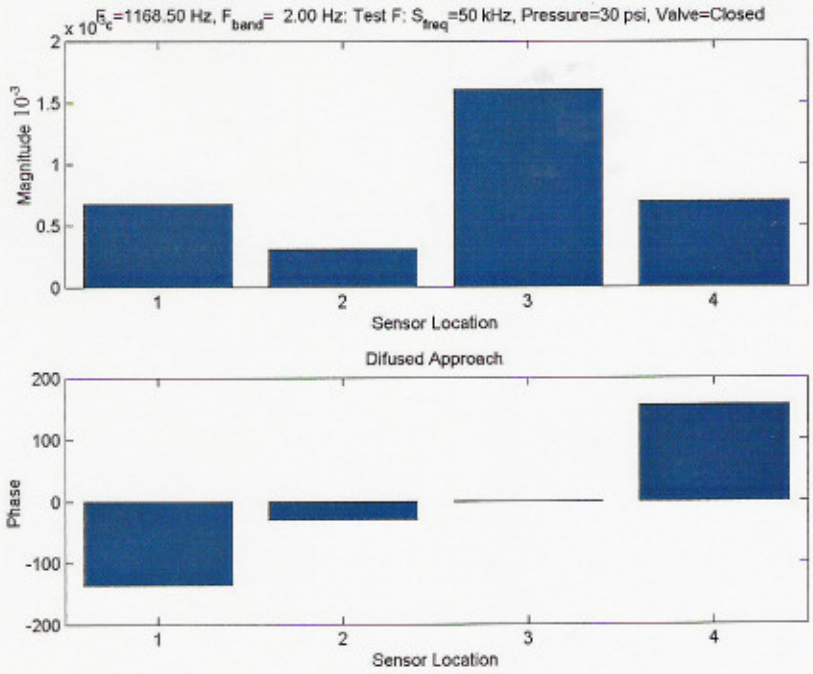

Figure 21: Integrated signal magnitude (top) and phase shift with respect to sensor 3 (bottom) at 1.168 kHz for pipe pressure at 30 psi and valve closed.

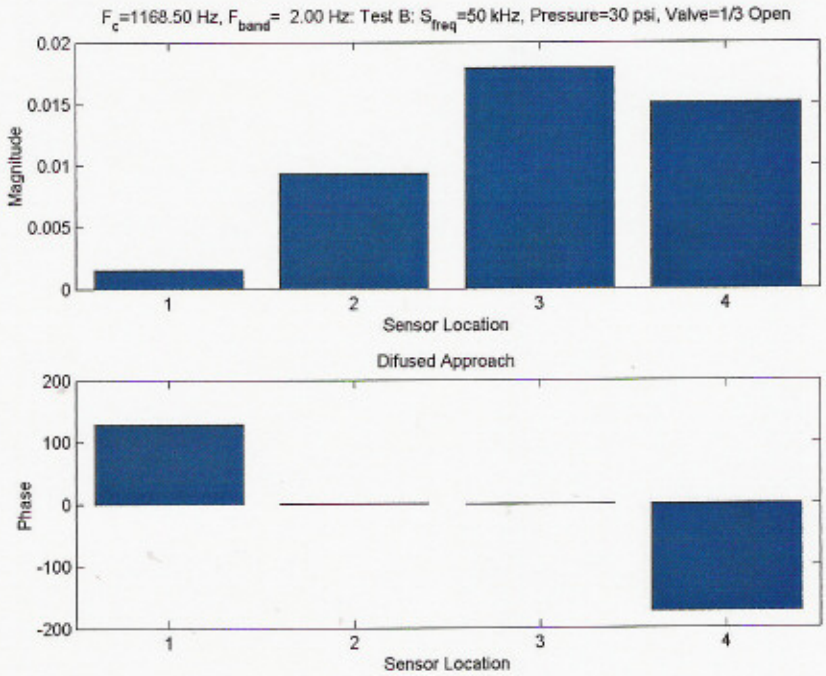

Figure 22: Integrated signal magnitude (top) and phase shift with respect to sensor 3 (bottom) at 1.168 kHz for pipe pressure at 30 psi and valve 1/3 open.

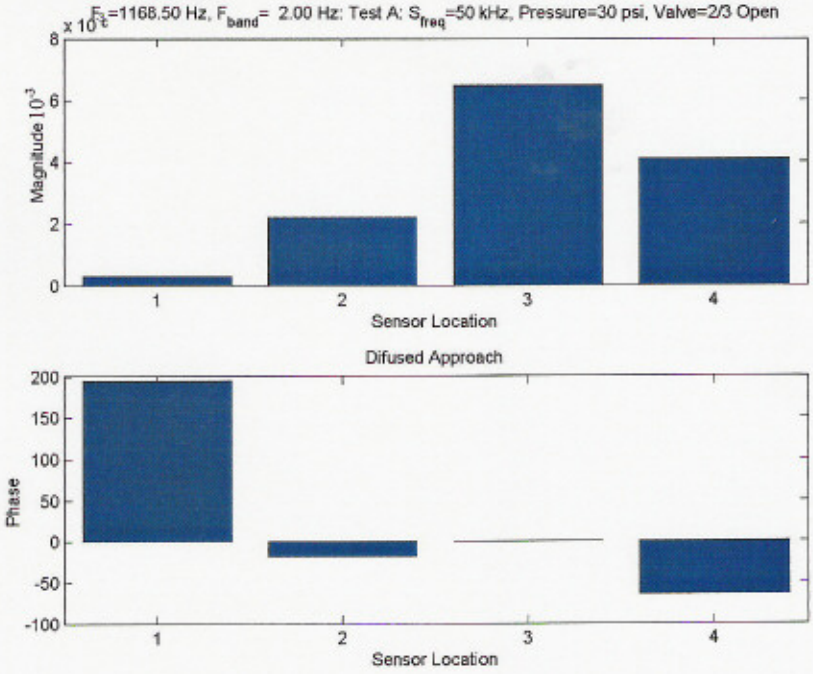

Figure 23: Integrated signal magnitude (top) and phase shift with respect to sensor 3 (bottom) at 1.168 kHz for pipe pressure at 30 psi and valve 2/3 open.

2.3.3.2.2 Sensor Signal Amplitudes and Phasing at 4000 Hz

At 4 kHz the maximum amplitude was near Sensor 4. Again, the phase results are more difficult to interpret and this will be completed in Phase II.

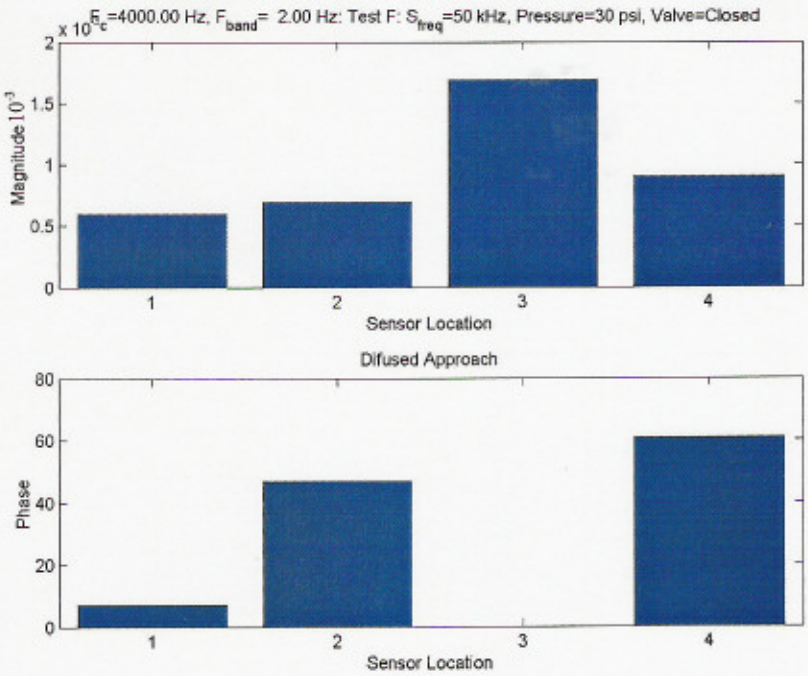

Figure 24: Integrated signal magnitude (top) and phase shift with respect to sensor 3 (bottom) at 4 kHz for pipe pressure at 30 psi and valve closed.

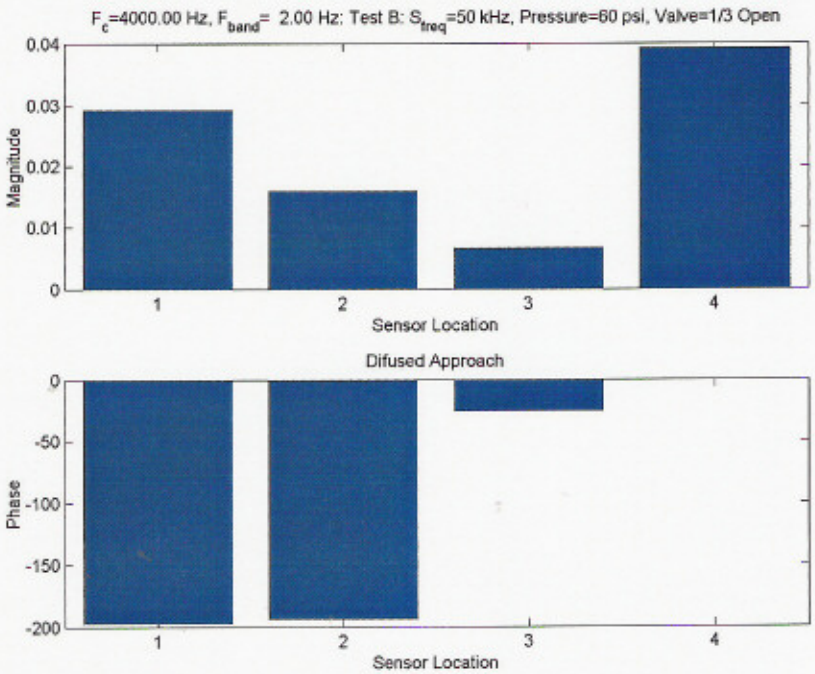

Figure 25: Integrated signal magnitude (top) and phase shift with respect to sensor 3 (bottom) at 4 kHz for pipe pressure at 60 psi and valve 1/3 open.

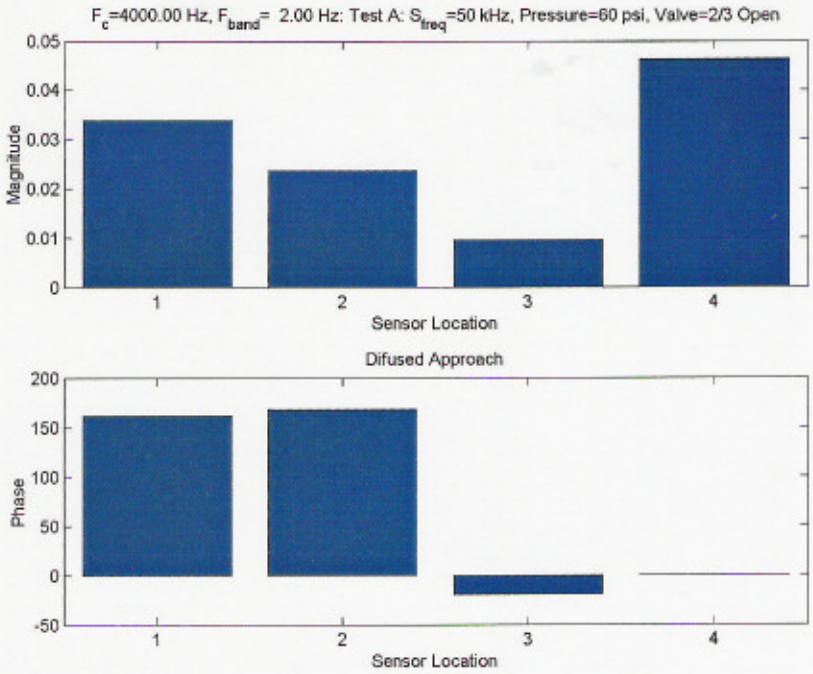

Figure 26: Integrated signal magnitude (top) and phase shift with respect to sensor 3 (bottom) at 4 kHz for pipe pressure at 60 psi and valve 2/3 open.

2.3.4. FEA Analysis on Test Setup

An FEA model was set up in order to corroborate the results of the tests. The results of this model, once compared and aligned with the test results, will serve as the cornerstone for the Phase II effort. Different boundary conditions, pipe diameters, pipe lengths and sensor placements can easily be evaluated using a calibrated model.

2.3.4.1. FEA Model

An FEA model was created in NASTRAN and is shown in Figure 27. The model consists of 2874 nodes and 2892 quadrilateral plate elements. This model in the free-free end condition is used to compare and corroborate test results.

Some of the modal results are shown in Figure 28. It is interesting to note that both string and radial vibrations contribute to the modes present in the pipe. Further analysis and modeling will be performed in the follow on contract. One of the tasks will be to instrument a pipe that is currently being used and compare the actual results with the predicted results of these models.

Figure 27: FEA model of the test article as created in NASTRAN. The model consists of 2874 nodes and 2892 quadrilateral plate elements.

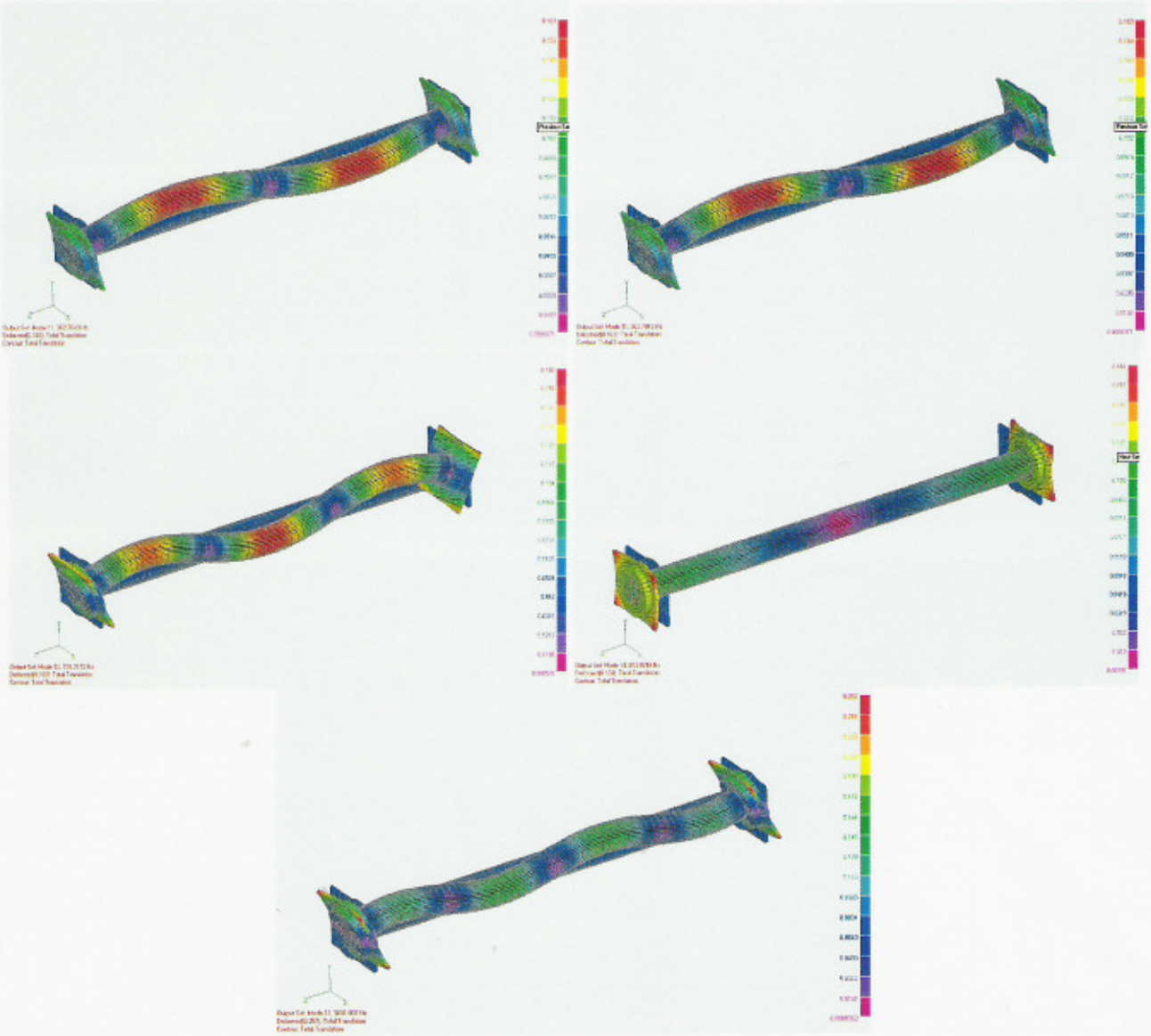

Figure 28: Results of the free-free FEA analysis. The modes from left to right, top to bottom are 359.5 Hz, 362.8 Hz, 708.3 Hz, 812 Hz and 1,091 Hz.

2.3.4.2. FEA Results

The FEA model described in the previous section was used to identify the natural frequencies (resonances) of the pipe test setup. The setup was modeled as free-free. Figure 29 shows the results of the modal calculations. In this figure, the each line represents a resonant frequency. The FEA analysis produces an array of natural frequencies. Representing a natural frequency with a 1 an all other frequencies with a 0 produced the graph of Figure 29.

It is interesting to compare Figure 29 with. Figure 20. As stated earlier, the dominant resonant frequencies of the test setup was determined to be at 362 Hz, 757 Hz, 1168 Hz and 4 kHz. These frequencies also clearly show up in Figure 29. It is thus concluded that the FEA analysis is a close approximation of the real test setup and that the model can be used for design purposes.

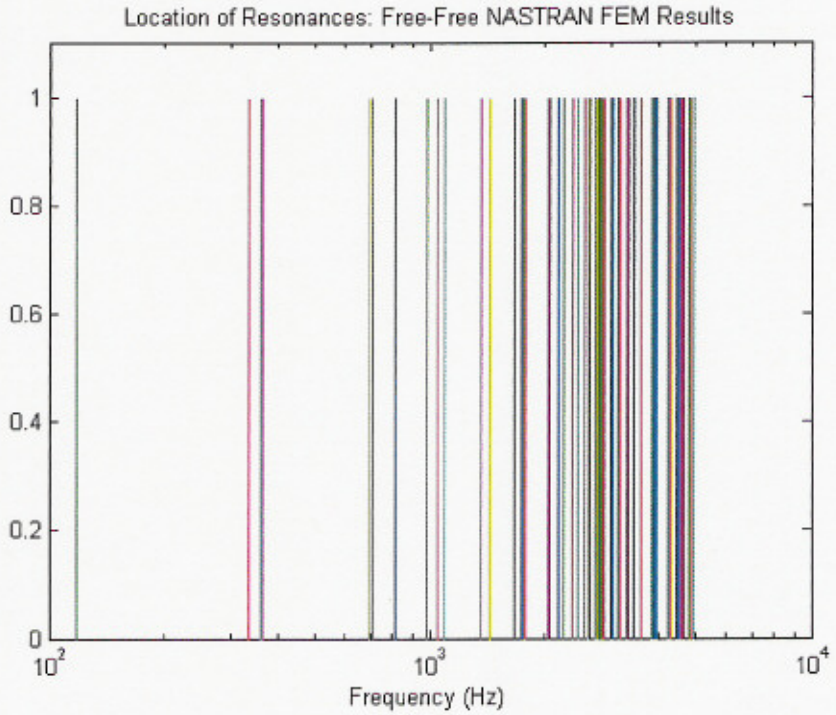

Figure 29: FEA results of fee-free modal calculation. Note the number of resonances at the 4 kHz range.

2.3.4.3. Utilizing the FEA Model for Design

2.3.4.3.1 Effect of Boundary conditions

One of the fist questions to answer with the FEA model is the effect of the boundary conditions on the response of the pipe. This is extremely important since the pipe will be buried in soil in the real application. Also, the type of soil will have a significant impact on how the pipe is supported. It will be worthless to design a sensing and location system that performs well on a suspended pipe system when the real pipe will be buried.

Since the dominant resonances are located in the 4 kHz region, the boundary conditions should not have a massive effect on the results. The FEA model was run with the four corners of each of the rectangular plates fixed. This produced a clamped-clamped boundary condition.

The result of the clamped-clamped analysis is shown in Figure 30. There is a striking resemblance in the high frequency resonances to the free-free condition of Figure 29.

In order to determine the exact differences between the free-free and clamped-clamped conditions, a summary of differences were performed. The result of this difference is shown in Figure 31. It is clear that there is a large difference in the modes at lower frequencies, but around 4 kHz, the difference is only 20%, confirming the suspicion that the pipe will perform similar with different boundary conditions at high frequencies.

Midé is therefore confident that the results presented for the test setup will carry over well for the real system, whether it is above or below ground level. These analyses also indicate that we should concentrate our efforts in the Phase II on the 4 kHz signals.

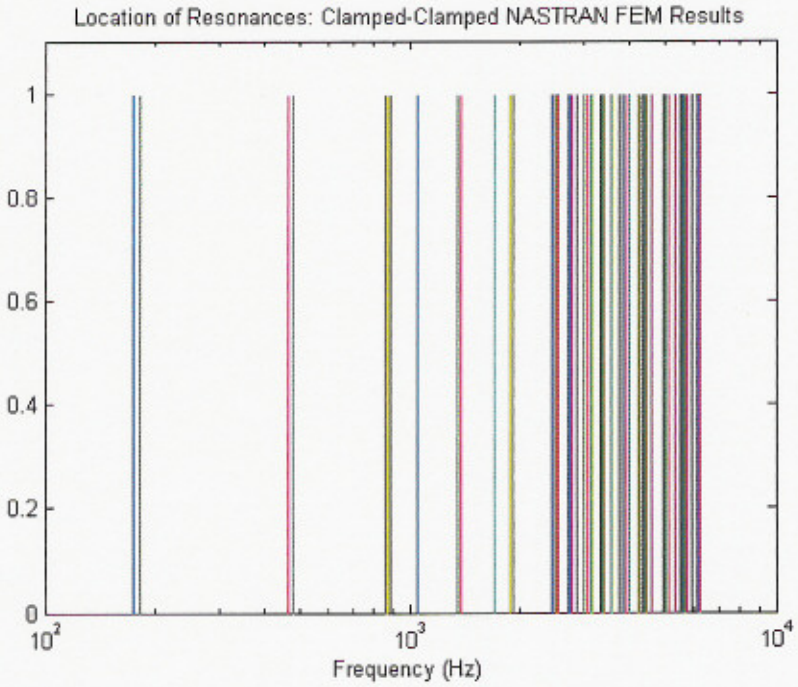

Figure 30: FEA results of clamped-clamped modal calculation. Note the similarities of the high frequency nodes to the free-free calculation in Figure 29.

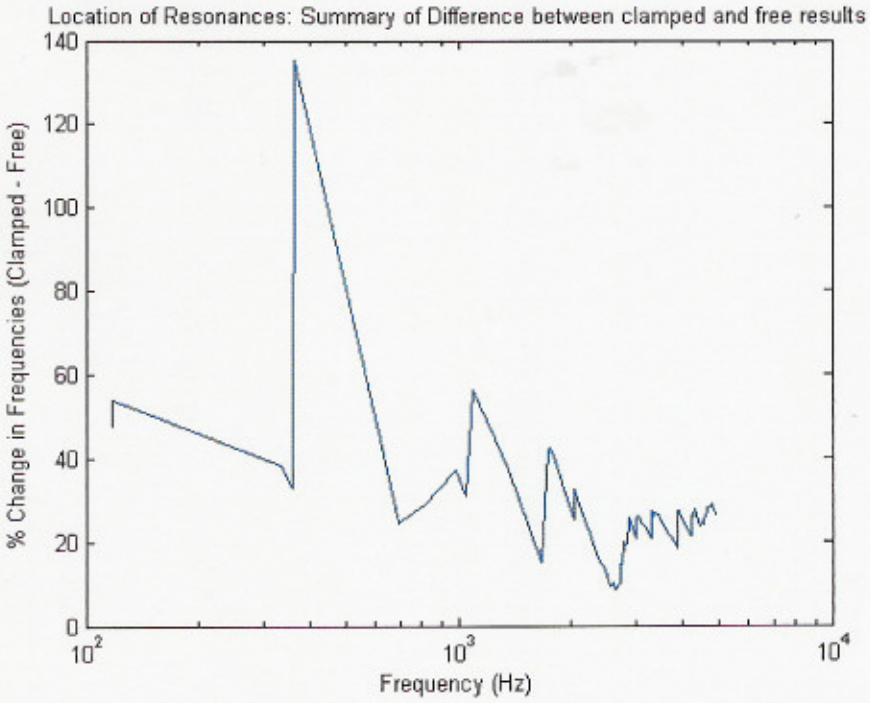

Figure 31: Percentage change in frequencies between the free-free and clamped-clamped conditions as calculated by the FEA model.

2.4. Protocol Development

This task will develop a protocol via which the monitors can communicate to a central processing station. Synchronization, common clocks and other issues will be considered and simulations will be performed.

Preliminary tests indicate that acoustic communications down the length of the pipe is viable (Section 2.3.2.3). A number of options exist for the communications protocol and these options must be compared on the basis of cost, performance and durability.

By cost we imply overall systems cost that include the following:

- Installation on the pipeline. The tradeoff is a complicated system that can be installed with minimal effort versus an inexpensive system that requires a lot of effort to install.

- Power cost. Battery or self propelled. The PowerAct actuator is able to generate moderate amounts of power when exposed to vibrations. The electronics required for such a power-harvesting scheme are more complicated and costly. Conversely a battery system, albeit simple and cheap, requires maintenance. An option exists to have the system wake when a leak event is sensed passively. A thermal battery or equivalent would then be activated to provide the power for computing information and transferring the data down the line. Since the pipe has to be uncovered and fixed in the case of a leak, the battery can be replaced at the same time.

- Data transfer past pipe connections. Connections can pose a problem for acoustic data transfer if they have elastomers for seals. Options to get the data past such seals include optical, acoustic or radio frequency (RF) systems. These need to be evaluated on the metrics of cost and performance. Fortunately, most natural gas pipes are welded to each other, posing few obstacles for high frequency acoustic data transfer.

- Flexibility. Since pipelines are exposed to corrosion, ground shifts and other natural phenomena, their boundary conditions are ever changing. This has the effect of shifting the natural frequency of the system. Since the highest power output to power input ratio for the data transfer system will be at the natural frequency of the system, a flexible system must be able to determine the optimal frequency before the data is sensed. Such a system is possible, but it will come at a cost of complexity, added components and increased power. The added performance must be weighed against these costs.

The protocol development must acknowledge the above factors and attempt to maximize efficiency while minimizing costs.

2.4.1. Communications System Design

Based on the work performed and the results obtained, a high-level system design for the communications protocol can be done. This system consists of two major parts, the sensor and the transmitting station as shown in Figure 32.

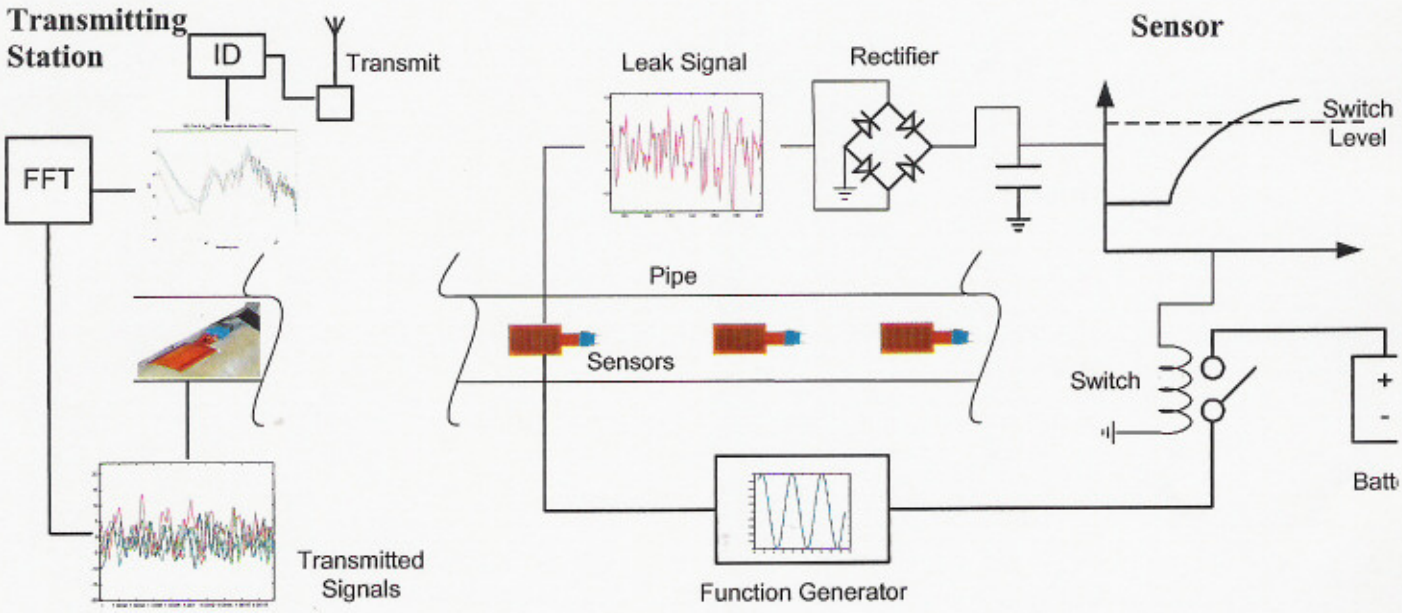

Figure 32: Communications system design. The sensors pick up the leak signal that is rectified to give an increasing DC signal. Once the DC signal is higher than the switch's power on level, the switch closes. A battery provides power to a function generator that powers the PowerAct™ to start acoustic data transfer. At the transmitting stations, the acoustic signals are picked up, analyzed and identified. This data is then transmitted through RF (above ground) to the monitoring stations that alert the relevant personnel.

The detection is done via a PowerAct™ sensor that is permanently mounted on the pipe. These sensors are spaced about 100m apart. When a leak appears, the PowerAct™ generates a voltage over its poles as was shown in Section 2.3.2.2. The voltage is rectified and turned into a direct current signal, without using any power. The voltage over the capacitor continues to build up, until it reaches the switch level. This is the voltage required by the switch to engage.

Once the switch closes, current is transferred from the battery to a function generator. This function generator is pre-programmed to produce a sinusoidal wave at a specific frequency and at high voltage. This specific frequency identifies the sensor that senses the leak. The high voltage signal is fed back to the PowerAct™ and now it is used as an actuator to generate its unique frequency in the pipe. The acoustic signal is broadcasted down the pipe as was shown in Section 2.3.2.1.

The acoustic wave traveling down the pipe will be picked up by all the other PowerAct's in the line between the original sensor and the transmitting station and will set them off as well. This will ensure that a considerable amount of acoustic energy will be forced into the pipe.

A transmitting station will sense all the frequencies coming down the line. The transmitting stations will be placed as far apart as possible, while maintaining functionality, because they need continuous power and also have an antenna that must be above ground. As the transmitting station senses the acoustic frequencies on the pipe, it will generate an FFT (Section 2.3.3.1). This FFT will identify the dominant frequencies that in turn will pinpoint the sensors that have been activated. It is expected that two stations will report leaks, thereby identifying the location of the leak between them. It is possible to pinpoint the leaks exactly by looking at the specific frequencies or arrival times of the signals.

The information about the leak gathered by the transmitting station will be sent via RF link to a base station. The transmitting stations communicate with each other to relay the information to the base station. Here the information about the location of the leak can be used to shut the pipeline down and send out emergency crews. It is envisioned that a whole pipe section in the vicinity of the leak will be dug up. During this operation, the batteries of the sensors that reported the leak can be replenished.

The only part of this system that will require continuous power is the transmitting stations. Since the reporting station will need at least its antennae above ground, its power supply can also be above ground. This supply can then be wall, solar or battery power, adding flexibility to the system so that the most cost effective solution can be realized.

2.5. System Design and Costing

This task will design and cost a complete leak monitoring system. This will be the system that will be fabricated and tested in Phase II.

This section will attempt to address the overall systems cost as decisions on the options from the previous sections are made. Overall systems cost includes some items that was not part of the Phase I effort. An estimation of the cost of these components will be made.

2.5.1. Bill of Materials

The bill of materials to complete the system is given in Table 6. This table is based on a few assumptions:

- The PowerAct™'s are spaced 100 meter apart.
- The Base Stations are 1 km apart.
- The system is built for the 230,000 km of interstate natural gas pipeline in the U.S.

Table 6: Cost estimate of the Midé system per km of pipeline.

Item Description	Cost/Unit	# Units / km	Total
Sensor			
PowerAct™	$2	10	$20
Rectifier and Switch	$8	10	$80
Function Generator	$12	10	$120
Lithium Ion Battery	$3	20	$30
Transmitting Station			
A/D Converter and Programmable Integrated Circuit (PIC)	$15	1	$15
RF Transmitting / Receiving Hardware – 1 km	$50	1	$50
Battery	$5	1	$5
		Grand Total / km	**$320**

2.5.2. PowerAct™

The PowerAct™ actuators used for this program were chosen because they are built on the concept of a very inexpensive product that was commercially sold to an OEM customer between 1999 and 2002. This product sold for under $3 a piece in volumes of 500,000 a year. However, since the PowerAct has the extra manufacturing process of laser machining to obtain conformability, this price might increase. The overall cost of the actuator is not expected to exceed $6 in quantity. As the system design matures, it will be possible to better estimate this component cost.

2.5.3. Actuator cost and performance

A comparison of different packaged piezoelectric actuators was performed. The objective of this effort was to compare the current commercially available packaged strain actuators – QuickPack, QuickPack IDE, PowerAct and MFC – in terms of performance, reliability, manufacturability and cost. These actuators are shown in Figure 33

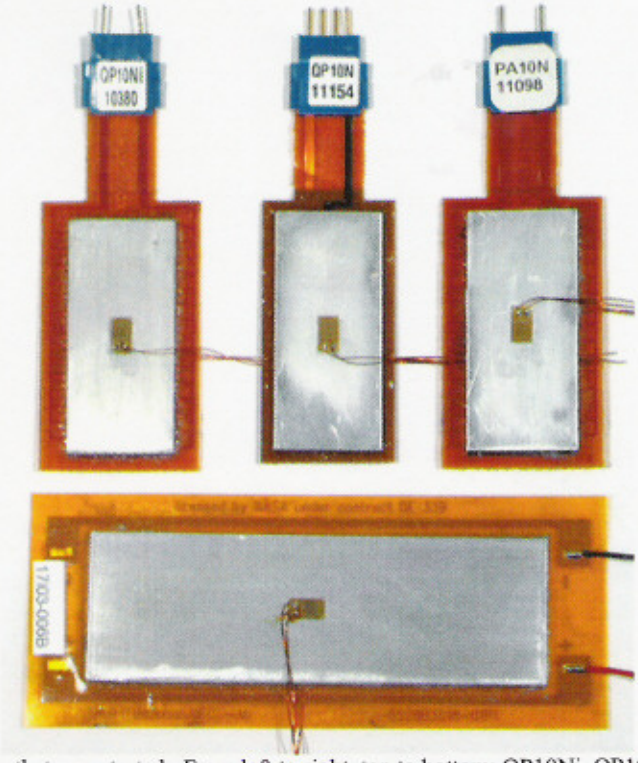

Figure 33: The actuators that were tested. From left to right, top to bottom: QP10Ni, QP10N, PA10N, MFC8528

Table 7 lists the different actuators, their characteristics and the type of substrates used for each actuator test. The table differentiates between the actuators on the basis of volume, actuation type and conformability. A short explanation of interdigitzed (IDE) versus traditional actuation and conformability will now be presented.

By convention, the direction of polarization in a piezoceramic defines the "3-axis". Traditional strain actuators like the QuickPack® and PowerAct™ use piezoceramic wafers poled through their thickness, with voltage applied also through the thickness. When these devices are bonded to a surface, actuation is in the plane of the wafer through the so-called "d_{31}" effect. In this case, the applied electric field couples equally to piezo actuation in both in-plane directions ($d_{31} = d_{32}$). The second type of actuator has inter-digitized electrodes (IDE) so that both the poling (3-axis) and the applied electric field are oriented down the length of the piezoelectric wafer. In this case, the applied electric field couples to piezo actuation along the length of the device according to d_{33}, and transversely according to d_{31}. For typical ceramics, $d_{33} \approx -3d_{31}$. These actuators, including the QuickPack® IDE and the MFC, take advantage of the more efficient electromechanical coupling in the 3-axis to provide greater actuation performance along their length.

The second metric of distinction between the four actuators considered here is their conformability. Piezoelectric wafers are brittle and break easily when bent. Packaging the monolithic piezoceramic element protects it from damage and crack propagation, but it still impractical to bond such an actuator to a curved surface. Removing some of the piezoceramic material in the actuator and replacing it with softer epoxy can form a composite material that has the ability to absorb more strain than the piezoceramic alone. This type of actuator can then be bonded to curved surfaces because it has the ability to conform to the shape of the surface. This type of composite actuator, including the PowerAct™ and MFC, will be referred to as a "conformable actuator" in this paper.

Table 7: Actuators used for comparative tests

Actuator	Aluminum substrate total thickness (in.)	Size of active area (in.)	Thickness of active material (in.)	Active material of frontal area	IDE / Tradi-tional	Conform-ability
QP10Ni	0.002 0.060	1.81 × 0.81	0.010	100%	IDE	None
QP10N	0.002 0.060	1.81 × 0.81	0.010	100%	Trad.	None
PA10N	0.002 0.060	1.81 × 0.81	0.010	88%	Trad.	Yes
MFC 8528	0.002 0.060	3.4 × 1.1	0.007	90%	IDE	Yes

These actuators were compared on the basis of stress and strain produced at a specific field density. The field density of 20 V/mil represent the maximum amount that will ensure high fatigue performance under high stress and strain conditions such as those expected on a pipeline. Figure 34 shows the result of the comparison. Midé's QP10Ni actuator produces the largest amount of stress and strain for a given field density.

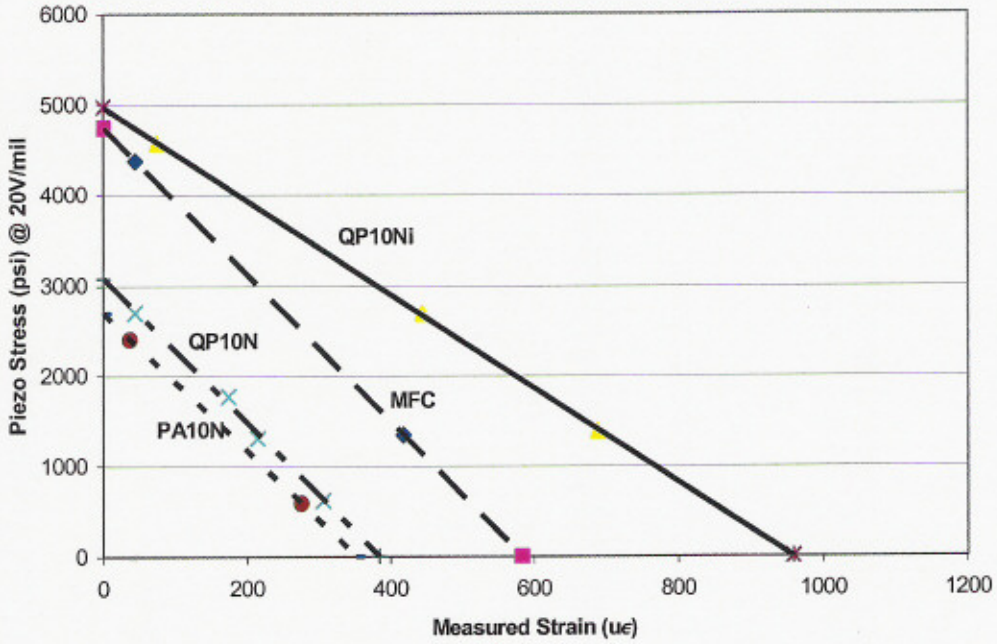

Figure 34: Piezo stress versus measured strain for 20V/mil field.

Table 8: Ranking of Commercial Packaged Strain Actuators

Trade Name:	QuickPack		PowerAct	MFC
PZT Element:	Wafer		Laser-Machined Wafer	Diced Wafer
Actuation Mode:	31	33	31	33

Authority per unit thickness…				
• principal strains in actuated structure having same sign:	1	4	3	2
• principal strains in actuated structure having opposite signs:	4	1	3	2
Feasibility of thick actuator (high force)	1	2	3	4
Conformability	4	4	2	1
Ease of electrical drive	1	4	1	2
Ease of fabrication	1	2	3	4
Overall technical maturity	1	2	3	3

Table 8 compares the actuators on other metrics. Short explanations of each of these metrics follow below:

Authority: While d_{33} is significantly larger, in the absolute sense, than d_{31}, real applications of packaged strain actuators involve two in-plane dimensions. In the classic application of controlling bending in a metallic cantilever beam, the desired pattern of the induced strain is very similar to the natural actuation pattern of the d_{33} actuator. The ratio d_{31}/d_{33} is very nearly equal to the Poisson ratio of metals like aluminum, so the IDE actuation couples very well into the strain field of the actuated structure. Traditional actuators, on the other hand, naturally expand in the transverse direction when expanding in the longitudinal axis, working against the natural transverse deformation of the bending beam and reducing the actuation effectiveness. But in more complex structures it is possible that the deformation of interest is associated with in-plane strains that have the same sign. This has been shown to be true, for example, on the vertical tails of the F/A-18 and F-22 aircraft in their first mode of vibration. In this case, d_{31} actuators can be as effective, if not more effective than d_{33} actuators· The rankings in the table for the PowerAct and MFC reflect their relative ineffectiveness at inducing stress and strain in the transverse direction due to the partial or total segmentation of the active element.

Thickness: In applications of packaged strain actuators requiring high forces, the use of d_{33} may not suffice. It may also (or alternatively) be necessary to use a thick PZT wafer. While it is always possible to achieve a given total thickness of PZT by using multiple layers, this is undesirable due to increased cost and loss of strain transfer through intervening packaging layers. In active applications, the increased voltages mitigate against this, but in passive damping applications thicker can be better. (For example. 0.060 inch thick wafers in the d_{31} configuration were used for the ACX ski damper) The traditional monolithic d_{31} configuration used in the QuickPack is most amenable to thick wafers.

Conformability: Conformability is desirable in a number of applications, particularly those involving shafts (like golf clubs). The MFC, with its completely diced elements, is the preferred technology under this criterion. PowerAct, with partially machined elements, follows behind. The QuickPack and QuickPack IDE do not apply well to surfaces with small radii of curvature. Anecdotally, QuickPack actuators were found to be flexible enough to conform to the surface of a full-scale F/A-18 vertical tail.

Electrical Drive: The IDE devices tend to require larger drive voltages to achieve similar electric fields. The QP10Ni uses voltages up to 1,200V, due to the 0.060 inch center-to-center spacing of its electrode lines. (This 6 to 1 ratio of spacing to PZT wafer thickness was chosen to maximize performance at the lowest possible voltage.) The MFC uses up to 1,500V due to the bias-and-overdrive scheme selected, but in the table above we have assumed 20 V/mil peak drive, or 400V. (If the MFC used the more efficient 6 to 1 ratio, 3kV would be required to achieve the maximum +75V/mil field specified for this device.) In any case, the cost, and often

the size of electronic components increases when rated for more than 100 to 200 volts. For overall system cost-effectiveness – including actuator and drive electronics – in high volume applications (such as automotive), IDE actuators may not be practical.

Fabrication: The true cost of packaged strain actuators is most likely not reflected in the low-volume sample prices published by the manufacturers. Low volume production can be labor-intensive, and great variability is possible in both the vendor cost agreements negotiated, as well as the amount of profit margin desired or required to achieve a particular business goal. While a given manufacturer will not publicize the costs associated with producing its products, it is possible to analyze qualitatively, in terms of manufacturing steps required, the true costs of the four packaged strain actuators considered here.

- Take the QuickPack as the baseline.
- QuickPack IDE requires the additional step of poling, which takes time and reduces end-to-end manufacturing yield.
- PowerAct requires the extra step of laser machining of the wafer part of the way through its thickness, which is likely slightly more costly (in low volume, at least) than the IDE poling.
- MFC requires a several-step process of dicing, and teardown of the dicing setup, as well as the IDE poling step. The poling yield, however, should be somewhat better than in the QP10Ni due to the reduced poling voltages required due to the smaller electrode spacing.

By this argument, with all else being equal the QuickPack actuator should be the cheapest to produce.

Figure 35 shows the available pricing data on the various technologies. The low-volume (up to 15 units) data points represent the average published "catalog" prices, on a per-unit-area basis. The QP10Ni is included in the QuickPack average, but none of the many 2-layer QuickPack catalog products are included in that average. By the argument above, the fact that the MFC is slightly less expensive than the QuickPack® does not reflect an inherent cost advantage of the MFC technology.

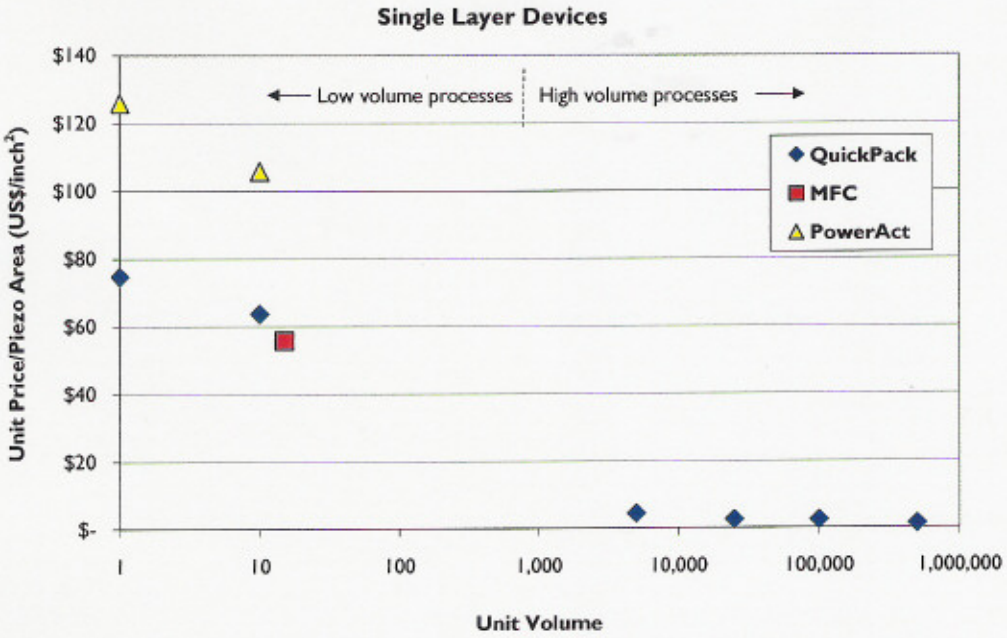

Figure 35: Pricing data for commercially available packaged strain actuators.

At high volumes, with more severe downward pressure on prices, it might be expected that unit prices more accurately reflect the actual costs to produce the product. However, the only product currently used in high volume applications is the QuickPack®, so no meaningful quantitative price comparison is not possible.

Reliability: As with cost, it is impossible to compare the various devices meaningfully in terms of reliability. Only the QuickPack® has been used widely enough to accumulate significant field data. To date, more than one million QuickPack® devices have been fielded, with an extremely low rate of field returns. The QuickPack® is the most mature of the commercially available packaged strain actuator technologies.

The QP10Ni is thus the preferred actuator for applications such as leak detection and data transfer in pipes. The only drawback of this actuator is that it is non-conformable. This means that a flat surface needs to be created on the pipe for it. Although this can be done, it will increase installation costs. Midé is currently developing a conformable actuator that has the performance of the QP10Ni and is conformable. In this form, the actuator will have the highest performance, the lowest manufacturing cost, the highest reliability and the lowest installation cost. This product, the PA10Ni, will soon be commercially available.

2.6. References

1. Hunaidi, Osama and Chu, Wing T. "Acoustical Characteristics of Leak Signals in Plastic Water Distribution Pipes", Applied Acoustics, Volume 58 (1999), pp.235-254.

2. Pilkey, Walter D. Formulas for Stress, Strain, and Structural Matrices. New York. John Wiley & Sons, 1994.

3. The vibration of a fixed-fixed string. 26 Jan 2004. http://www.gmi.edu/~drussell/Demos/string/Fixed.html

4. D. B. Sharp and D. M. Campbell (1997), "Leak detection in pipes using acoustic pulse reflectometry," Acustica (1997), 83(3), pp.560-566.

5. Jinguji, M., Imaizumi, H., Kunimatsu, S., Isei, T., "Fundamental Study on Leak Detection of UnderGround Gas Pipeline Using Passive Acoustic Method", Proceedings of the 96th Conference of the Society of Exploration Geophysicists of Japan; Tokyo, Japan (1997), pp. 174-176

6. Famiglietti, M.; Scandolo, D.; Tonolini, F.; Ghia, S., Regis, V., "Leak detection by acoustic emission monitoring in power plant high pressure preheaters", 2001

7. Morishita, Y., Mochizuki, H., Watanabe, K., Nakamura, T., Nakazima, Y., Tamauchi, T., "Development of Leak detection system using high temperature-resistant microphones", Journal of Nuclear Science and Technology, Vol. 32, No. 3, (1995), pp 237-244

8. Pretorius, J, Hugo, M, Spangler, R, "A Comparison of Packaged Piezoactuators for Industrial Applications", presented at the SPIE 11th Annual International Symposium on Smart Materials and Structures, 14-18 March 2004.

3. Appendix

3.1. Appendix A: Preliminary FEA

Mode	Frequency (Hz)	Figure #
1	1581.4	Figure 36
2	1581.5	Figure 37
3	3622.3	Figure 38
4	3622.5	Figure 39
5	3726.2	Figure 40
6	4440.1	Figure 41
7	4446.2	Figure 42
8	4942	Figure 43
9	4943.7	Figure 44
10	5629.5	Figure 45
11	5632.4	Figure 46
12	5948	Figure 47
13	6132.8	Figure 48
14	6133.3	Figure 49
15	6681.8	Figure 50
16	6683	Figure 51
17	7264.8	Figure 52
18	8200.6	Figure 53

19	8200.7	Figure 54
20	8877.3	Figure 55
21	8877.7	Figure 56
22	9943.9	Figure 57
23	9946.1	Figure 58
24	11327	Figure 59
25	11455	Figure 60
26	11455	Figure 61
27	11615	Figure 62
28	11711	Figure 63
29	11711	Figure 64
30	12009	Figure 65

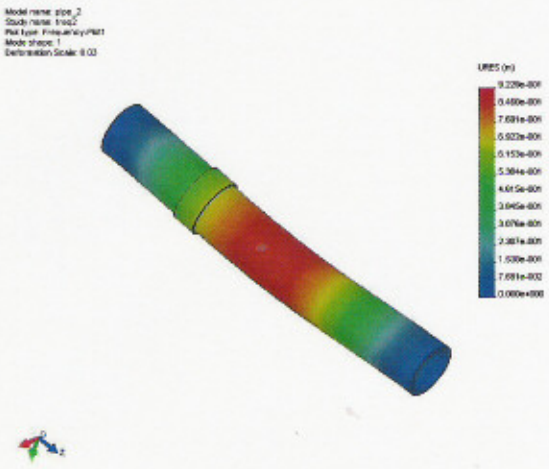

Figure 36 - Mode 1

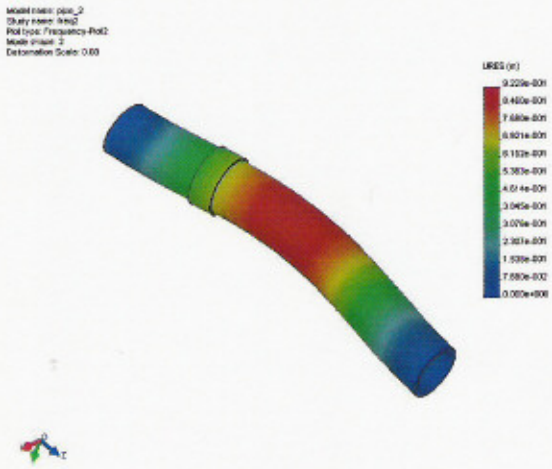

Figure 37 - Mode 2

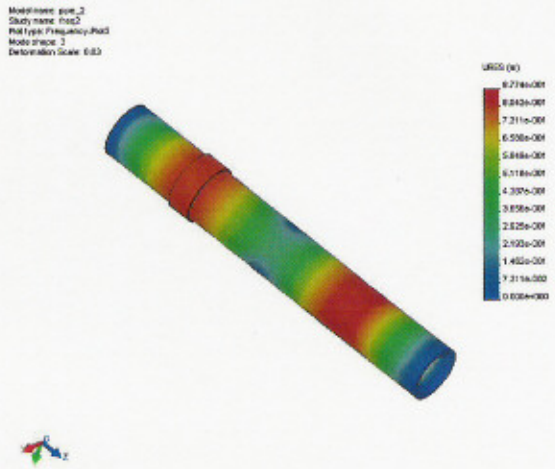

Figure 38 - Mode 3

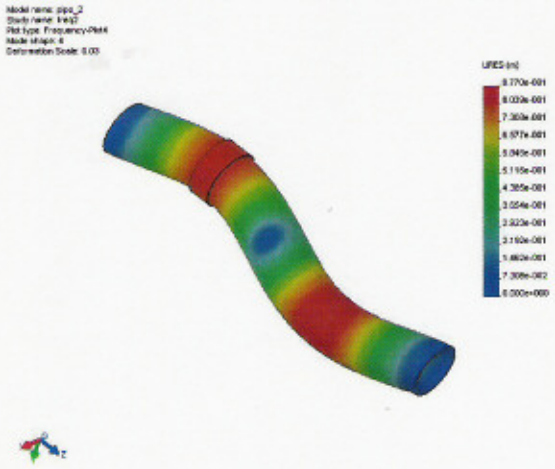

Figure 39 - Mode 4

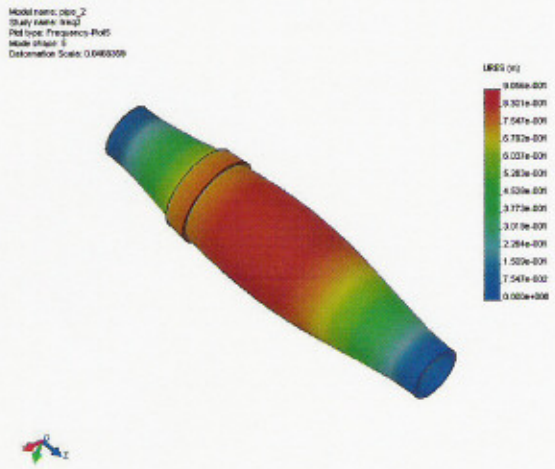

Figure 40 - Mode 5

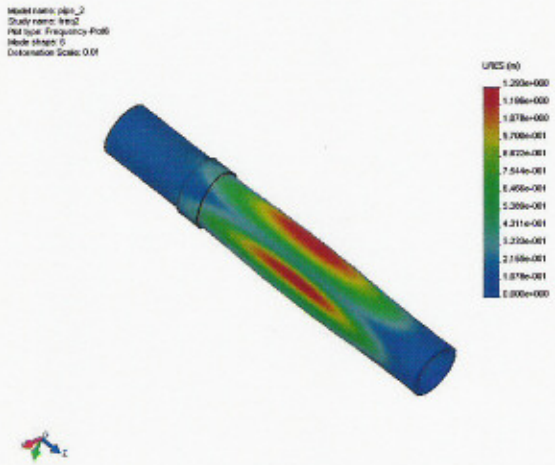

Figure 41 - Mode 6

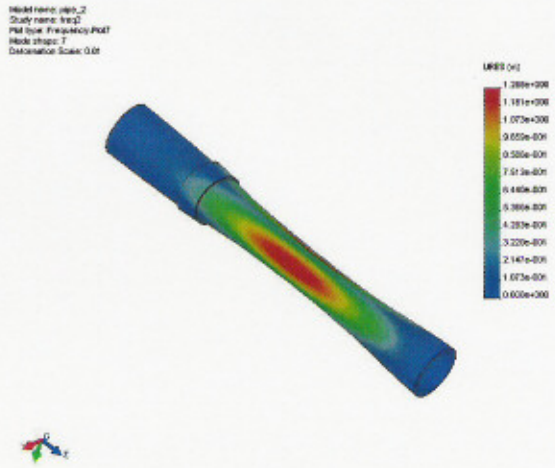

Figure 42 - Mode 7

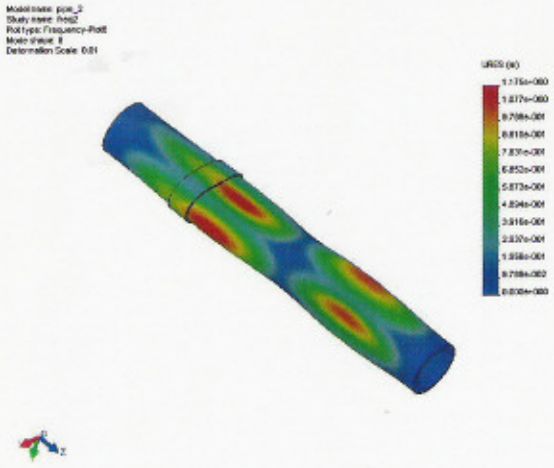

Figure 43 - Mode 8

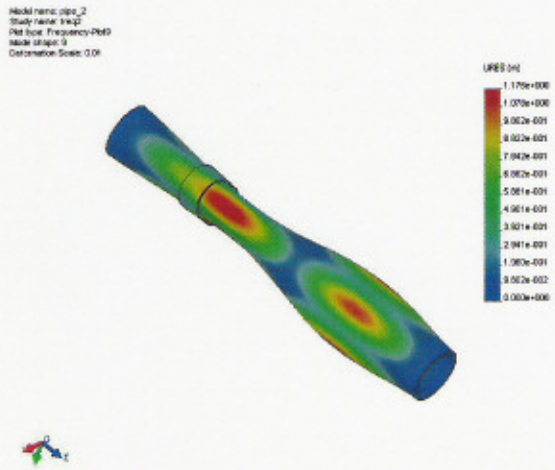

Figure 44 - Mode 9

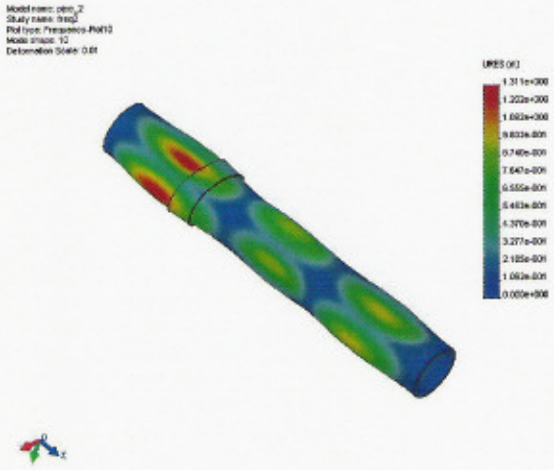

Figure 45 - Mode 10

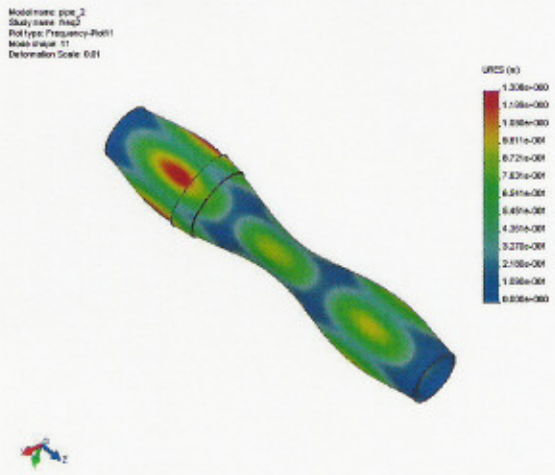

Figure 46 - Mode 11

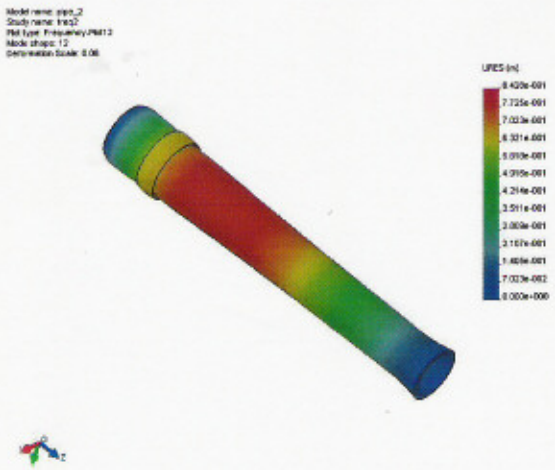

Figure 47 - Mode 12

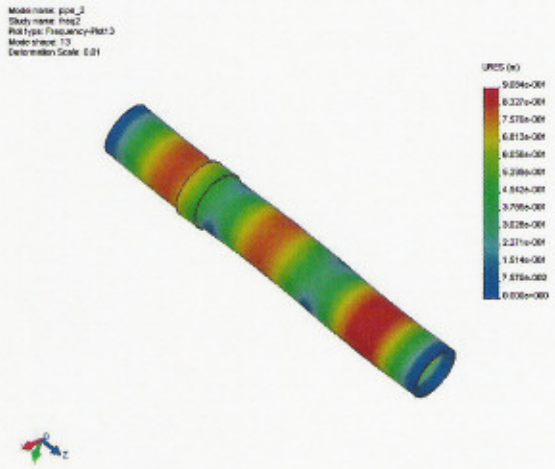

Figure 48 - Mode 13

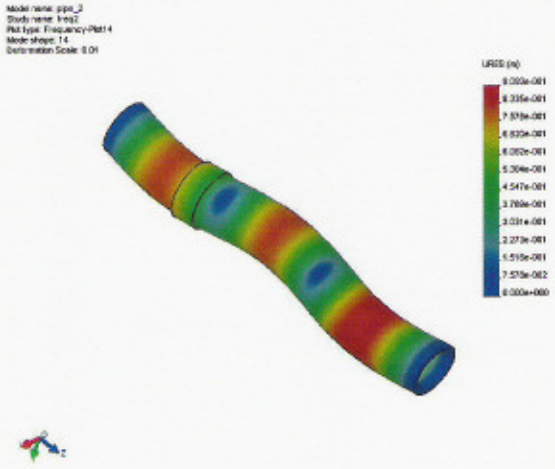

Figure 49 - Mode 14

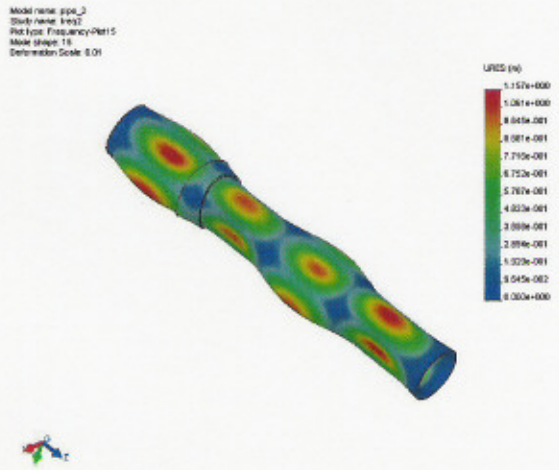

Figure 50 - Mode 15

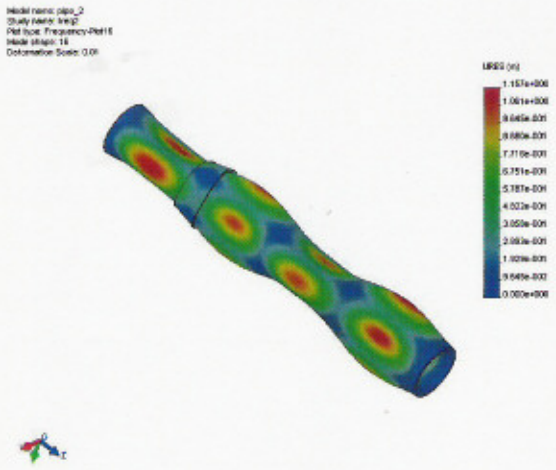

Figure 51 - Mode 16

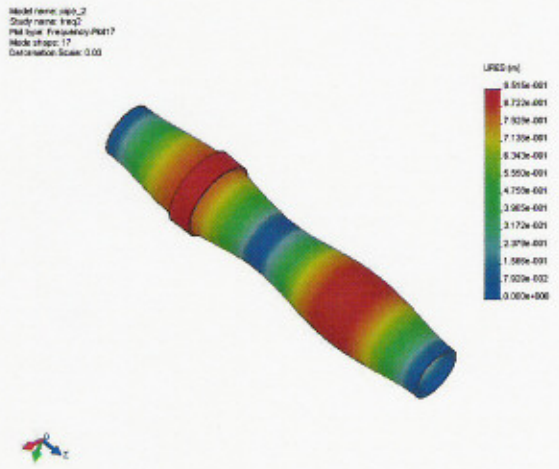

Figure 52 - Mode 17

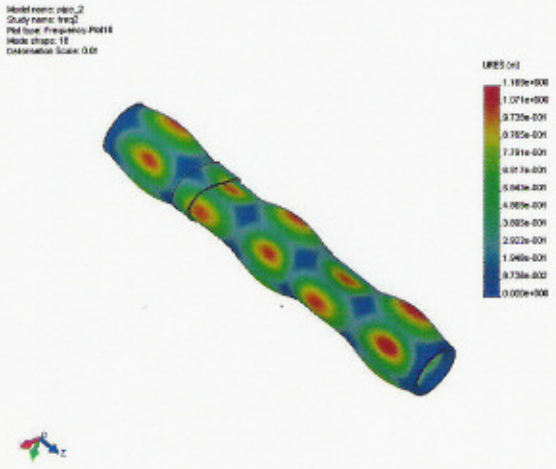

Figure 53 - Mode 18

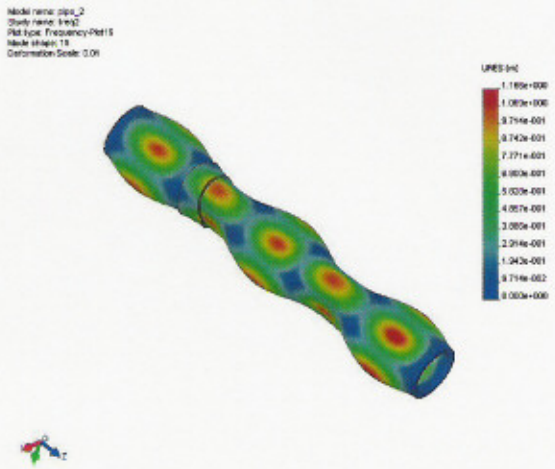

Figure 54 - Mode 19

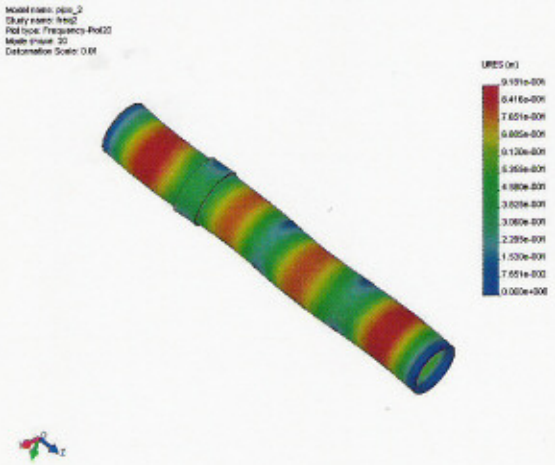

Figure 55 - Mode 20

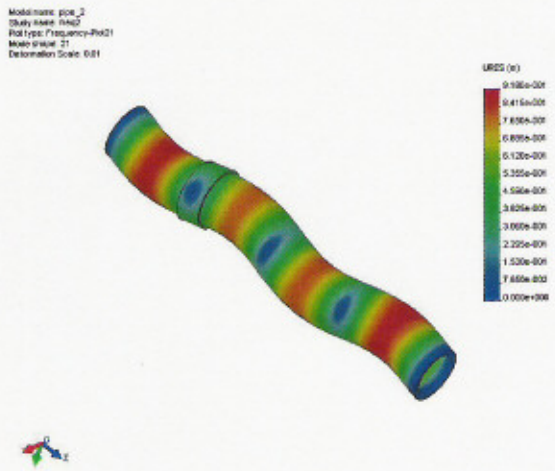

Figure 56 - Mode 21

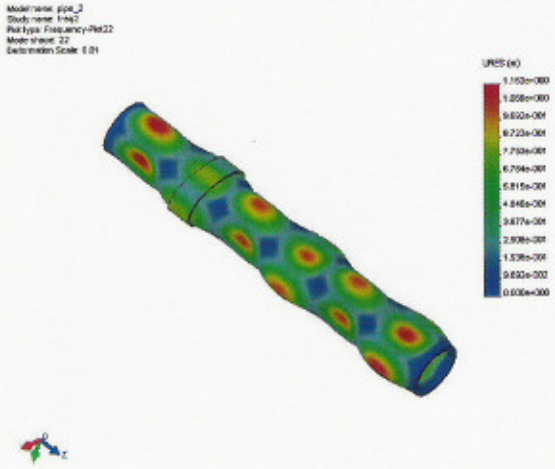

Figure 57 - Mode 22

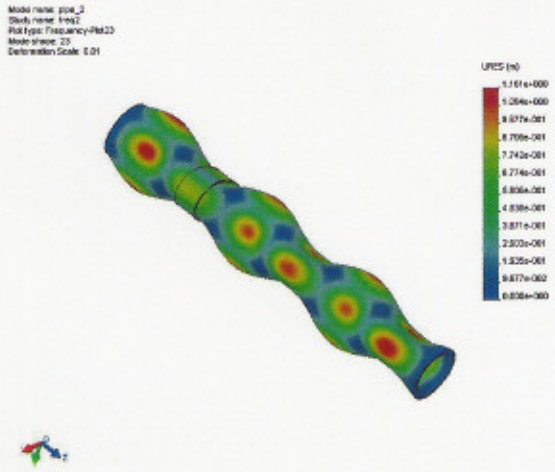

Figure 58 - Mode 23

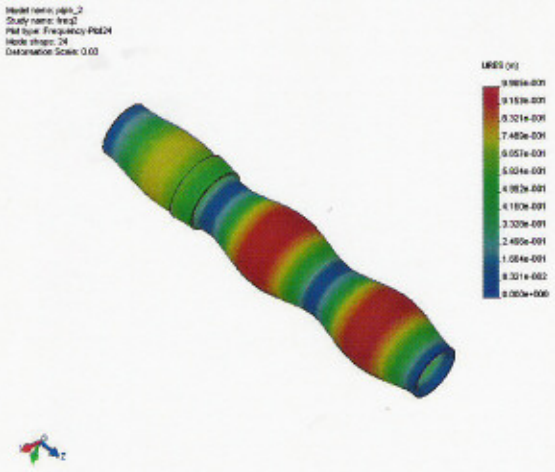

Figure 59 - Mode 24

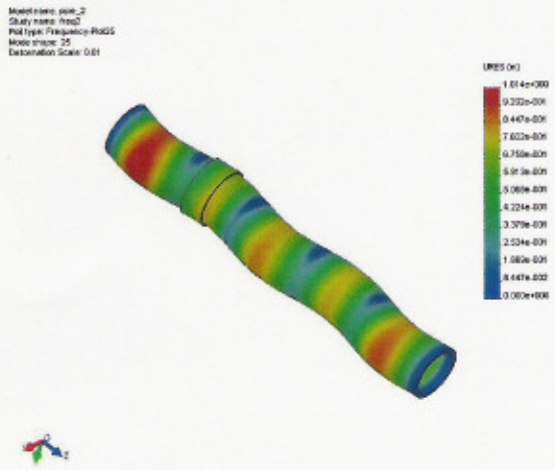

Figure 60 - Mode 25

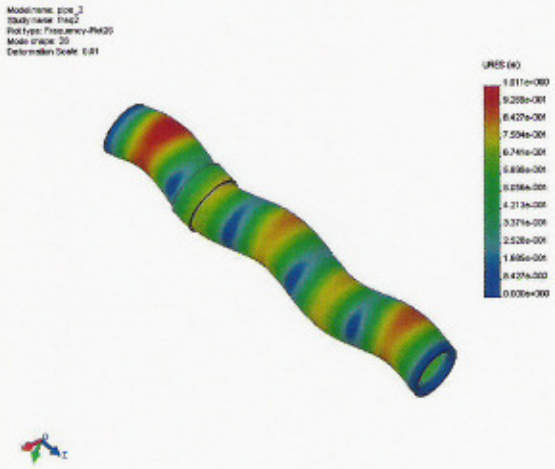

Figure 61 - Mode 26

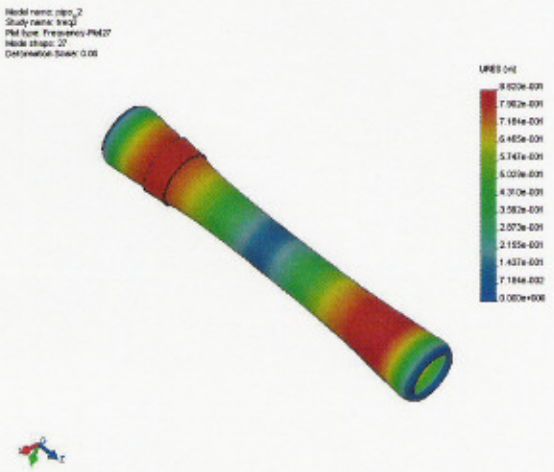

Figure 62 - Mode 27

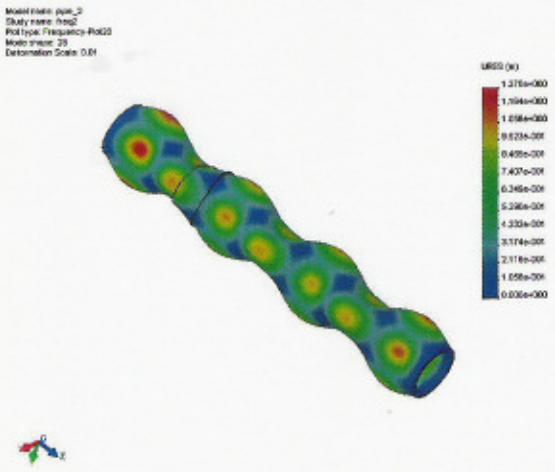

Figure 63 - Mode 28

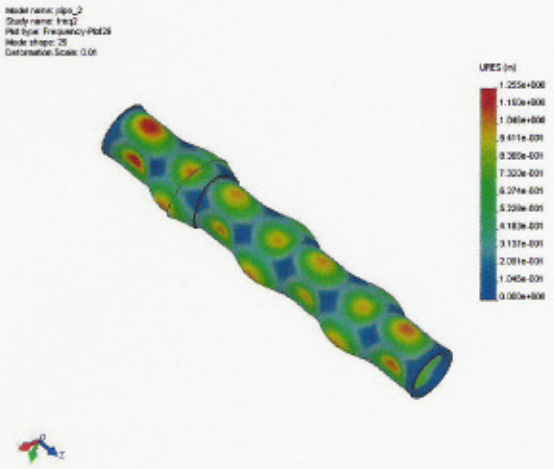

Figure 64 - Mode 29

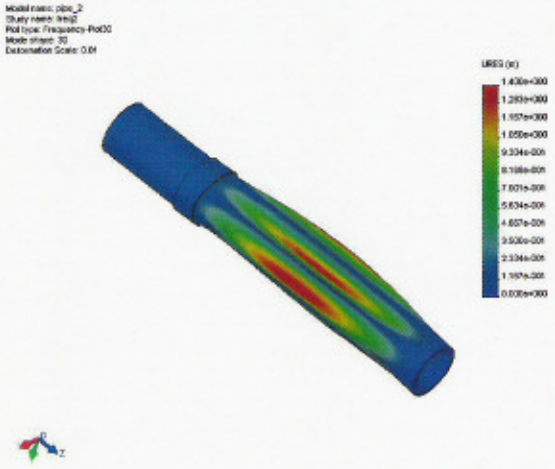

Figure 65 - Mode 30

3.2. Appendix B: Test Results

3.2.1. Auto-Spectra and Power Spectral Density Results

This section presents the Auto-Spectra (FFT) and Power Spectral Densities (PSD) of the measured sensor outputs. When the "leak" and "no-leak" results are compared, it is clear that leaks are detectable. It is also clear that the sensor outputs increase with increased pressure and size of leak. These conclusions are also supported by the results presented in the next section.

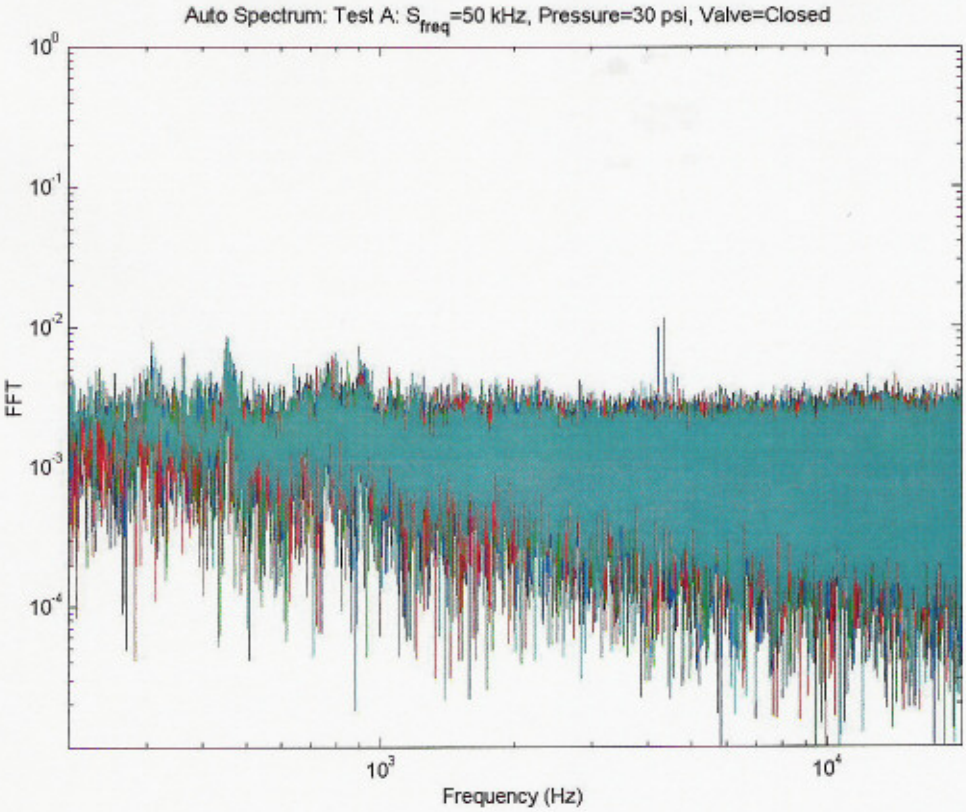
Auto Spectrum: Test A: S_{freq}=50 kHz, Pressure=30 psi, Valve=Closed
10^0
10^{-1}
10^{-2}
10^{-3}
10^{-4}
FFT
10^3
10^4
Frequency (Hz)

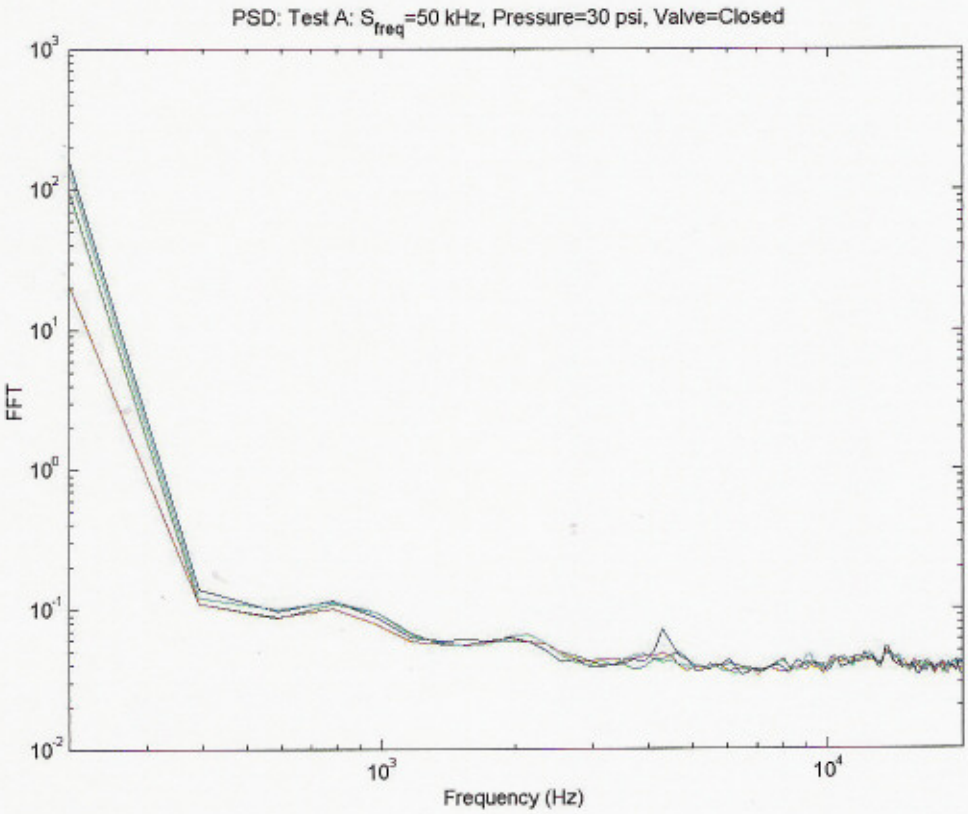
PSD: Test A: S_{freq}=50 kHz, Pressure=30 psi, Valve=Closed
10^3
10^2
10^1
10^0
10^{-1}
10^{-2}
FFT
10^3
10^4
Frequency (Hz)

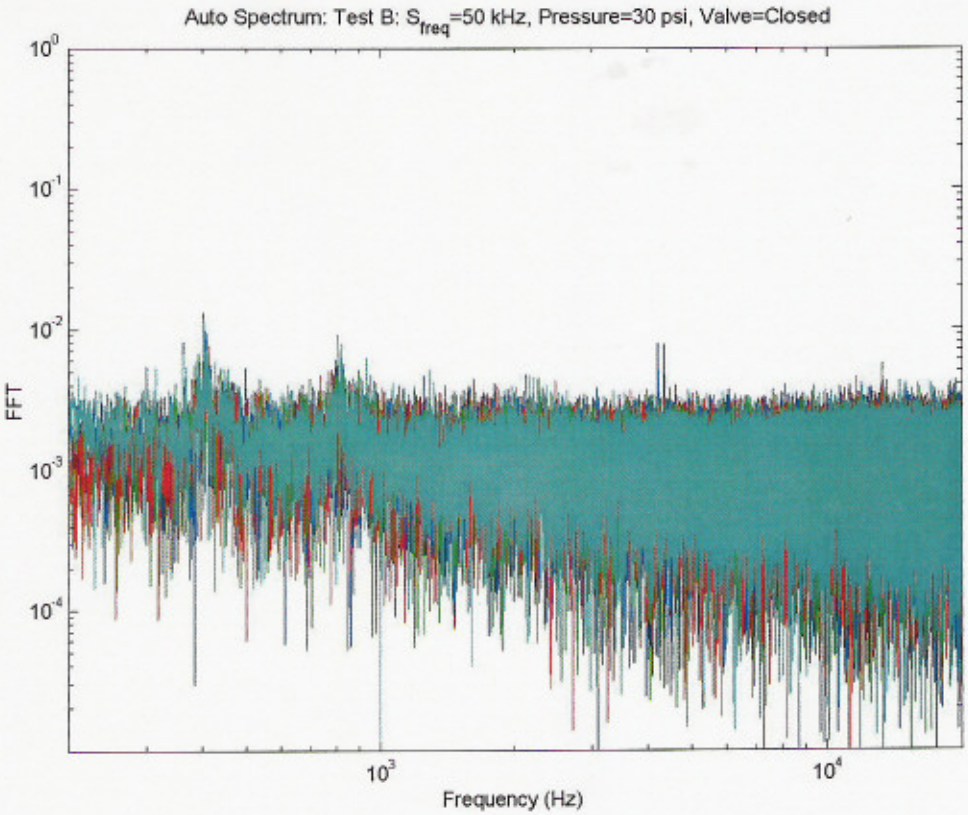
Auto Spectrum: Test B: S_{freq}=50 kHz, Pressure=30 psi, Valve=Closed
FFT
Frequency (Hz)

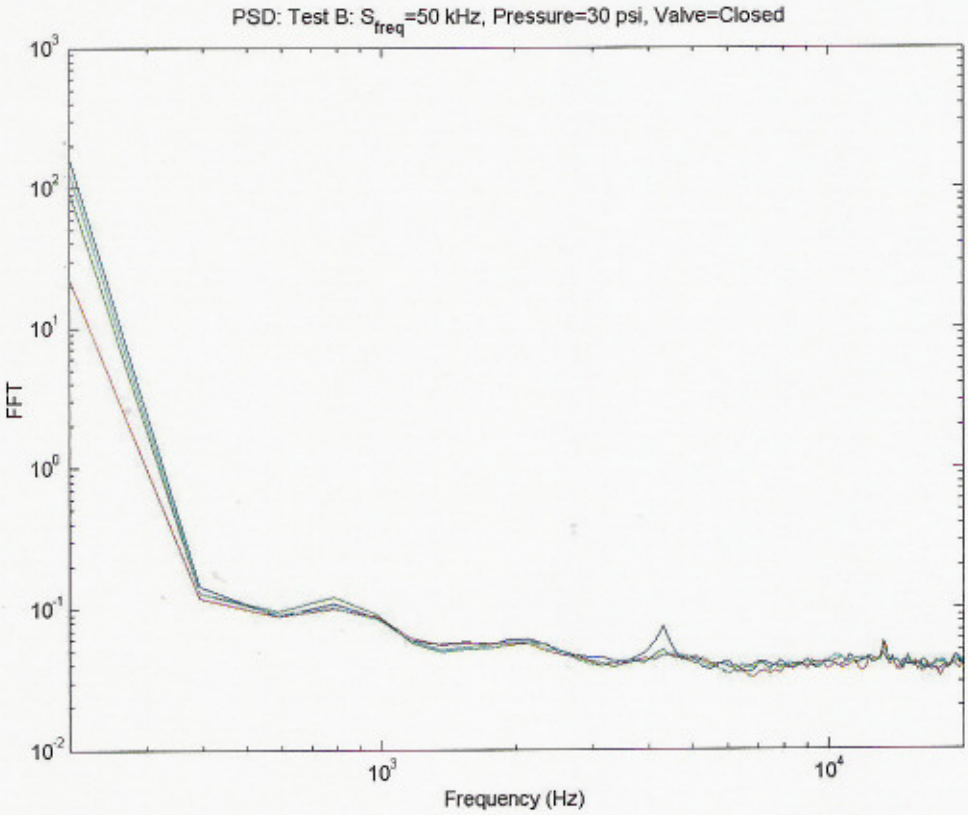
PSD: Test B: S_{freq}=50 kHz, Pressure=30 psi, Valve=Closed
FFT
Frequency (Hz)

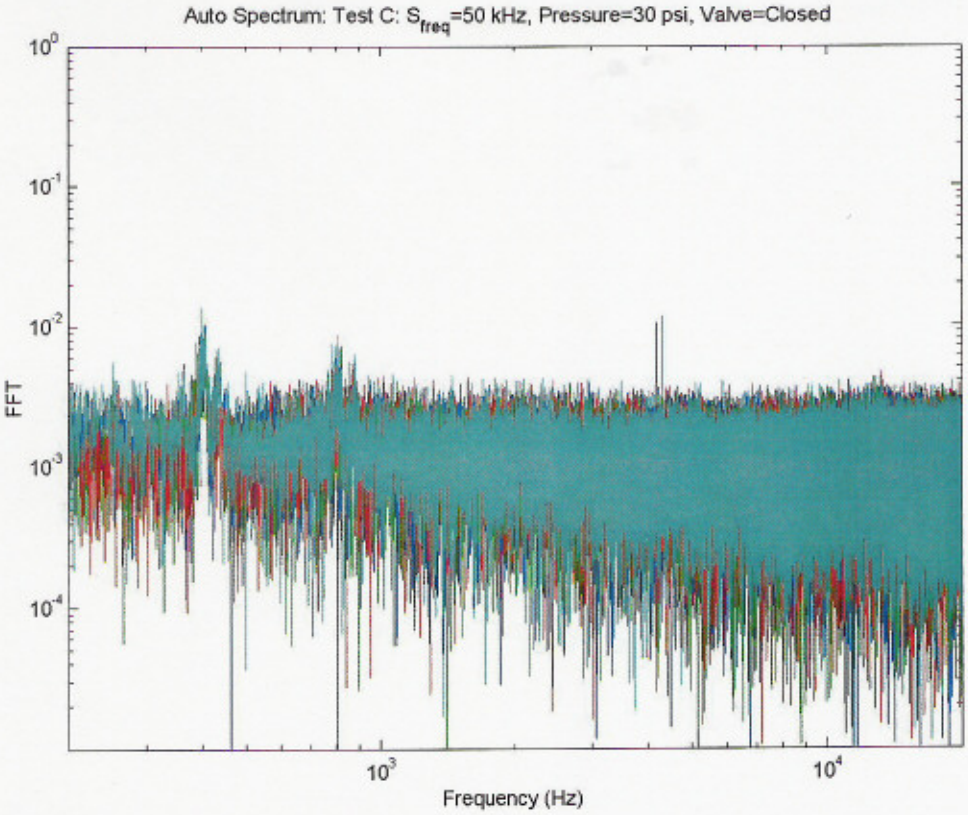
Auto Spectrum: Test C: S_{freq}=50 kHz, Pressure=30 psi, Valve=Closed
FFT
Frequency (Hz)

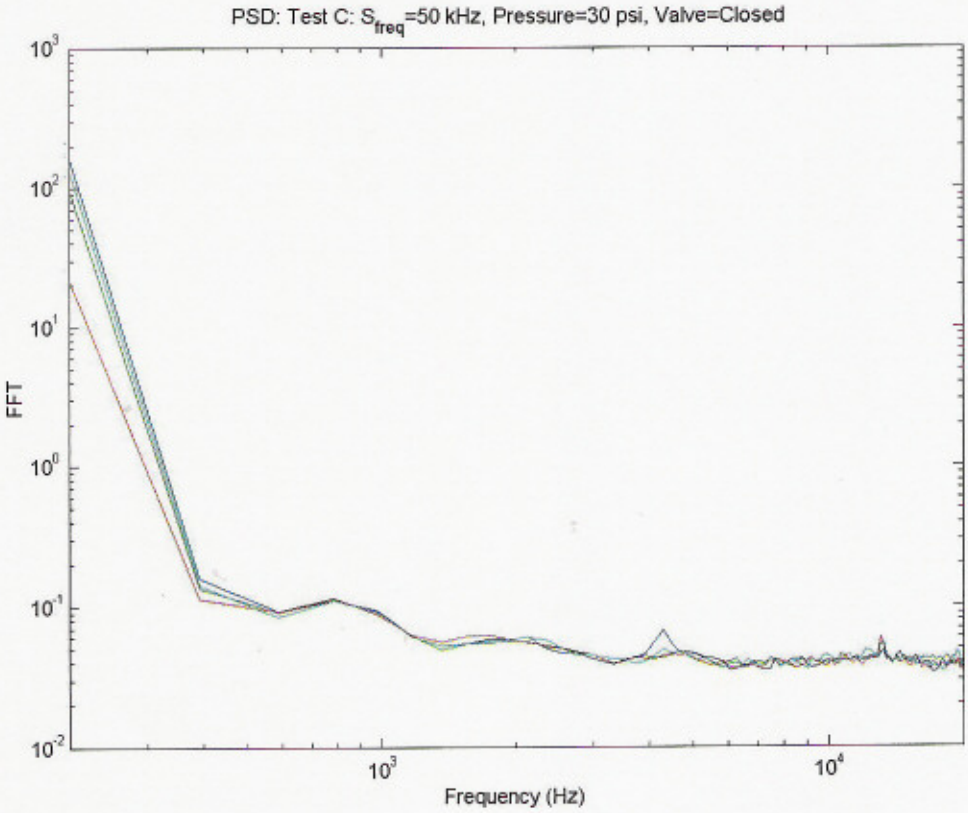
PSD: Test C: S_{freq}=50 kHz, Pressure=30 psi, Valve=Closed
FFT
Frequency (Hz)

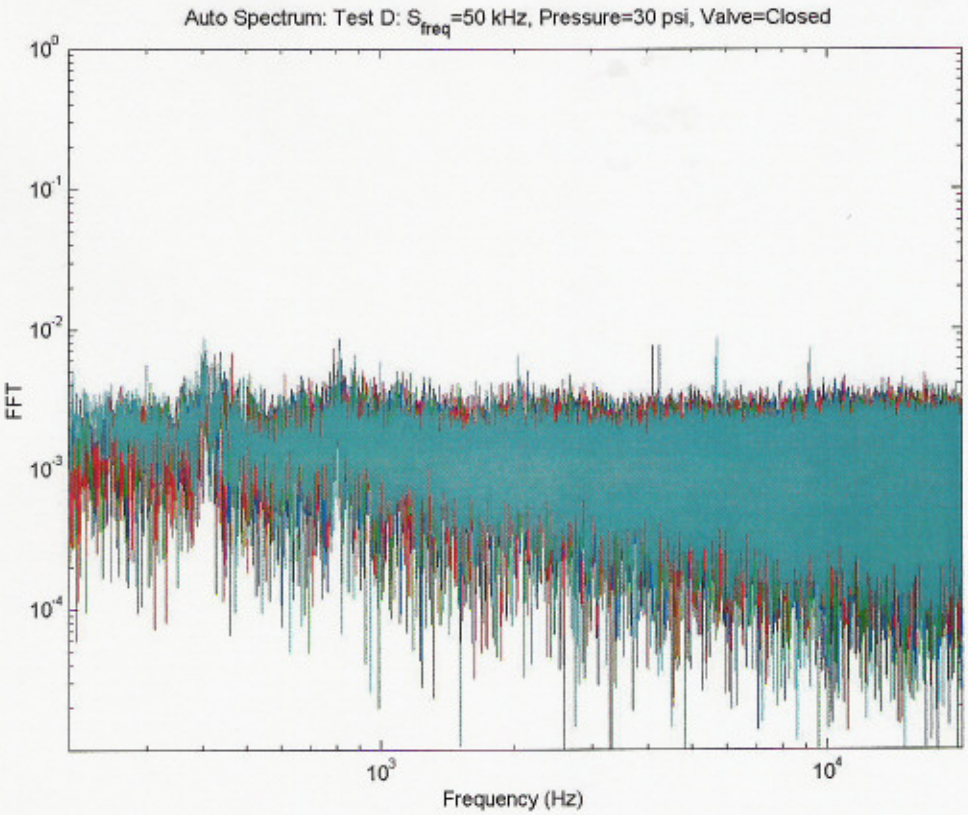
Auto Spectrum: Test D: S_{freq}=50 kHz, Pressure=30 psi, Valve=Closed
FFT
Frequency (Hz)

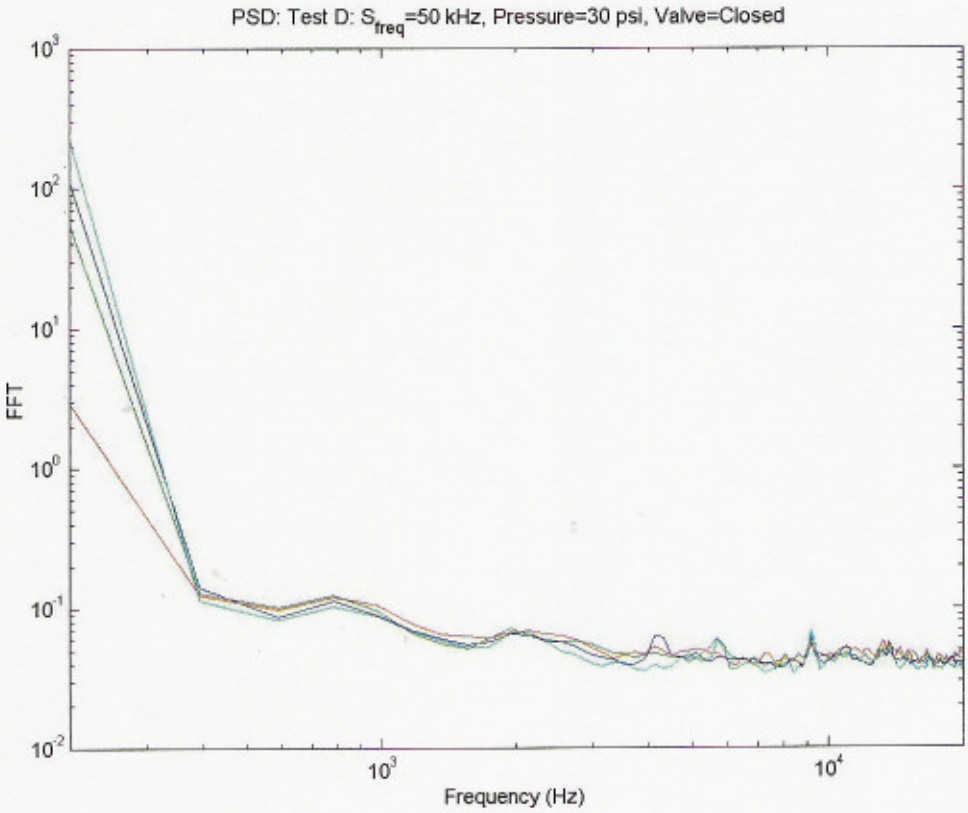
PSD: Test D: S_{freq}=50 kHz, Pressure=30 psi, Valve=Closed
FFT
Frequency (Hz)

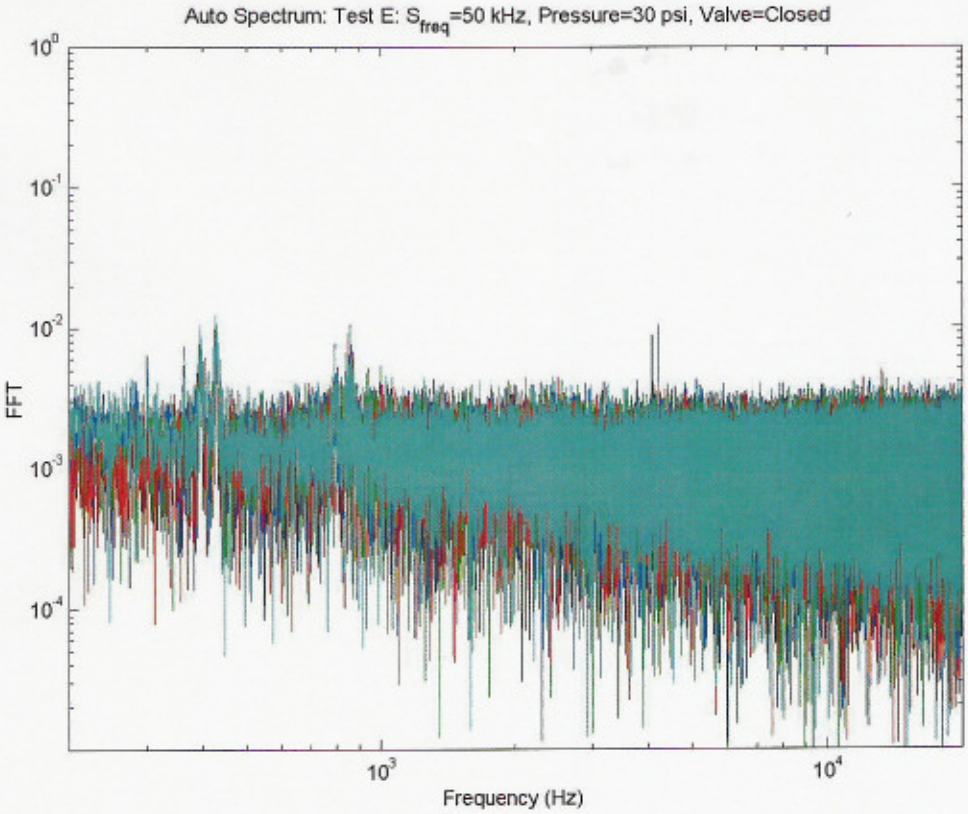
Auto Spectrum: Test E: S_{freq}=50 kHz, Pressure=30 psi, Valve=Closed
FFT
Frequency (Hz)

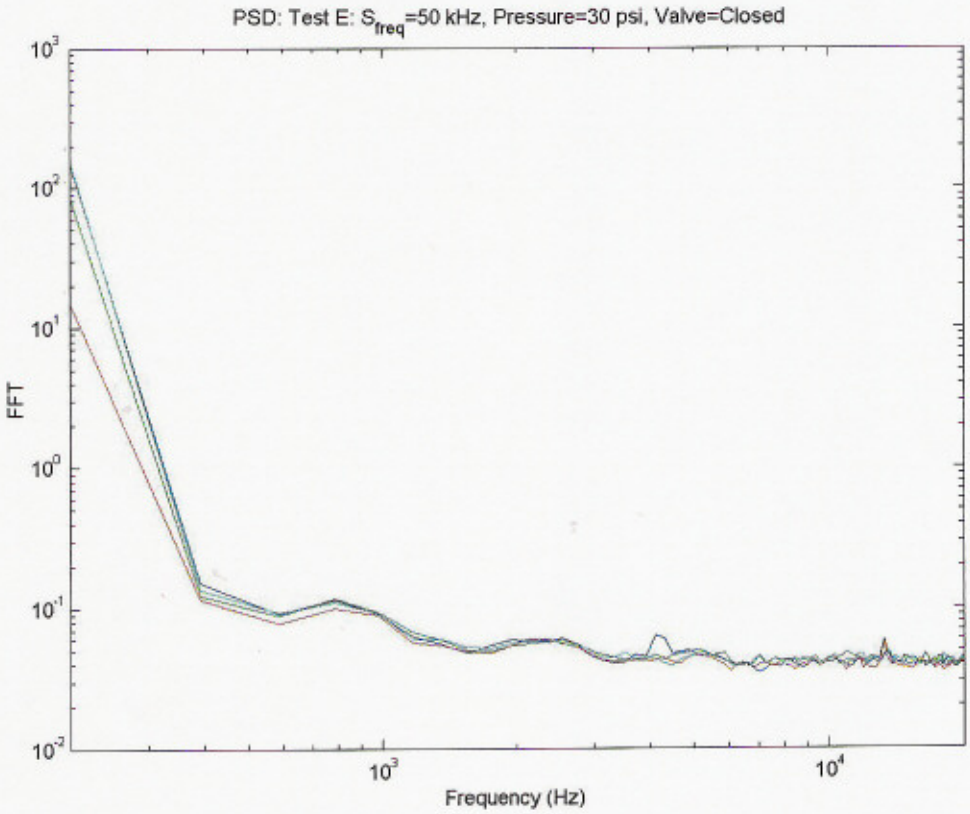
PSD: Test E: S_{freq}=50 kHz, Pressure=30 psi, Valve=Closed
FFT
Frequency (Hz)

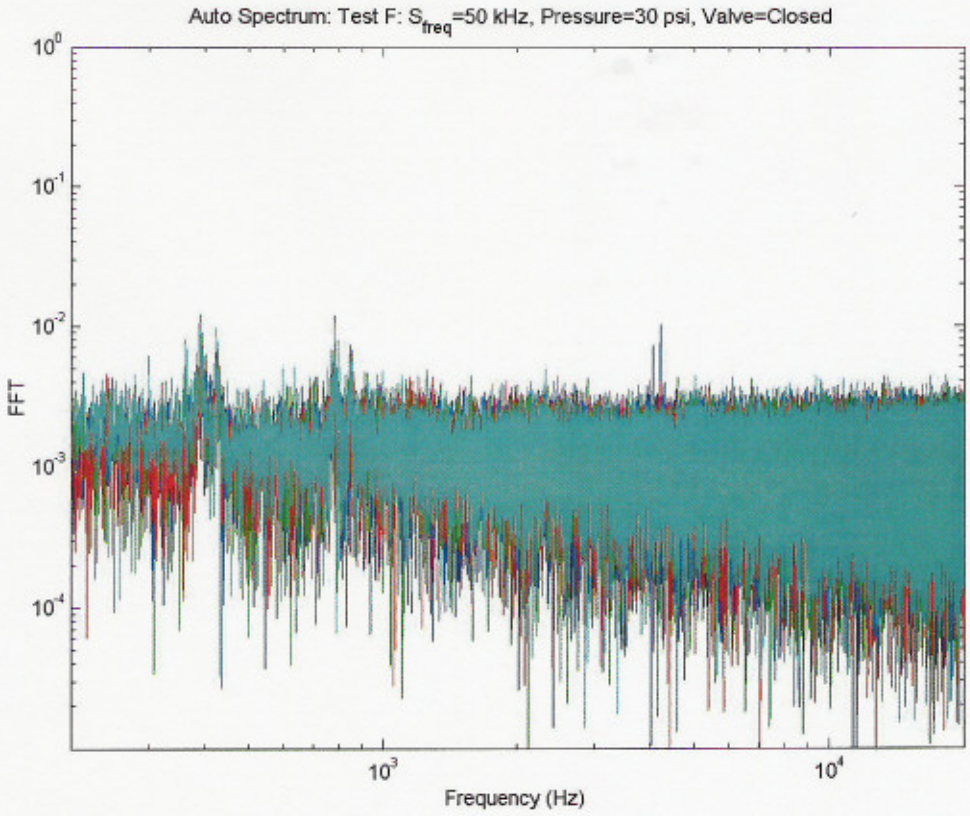
Auto Spectrum: Test F: S_{freq}=50 kHz, Pressure=30 psi, Valve=Closed
FFT
Frequency (Hz)

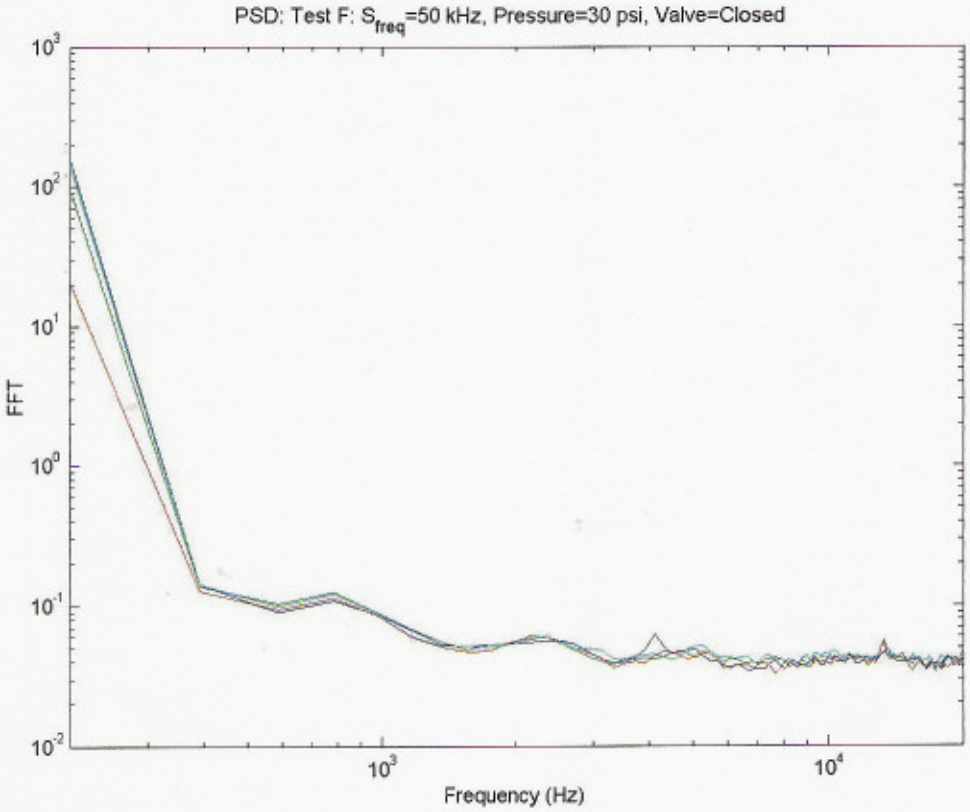
PSD: Test F: S_{freq}=50 kHz, Pressure=30 psi, Valve=Closed
FFT
Frequency (Hz)

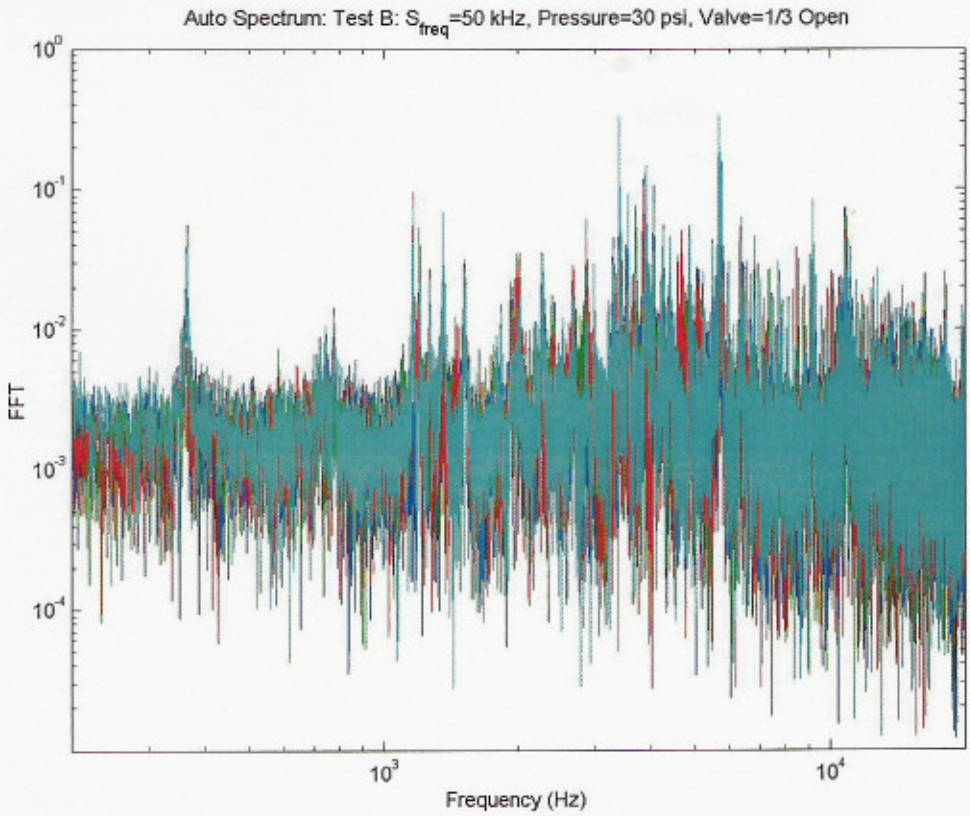
Auto Spectrum: Test B: S_{freq}=50 kHz, Pressure=30 psi, Valve=1/3 Open
10^0
10^{-1}
10^{-2}
10^{-3}
10^{-4}
FFT
10^3
10^4
Frequency (Hz)

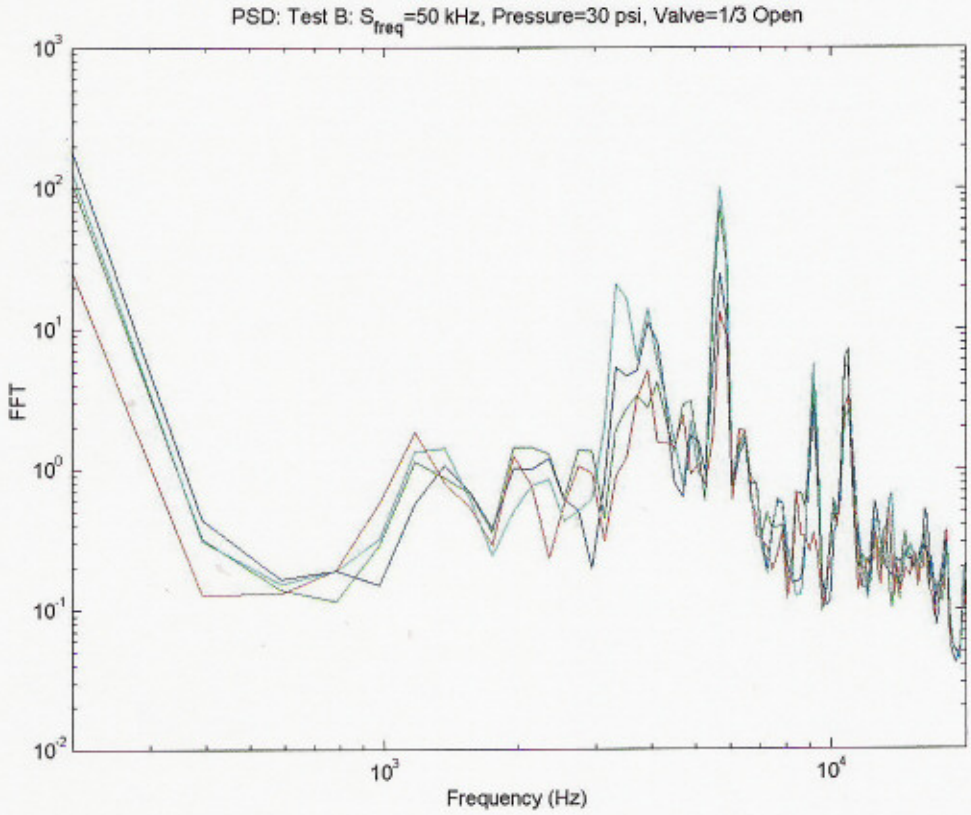
PSD: Test B: S_{freq}=50 kHz, Pressure=30 psi, Valve=1/3 Open
10^3
10^2
10^1
10^0
10^{-1}
10^{-2}
FFT
10^3
10^4
Frequency (Hz)

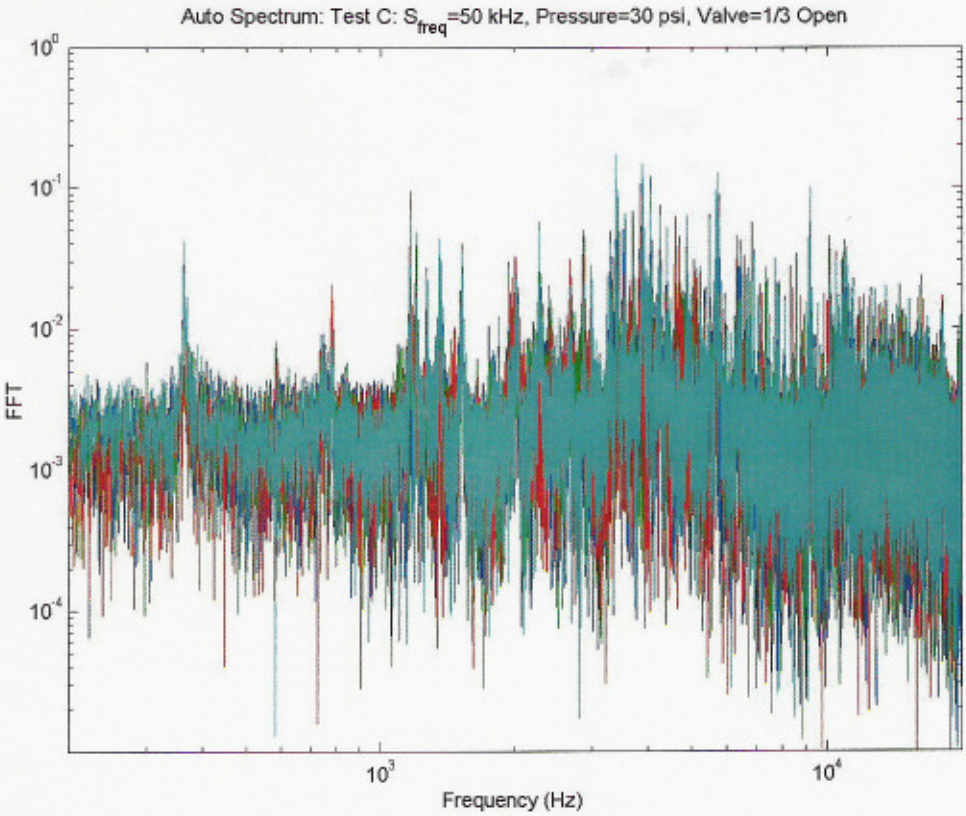
Auto Spectrum: Test C: S_{freq}=50 kHz, Pressure=30 psi, Valve=1/3 Open
FFT
Frequency (Hz)

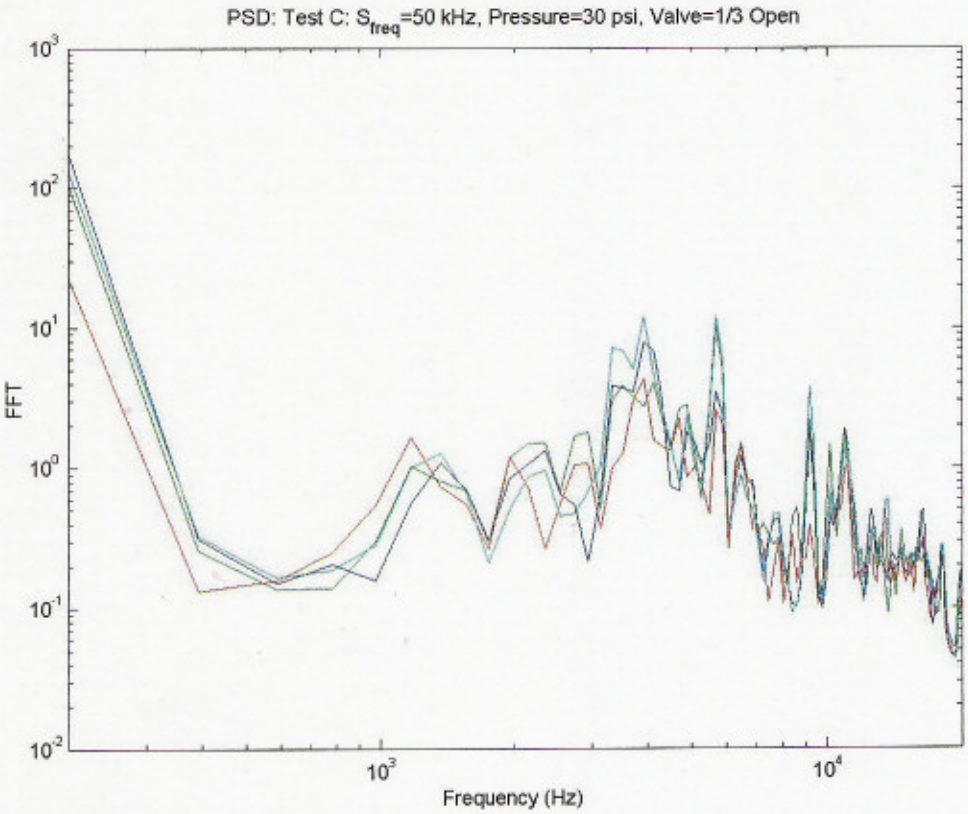
PSD: Test C: S_{freq}=50 kHz, Pressure=30 psi, Valve=1/3 Open
FFT
Frequency (Hz)

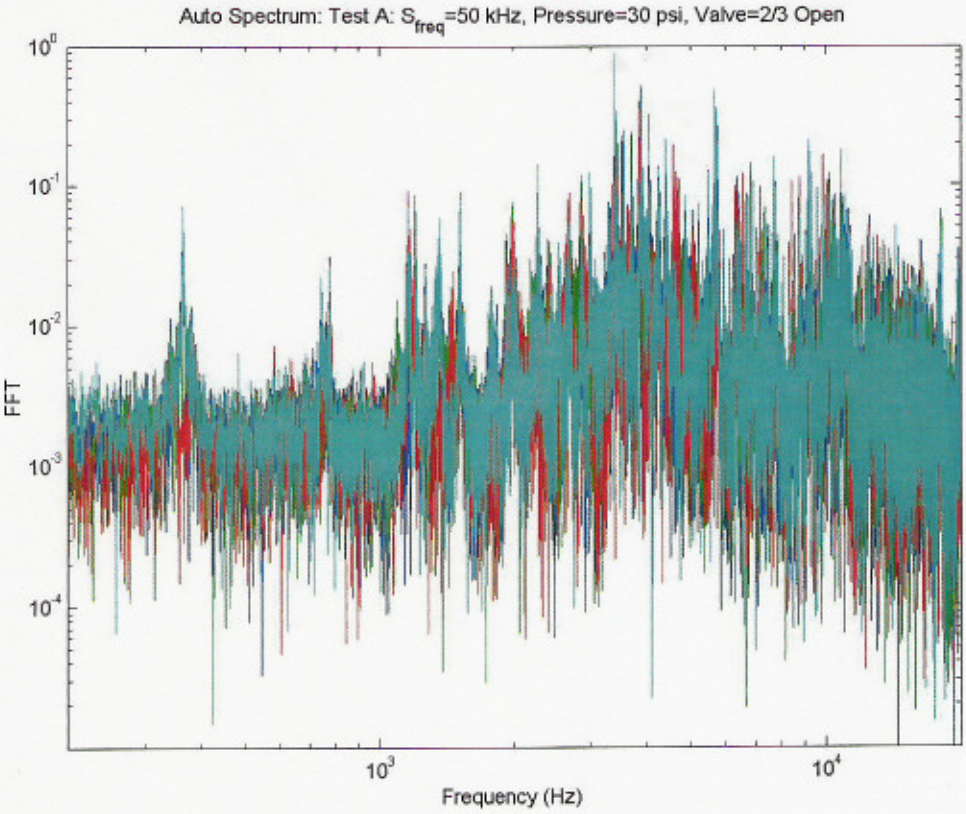
Auto Spectrum: Test A: S_{freq}=50 kHz, Pressure=30 psi, Valve=2/3 Open
FFT
Frequency (Hz)

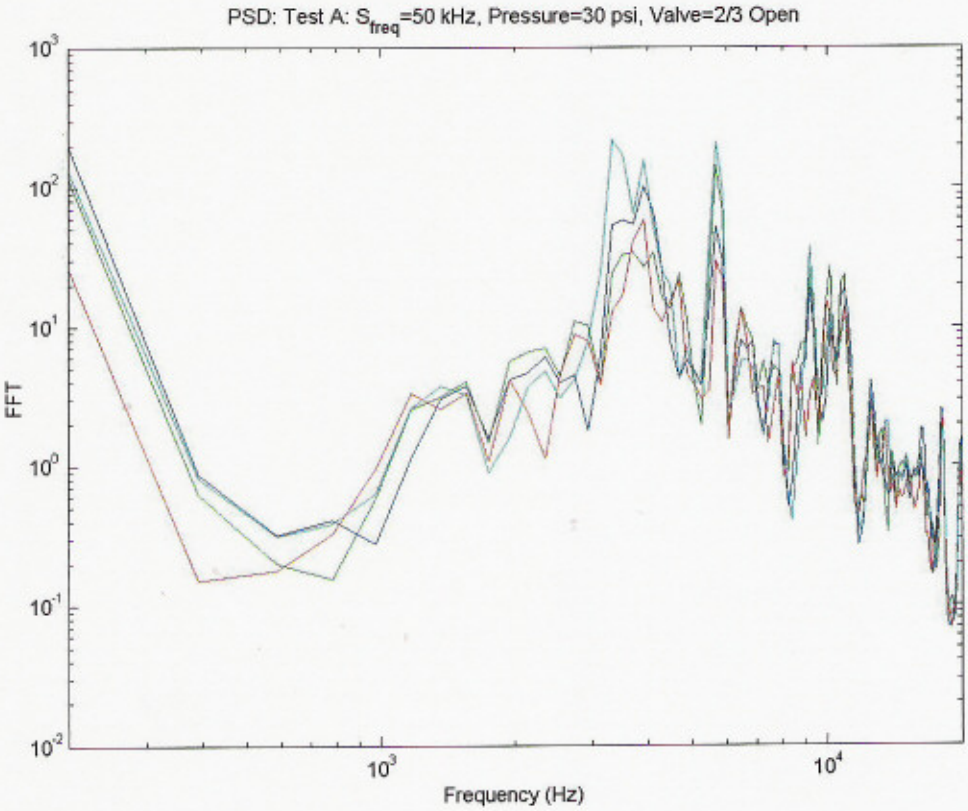
PSD: Test A: S_{freq}=50 kHz, Pressure=30 psi, Valve=2/3 Open
FFT
Frequency (Hz)

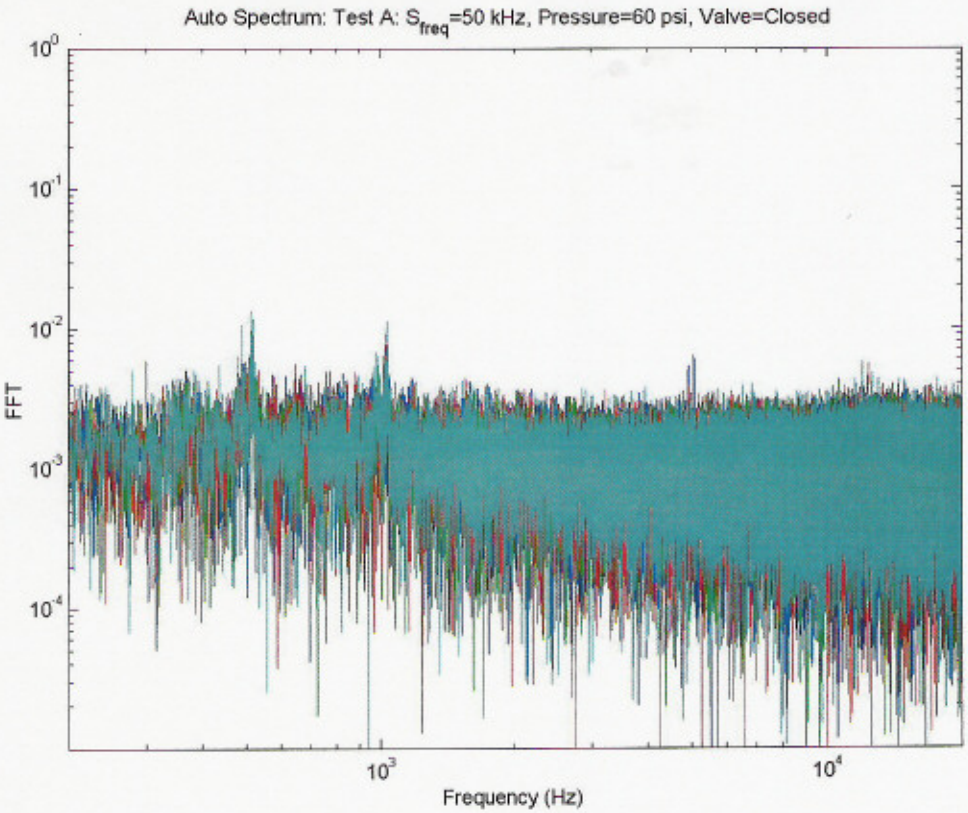
Auto Spectrum: Test A: S_{freq}=50 kHz, Pressure=60 psi, Valve=Closed
FFT
Frequency (Hz)

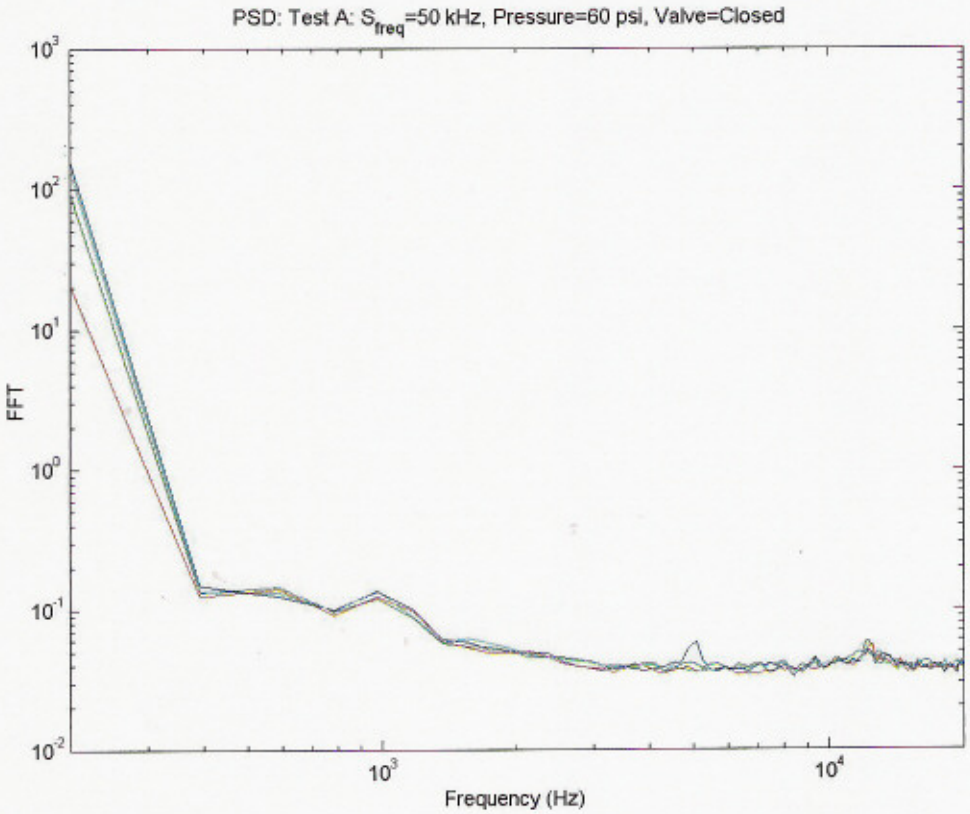
PSD: Test A: S_{freq}=50 kHz, Pressure=60 psi, Valve=Closed
FFT
Frequency (Hz)

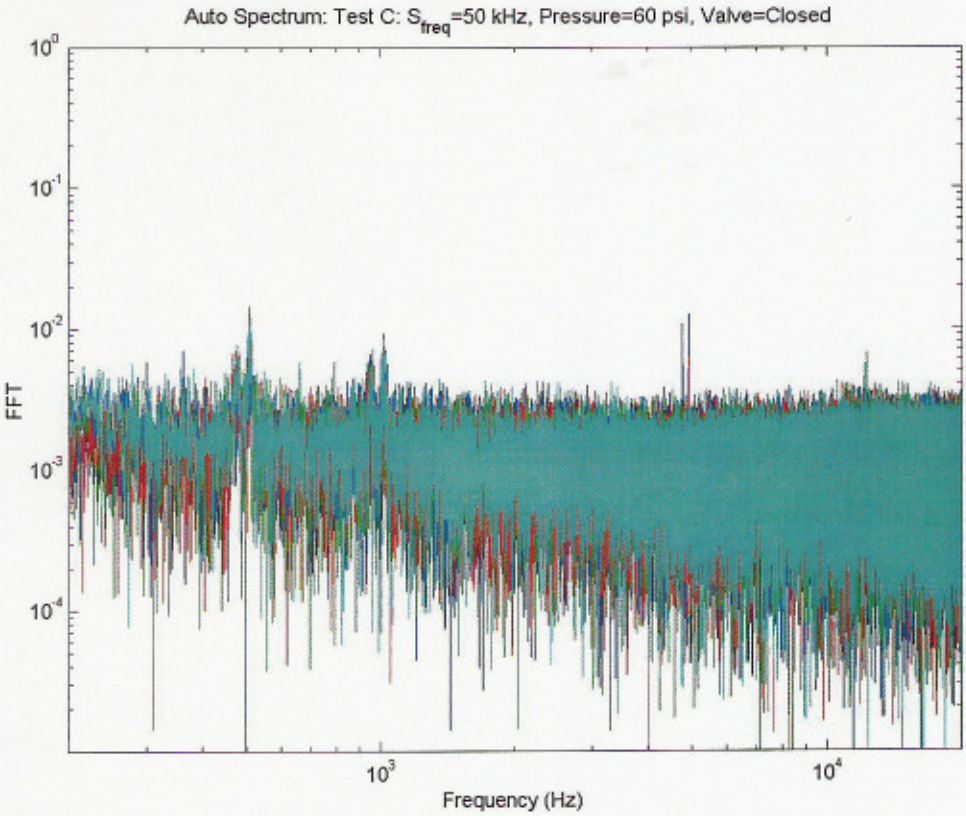
Auto Spectrum: Test C: S_{freq}=50 kHz, Pressure=60 psi, Valve=Closed
FFT
Frequency (Hz)

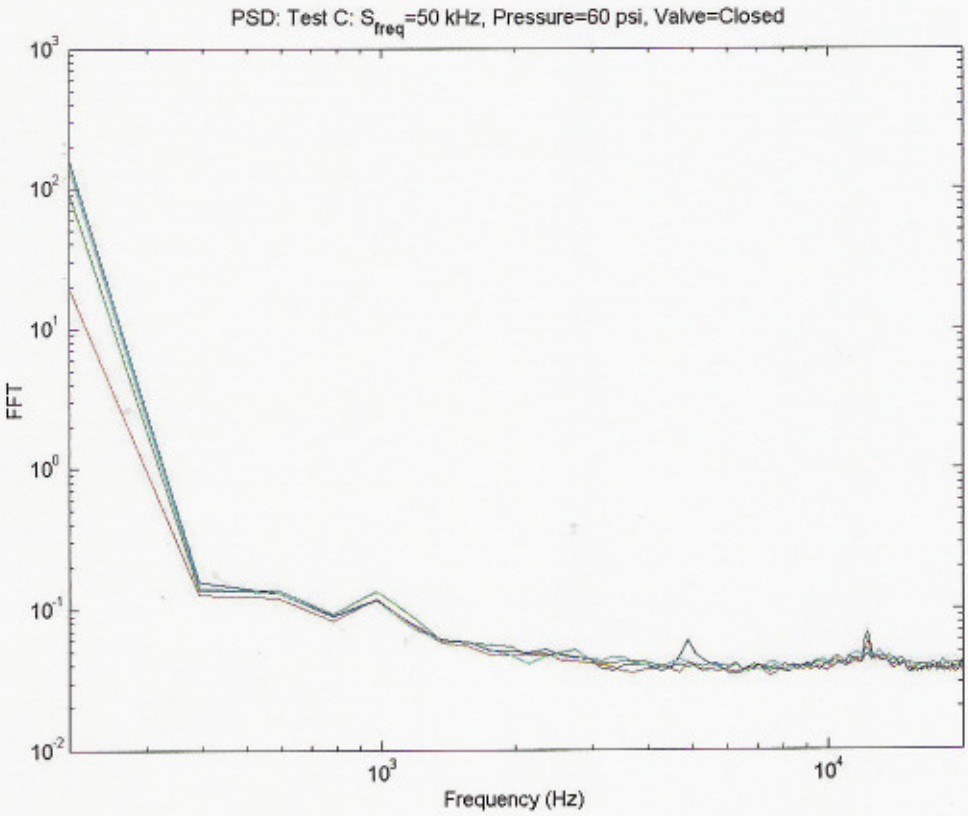
PSD: Test C: S_{freq}=50 kHz, Pressure=60 psi, Valve=Closed
FFT
Frequency (Hz)

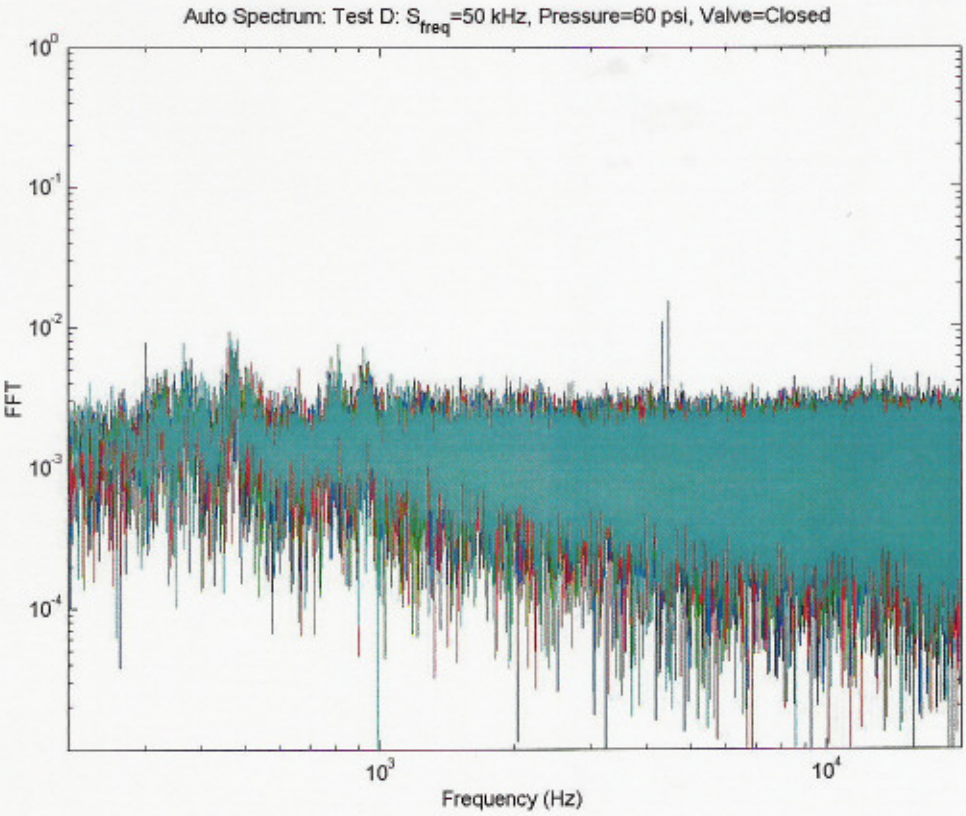
Auto Spectrum: Test D: S_{freq}=50 kHz, Pressure=60 psi, Valve=Closed
FFT
Frequency (Hz)

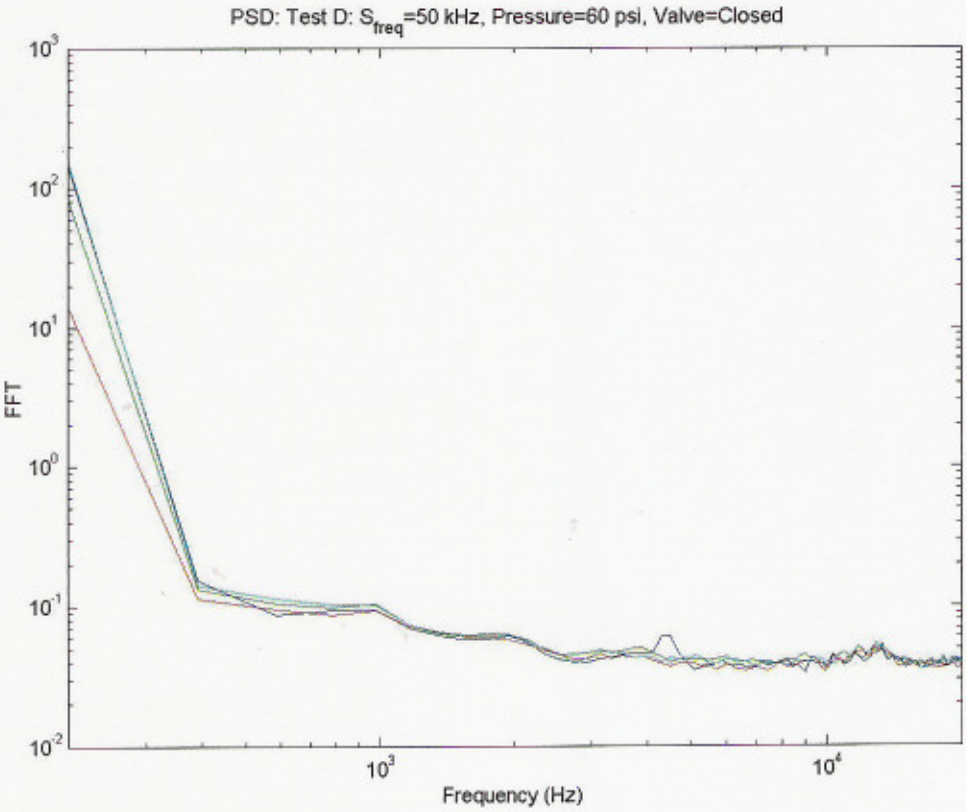
PSD: Test D: S_{freq}=50 kHz, Pressure=60 psi, Valve=Closed
FFT
Frequency (Hz)

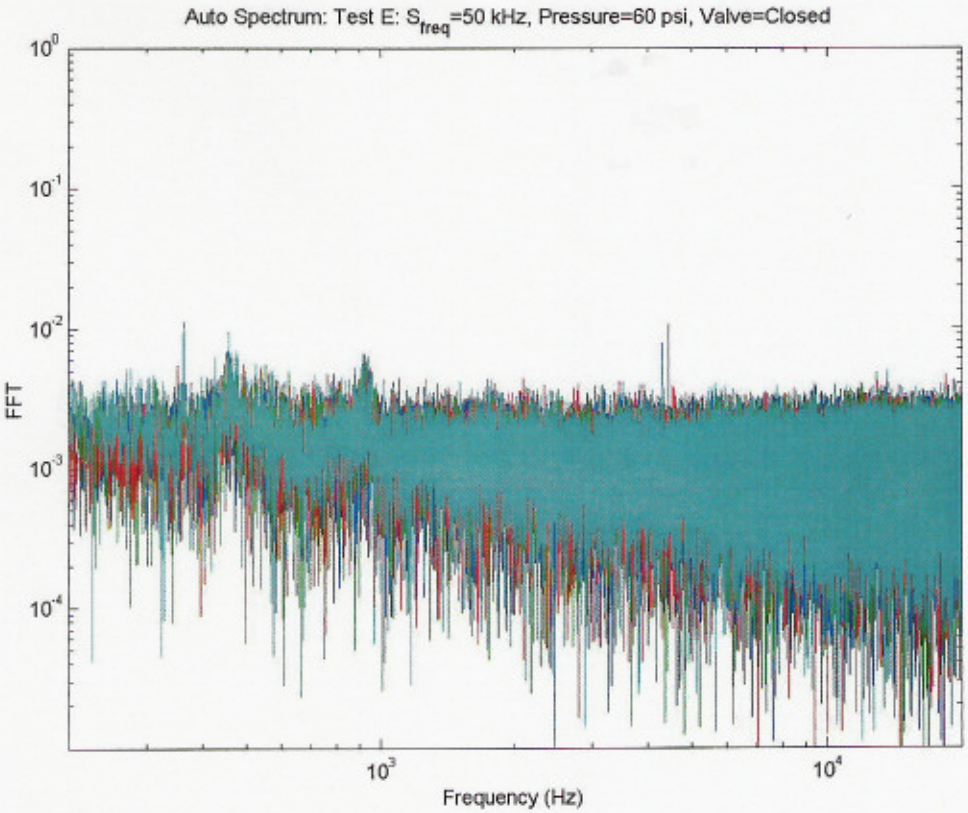
Auto Spectrum: Test E: S_{freq}=50 kHz, Pressure=60 psi, Valve=Closed
FFT
Frequency (Hz)

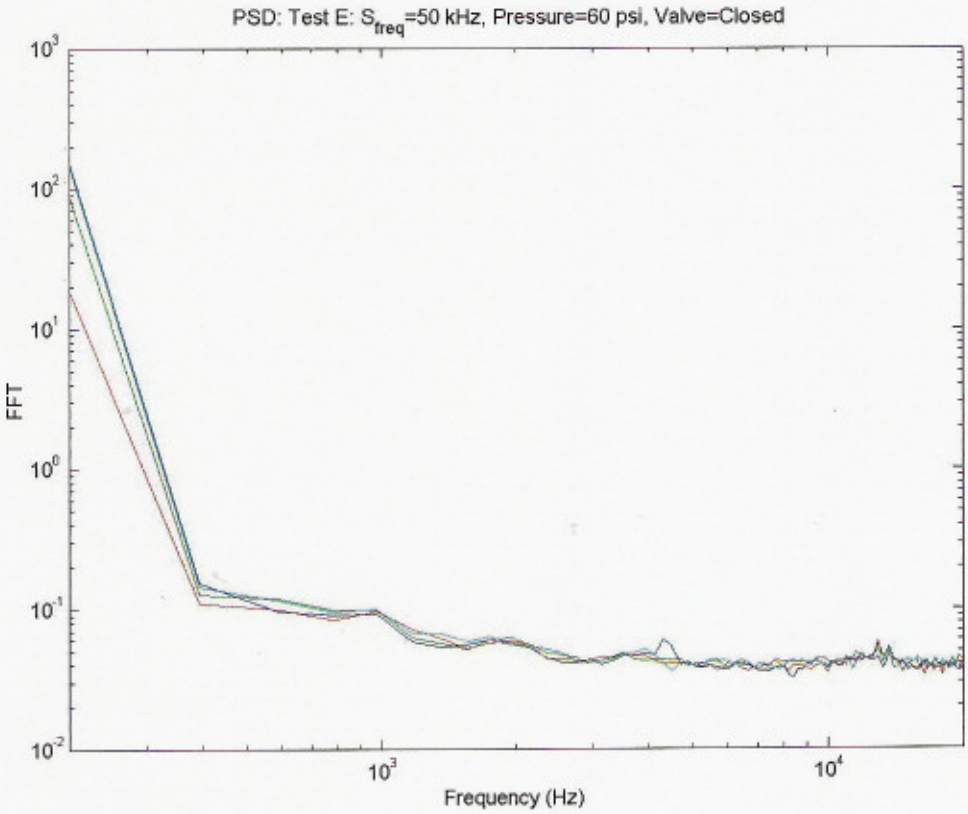
PSD: Test E: S_{freq}=50 kHz, Pressure=60 psi, Valve=Closed
FFT
Frequency (Hz)

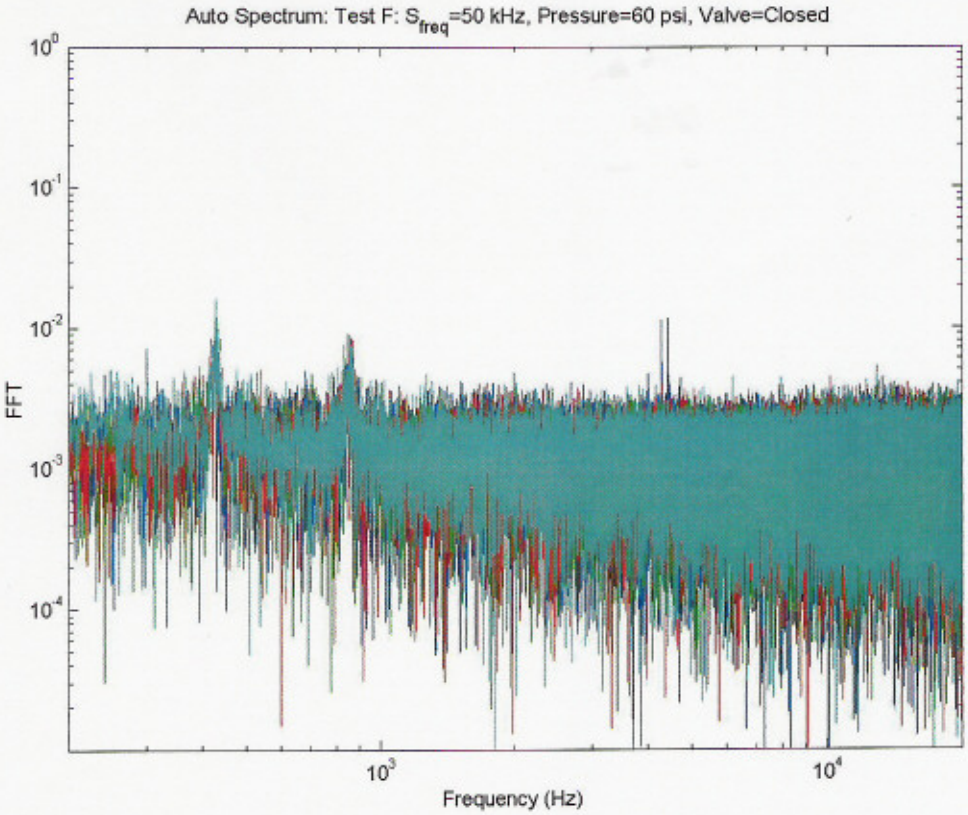
Auto Spectrum: Test F: S_{freq}=50 kHz, Pressure=60 psi, Valve=Closed
10^0
10^{-1}
10^{-2}
10^{-3}
10^{-4}
FFT
10^3
10^4
Frequency (Hz)

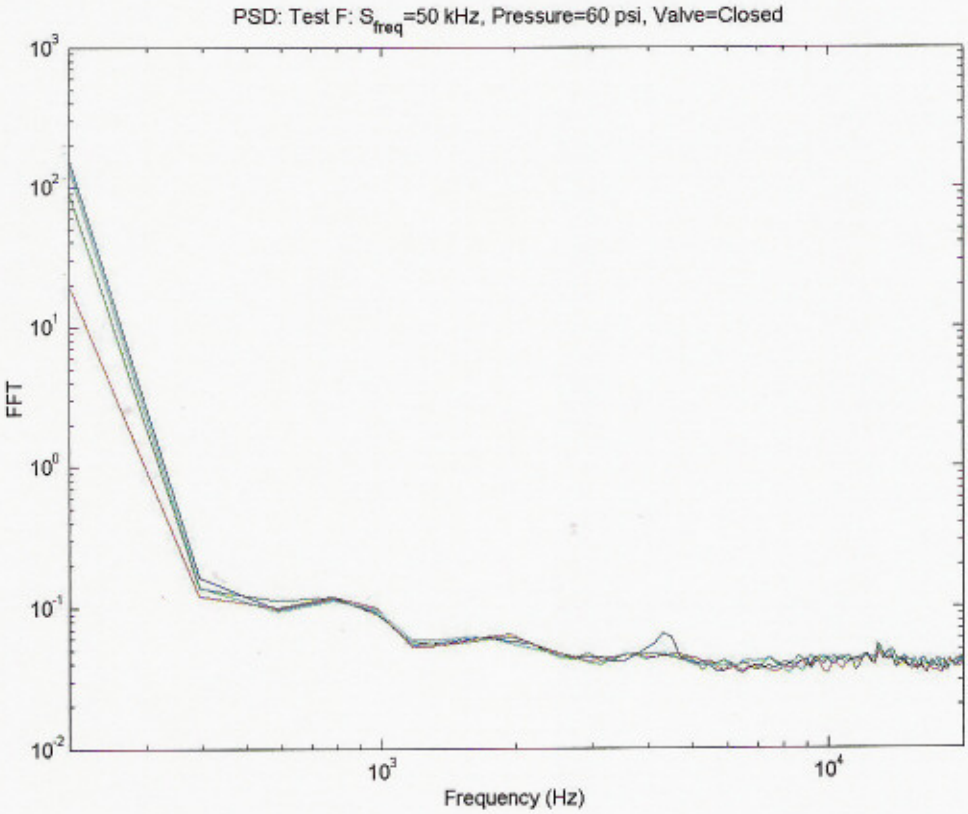
PSD: Test F: S_{freq}=50 kHz, Pressure=60 psi, Valve=Closed
10^3
10^2
10^1
10^0
10^{-1}
10^{-2}
FFT
10^3
10^4
Frequency (Hz)

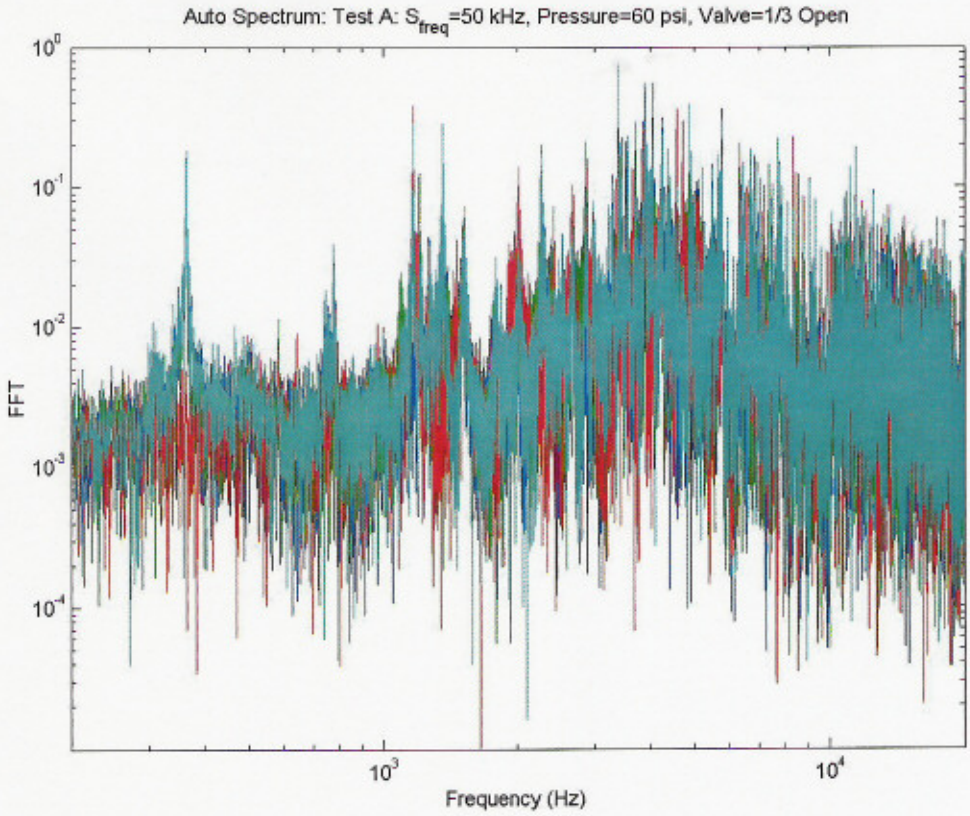
Auto Spectrum: Test A: S_{freq}=50 kHz, Pressure=60 psi, Valve=1/3 Open
FFT
Frequency (Hz)

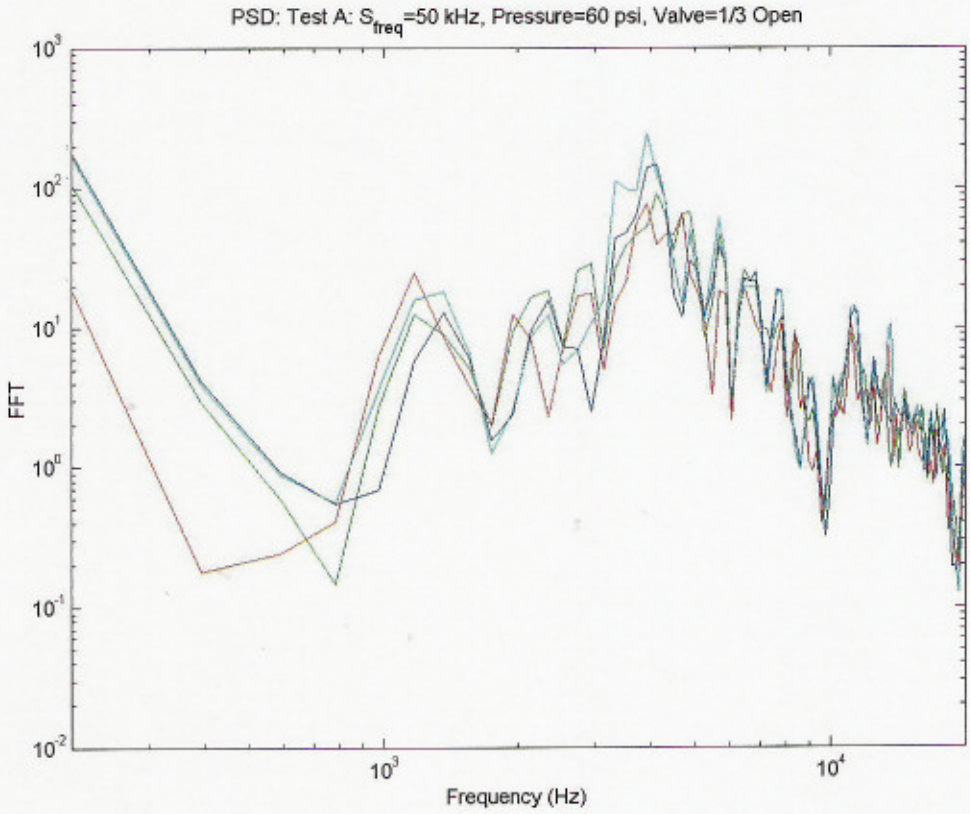
PSD: Test A: S_{freq}=50 kHz, Pressure=60 psi, Valve=1/3 Open
FFT
Frequency (Hz)

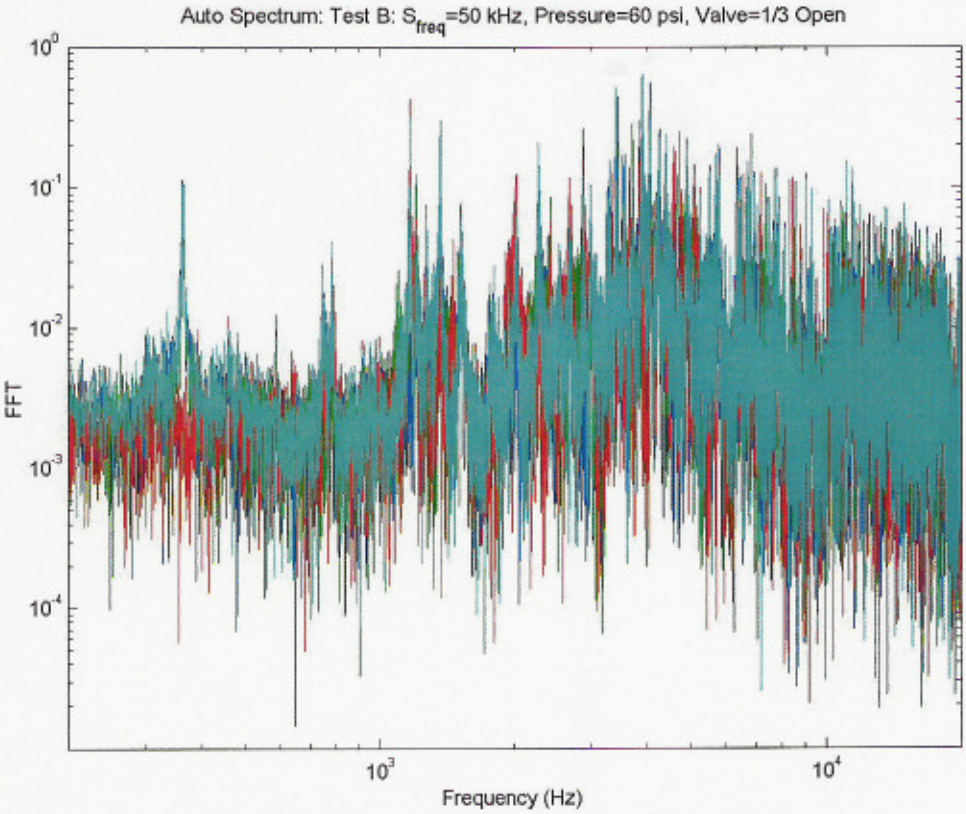
Auto Spectrum: Test B: S_{freq}=50 kHz, Pressure=60 psi, Valve=1/3 Open
FFT
Frequency (Hz)

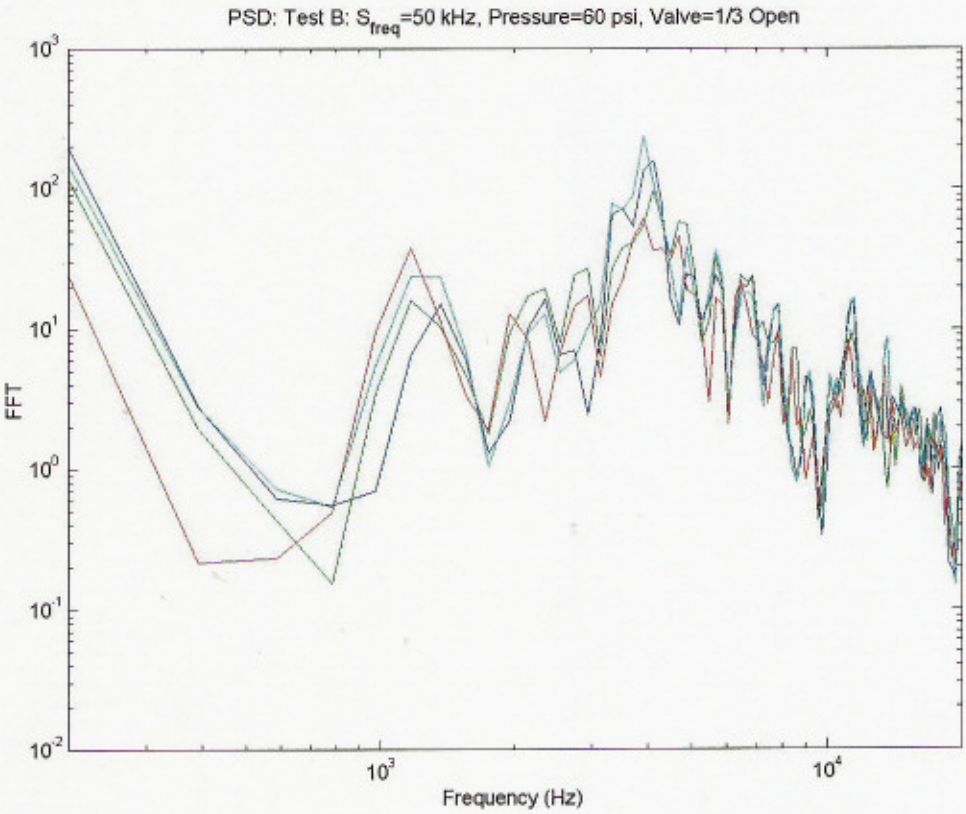
PSD: Test B: S_{freq}=50 kHz, Pressure=60 psi, Valve=1/3 Open
FFT
Frequency (Hz)

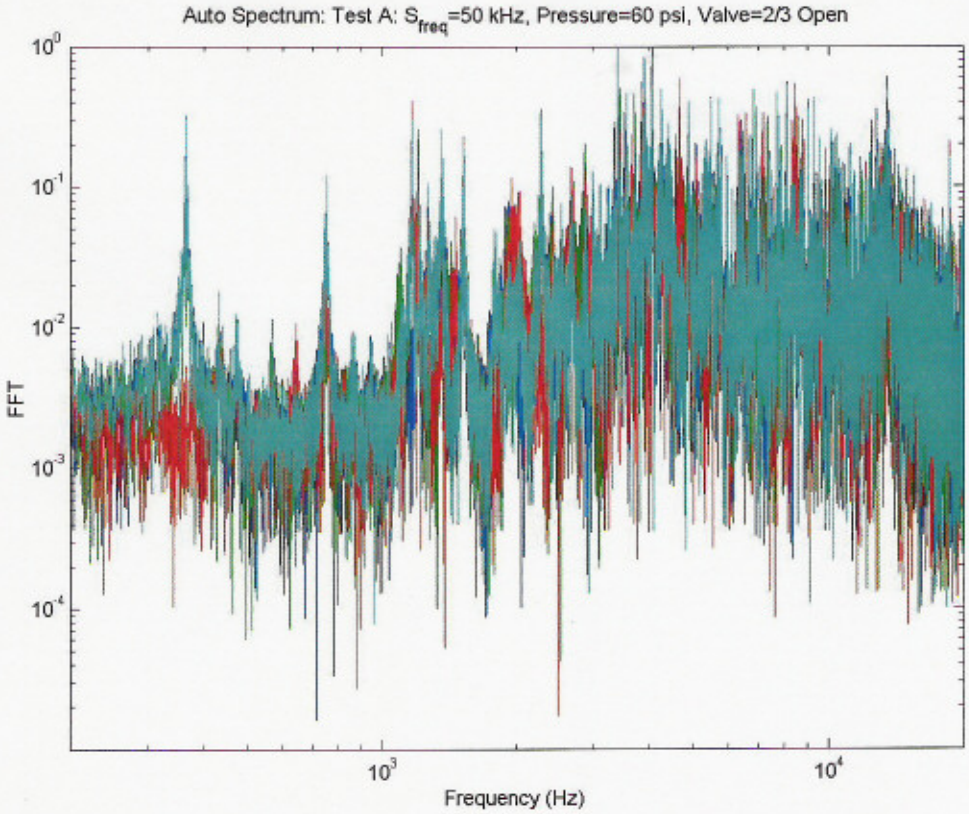
Auto Spectrum: Test A: S_{freq}=50 kHz, Pressure=60 psi, Valve=2/3 Open
10^0
10^{-1}
10^{-2}
10^{-3}
10^{-4}
FFT
10^3
10^4
Frequency (Hz)

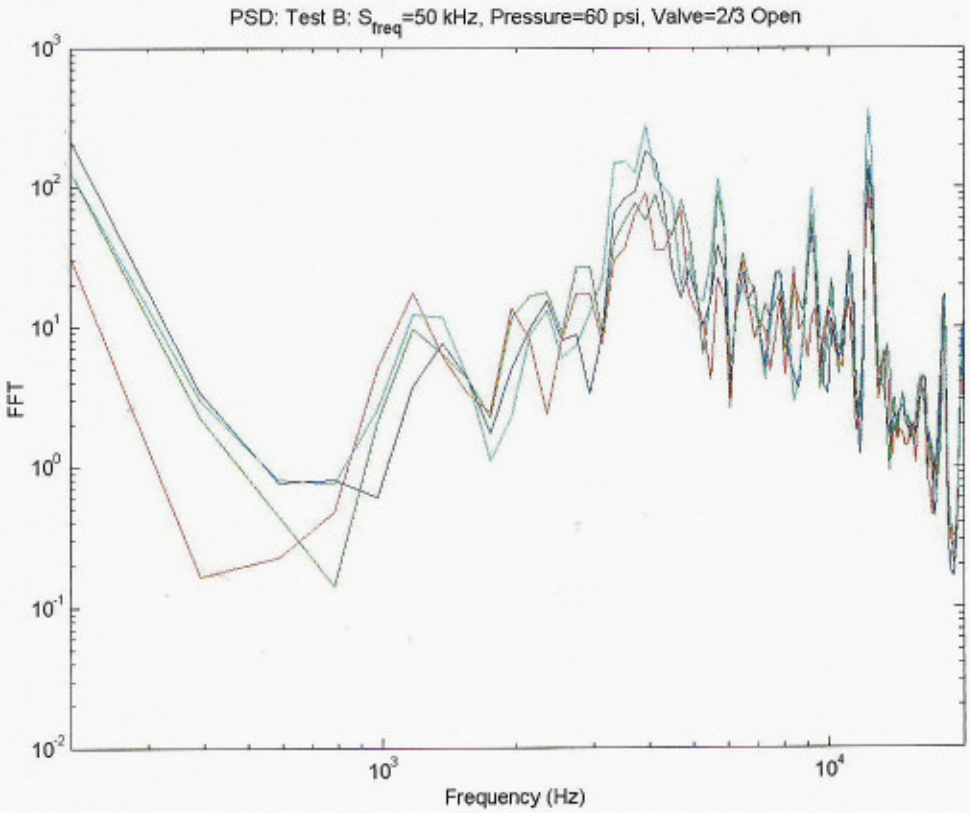
PSD: Test B: S_{freq}=50 kHz, Pressure=60 psi, Valve=2/3 Open
10^3
10^2
10^1
10^0
10^{-1}
10^{-2}
FFT
10^3
10^4
Frequency (Hz)

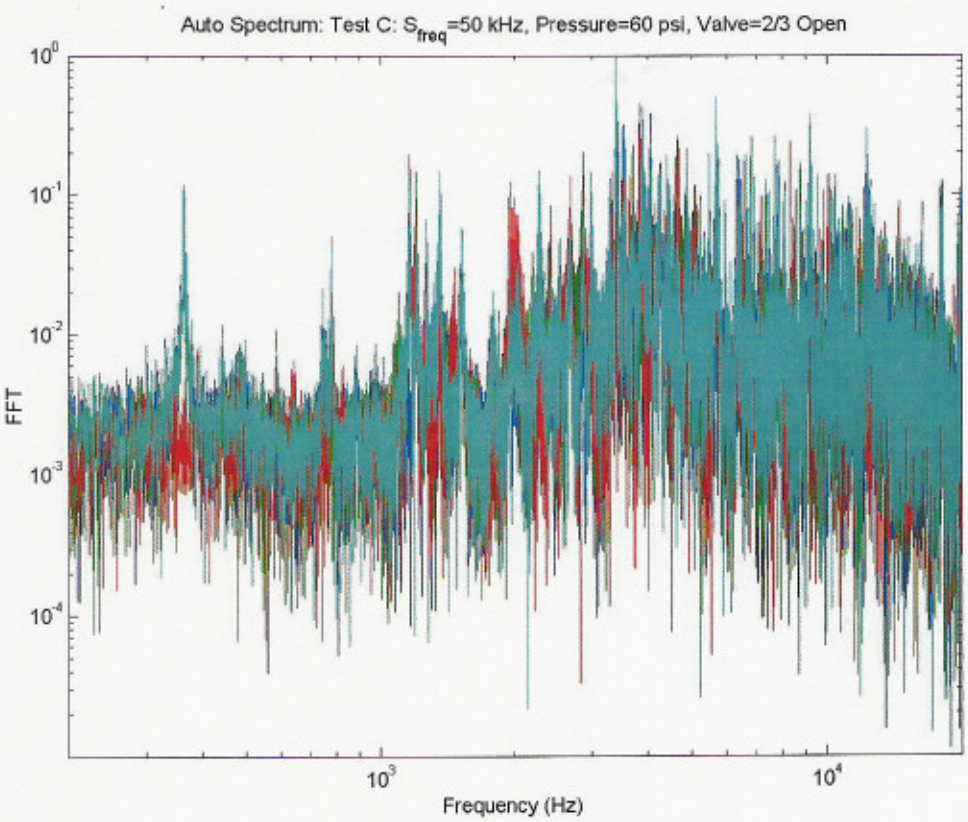
Auto Spectrum: Test C: S_{freq}=50 kHz, Pressure=60 psi, Valve=2/3 Open
10^0
10^{-1}
10^{-2}
10^{-3}
10^{-4}
FFT
10^3
10^4
Frequency (Hz)

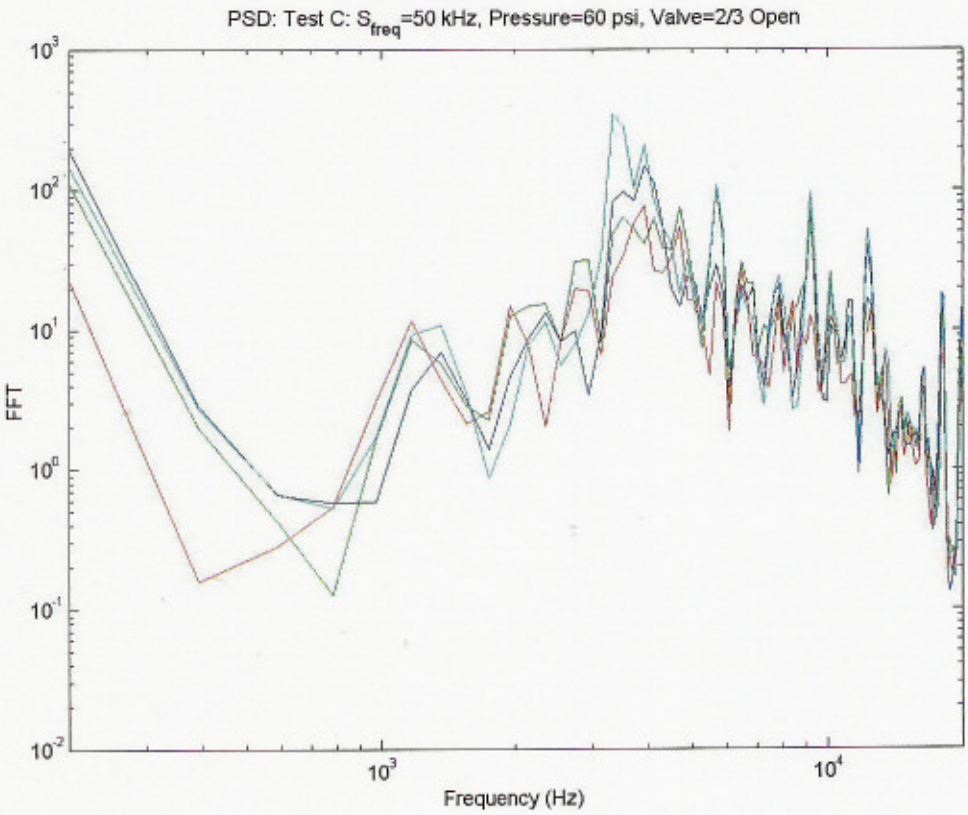
PSD: Test C: S_{freq}=50 kHz, Pressure=60 psi, Valve=2/3 Open
10^3
10^2
10^1
10^0
10^{-1}
10^{-2}
FFT
10^3
10^4
Frequency (Hz)

3.2.2. Location and Magnitude of the Leak

In order to determine the location and the size of the leak, the phasing and amplitude of the measured disturbances were examined near the peak or resonant frequencies. Four "resonant" frequencies were identified, namely:

- 362.5 Hz
- 751.0 Hz
- 1168.5 Hz
- 4000.0 Hz

It is expected that these four frequencies are structural resonant frequencies and Midé is in the process of constructing a structural Finite Element Model to confirm this.

The data was examined by either looking at the phase and amplitude near the peak or at the peak. Preliminary results concluded that more accurate phasing information can be obtained when only the phasing and amplitude at the peak is used. The amplitude and phase was obtained by numerically integrating for the Fourier coefficients. These results are graphically summarized in the Figures below.

It should be noted that Midé that the data acquisition system does not have a simultaneous sample and hold and that the phase must still be adjusted according to the following:

$\bar{\phi}_i = \phi_i - 0.0018(i-1)f$ Where f is the frequency in Hz, i is the sensor channel number, ϕ_i is the uncorrected phase of channel number i and $\bar{\phi}$ is the corrected phase.

3.2.2.1. Sensor Signal Amplitudes and Phasing at 1168.5 Hz

For the case where there is no leak, the amplitudes are below .002, about an order of magnitude lower than any one of the leak tests. In all these tests, the maximum amplitude was near Sensor 3. In most cases the next strongest output is from Sensor 4, indicating the leak is between these two sensors. The phase results are more difficult to interpret and this work is in progress.

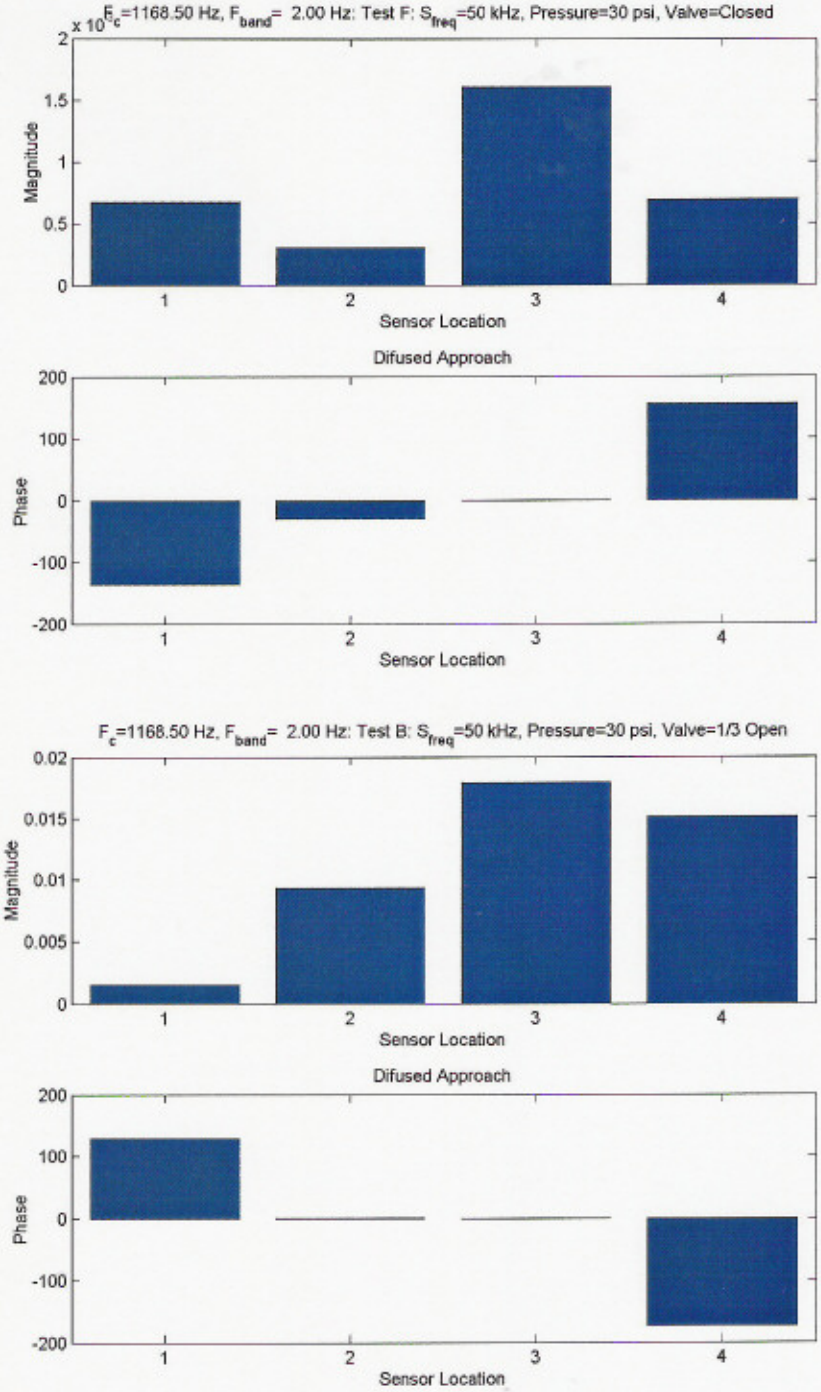
F_c=1168.50 Hz, F_{band}= 2.00 Hz: Test F: S_{freq}=50 kHz, Pressure=30 psi, Valve=Closed
x 10
Magnitude
Sensor Location
Difused Approach
Phase
Sensor Location
F_c=1168.50 Hz, F_{band}= 2.00 Hz: Test B: S_{freq}=50 kHz, Pressure=30 psi, Valve=1/3 Open
Magnitude
Sensor Location
Difused Approach
Phase
Sensor Location

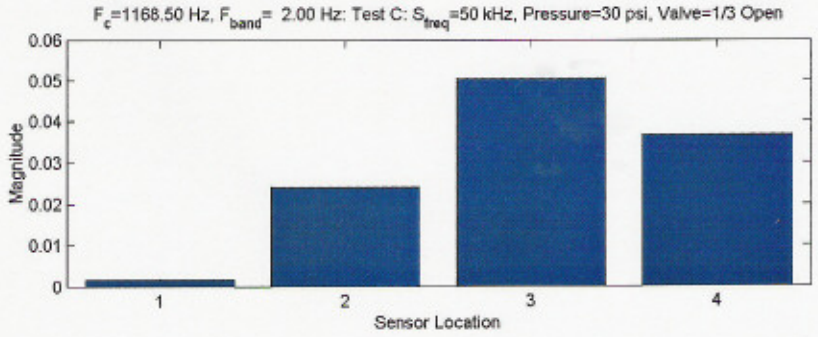
F_c=1168.50 Hz, F_{band}= 2.00 Hz: Test C: S_{freq}=50 kHz, Pressure=30 psi, Valve=1/3 Open
Magnitude
0.06
0.05
0.04
0.03
0.02
0.01
0
1
2
3
4
Sensor Location

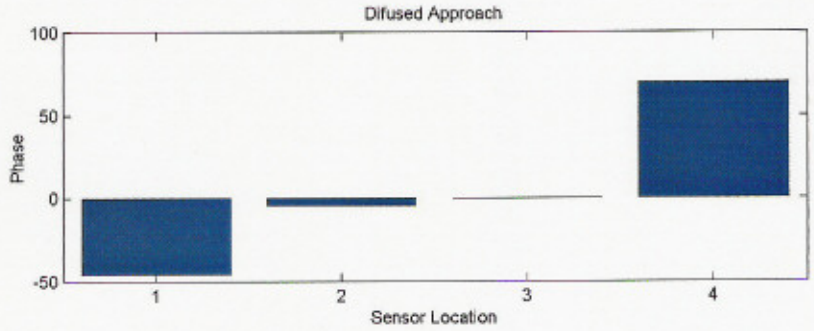
Difused Approach
Phase
100
50
0
-50
1
2
3
4
Sensor Location

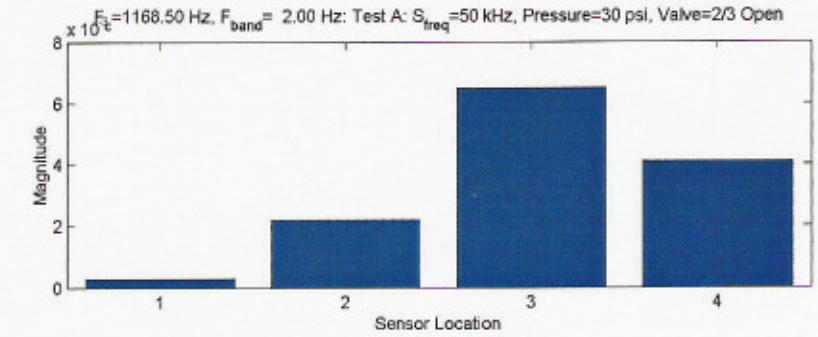
F_c=1168.50 Hz, F_{band}= 2.00 Hz: Test A: S_{freq}=50 kHz, Pressure=30 psi, Valve=2/3 Open
x 10^4
Magnitude
8
6
4
2
0
1
2
3
4
Sensor Location

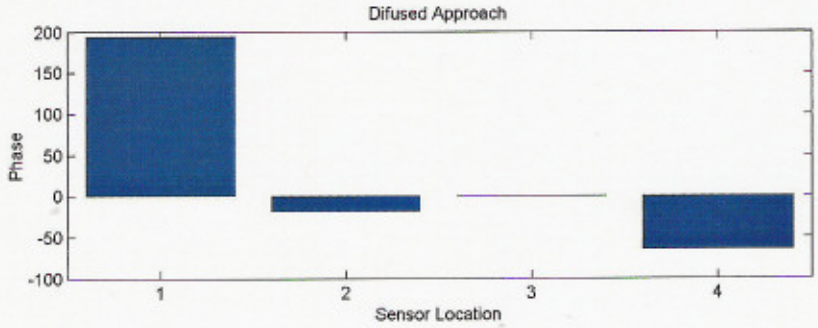
Difused Approach
Phase
200
150
100
50
0
-50
-100
1
2
3
4
Sensor Location

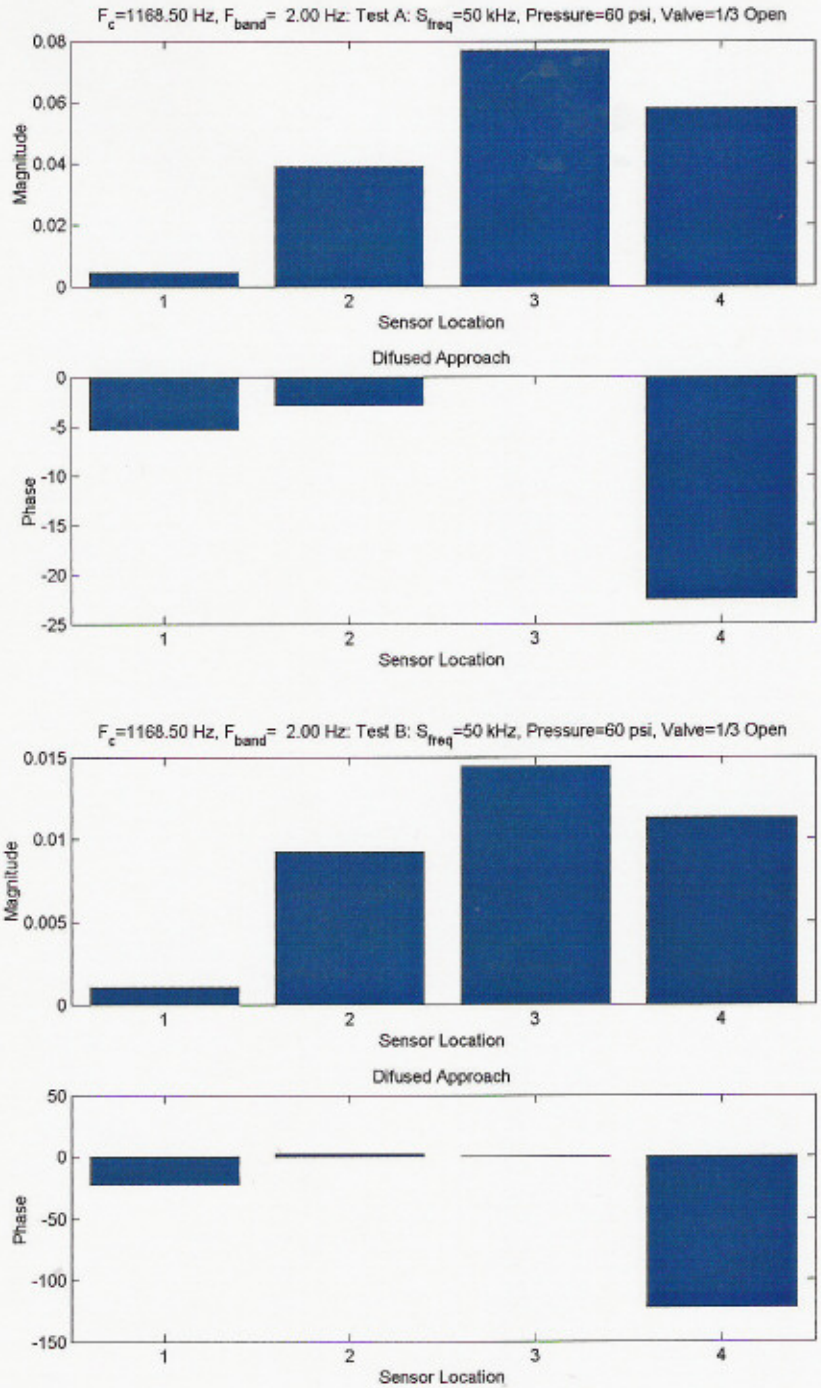
F_c=1168.50 Hz, F_{band}= 2.00 Hz: Test A: S_{freq}=50 kHz, Pressure=60 psi, Valve=1/3 Open
Magnitude
Sensor Location
Difused Approach
Phase
Sensor Location
F_c=1168.50 Hz, F_{band}= 2.00 Hz: Test B: S_{freq}=50 kHz, Pressure=60 psi, Valve=1/3 Open
Magnitude
Sensor Location
Difused Approach
Phase
Sensor Location

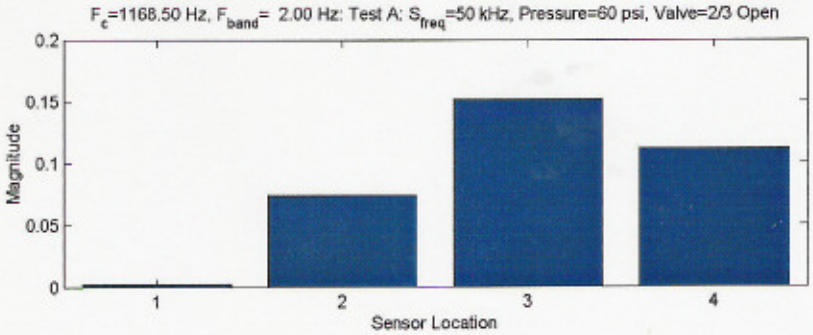
F_c=1168.50 Hz, F_{band}= 2.00 Hz: Test A: S_{freq}=50 kHz, Pressure=60 psi, Valve=2/3 Open
Magnitude
0.2
0.15
0.1
0.05
0
1
2
3
4
Sensor Location

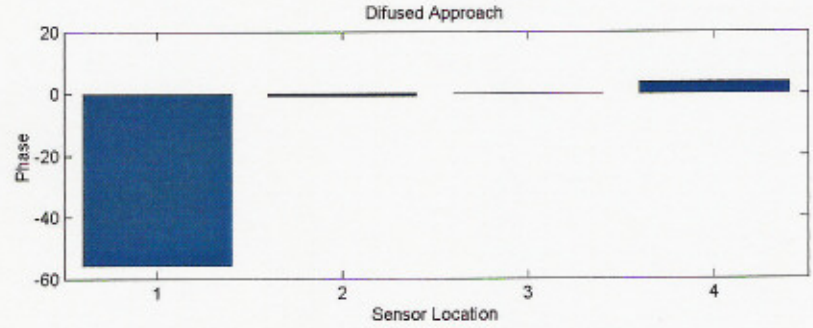
Difused Approach
Phase
20
0
-20
-40
-60
1
2
3
4
Sensor Location

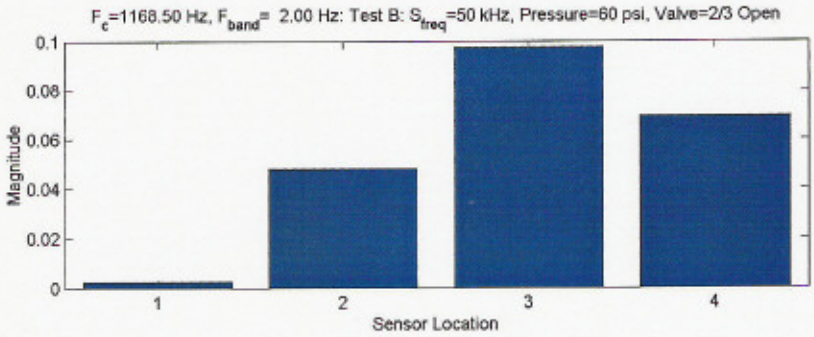
F_c=1168.50 Hz, F_{band}= 2.00 Hz: Test B: S_{freq}=50 kHz, Pressure=60 psi, Valve=2/3 Open
Magnitude
0.1
0.08
0.06
0.04
0.02
0
1
2
3
4
Sensor Location

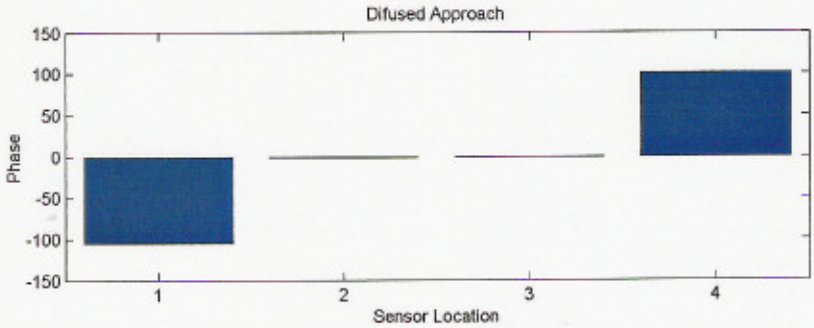
Difused Approach
Phase
150
100
50
0
-50
-100
-150
1
2
3
4
Sensor Location

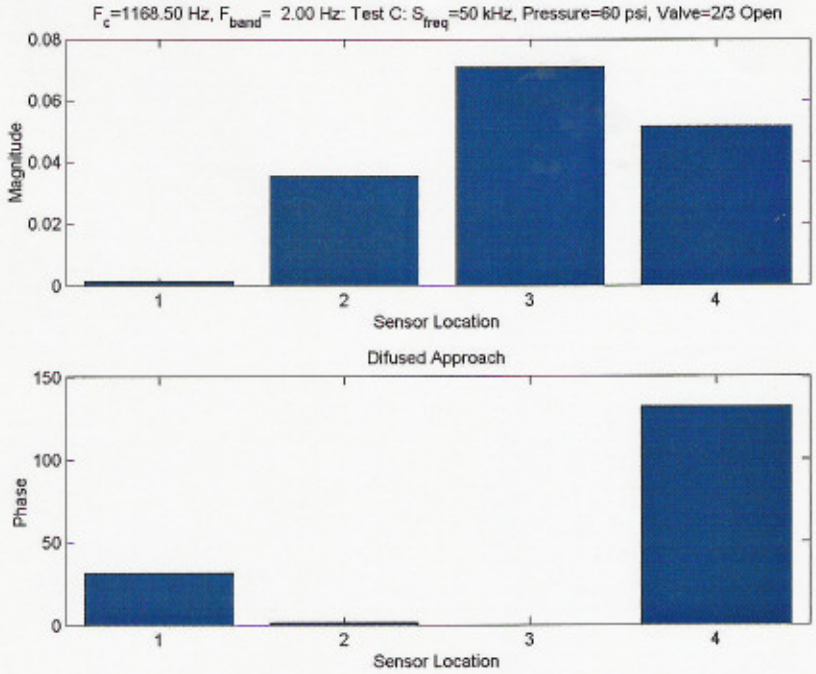

3.2.2.2. Sensor Signal Amplitudes and Phasing at 4000 Hz

At 4 kHz the maximum amplitude was near Sensor 4. The phase results are more difficult to interpret and this work is in progress.

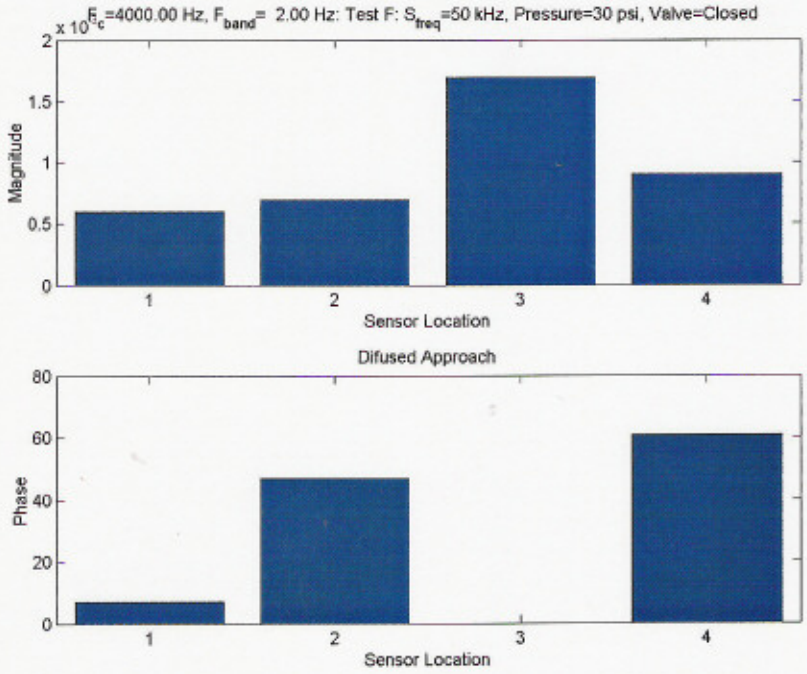

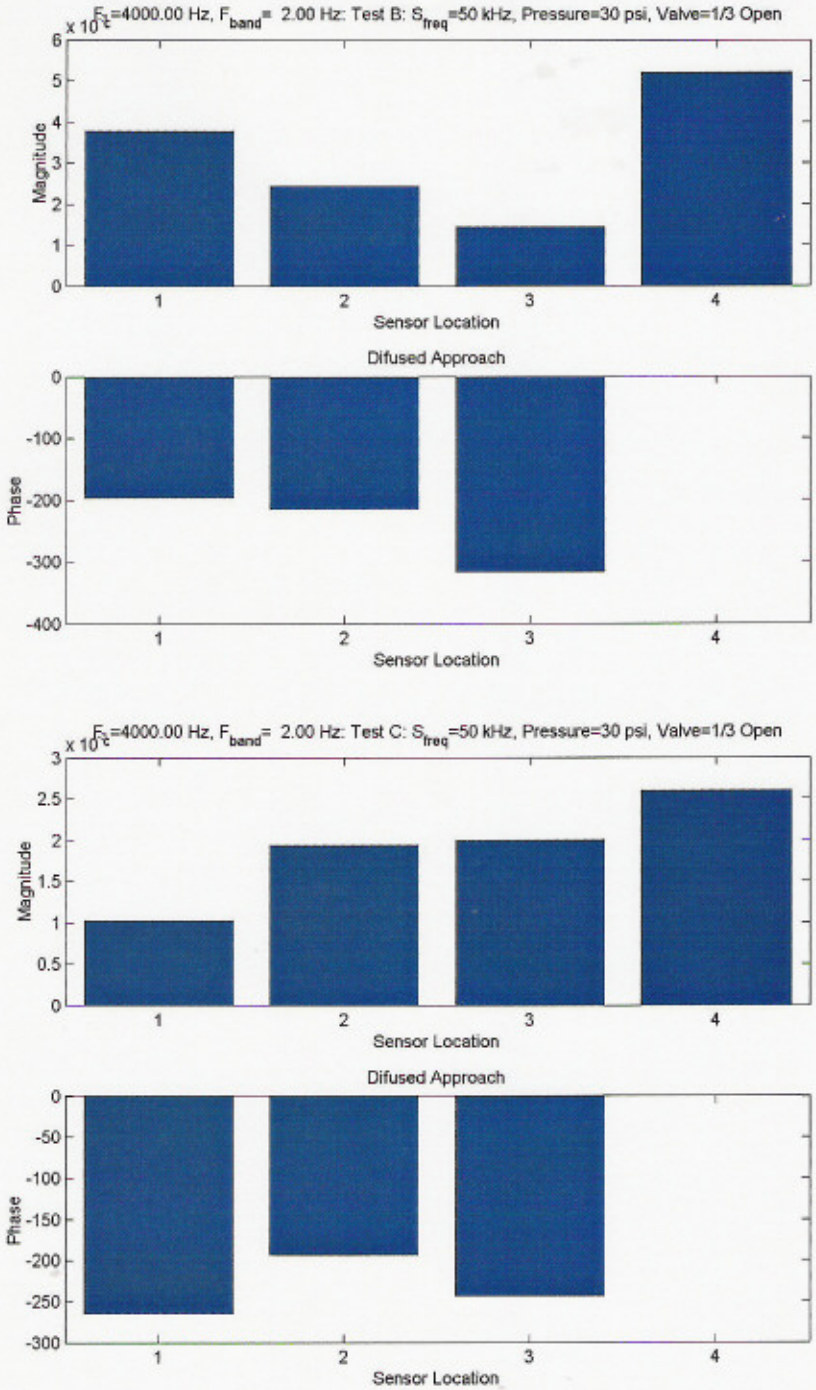
F_c=4000.00 Hz, F_band= 2.00 Hz: Test B: S_freq=50 kHz, Pressure=30 psi, Valve=1/3 Open
x 10^6
Magnitude
Sensor Location
Difused Approach
Phase
Sensor Location
F_c=4000.00 Hz, F_band= 2.00 Hz: Test C: S_freq=50 kHz, Pressure=30 psi, Valve=1/3 Open
x 10^6
Magnitude
Sensor Location
Difused Approach
Phase
Sensor Location

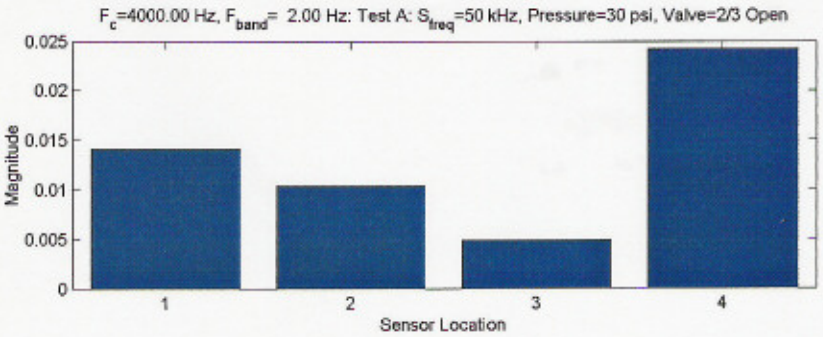
F_c=4000.00 Hz, F_{band}= 2.00 Hz: Test A: S_{freq}=50 kHz, Pressure=30 psi, Valve=2/3 Open
Magnitude
0.025
0.02
0.015
0.01
0.005
0
1
2
3
4
Sensor Location

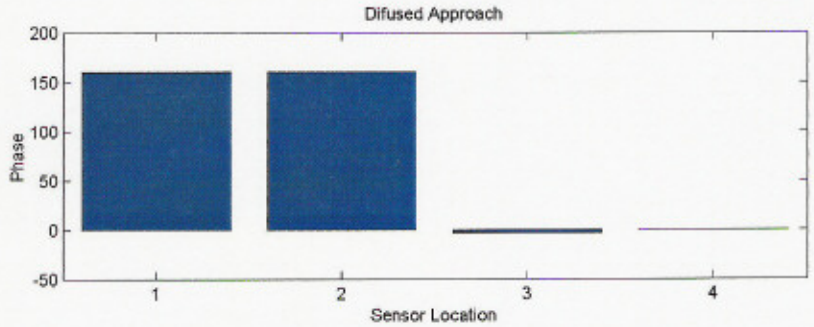
Difused Approach
Phase
200
150
100
50
0
-50
1
2
3
4
Sensor Location

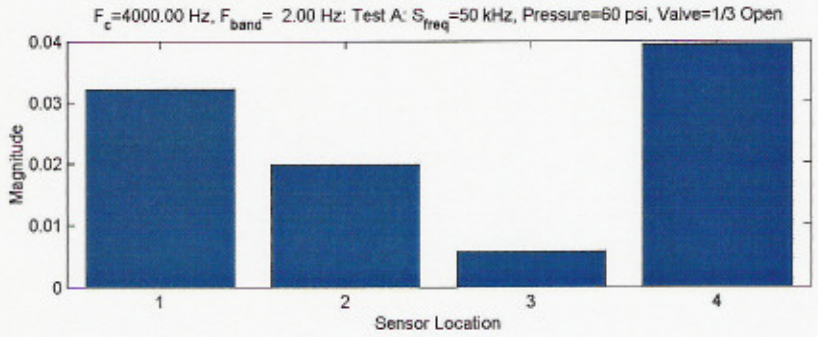
F_c=4000.00 Hz, F_{band}= 2.00 Hz: Test A: S_{freq}=50 kHz, Pressure=60 psi, Valve=1/3 Open
Magnitude
0.04
0.03
0.02
0.01
0
1
2
3
4
Sensor Location

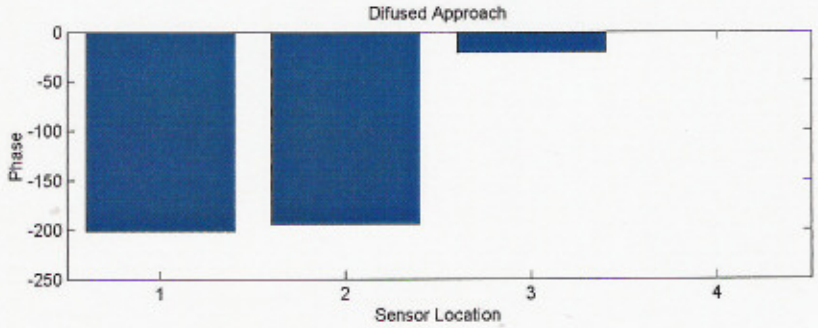
Difused Approach
Phase
0
-50
-100
-150
-200
-250
1
2
3
4
Sensor Location

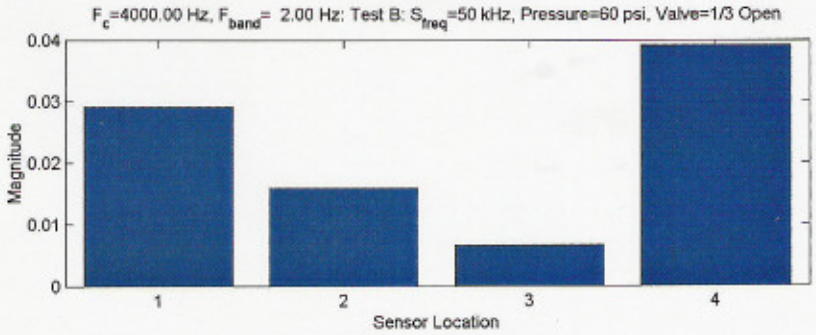
F_c=4000.00 Hz, F_{band}= 2.00 Hz: Test B: S_{freq}=50 kHz, Pressure=60 psi, Valve=1/3 Open
Magnitude
0.04
0.03
0.02
0.01
0
1
2
3
4
Sensor Location

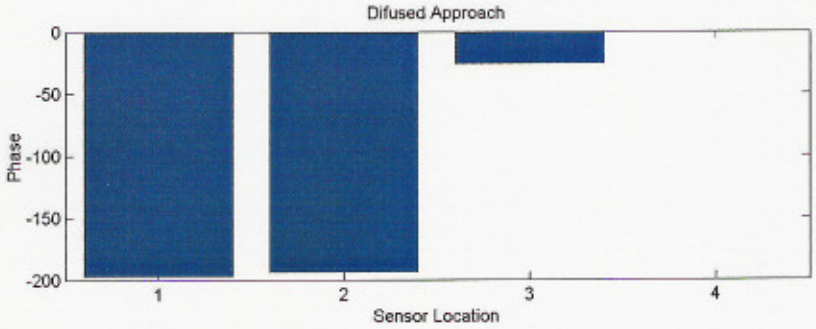
Difused Approach
Phase
0
-50
-100
-150
-200
1
2
3
4
Sensor Location

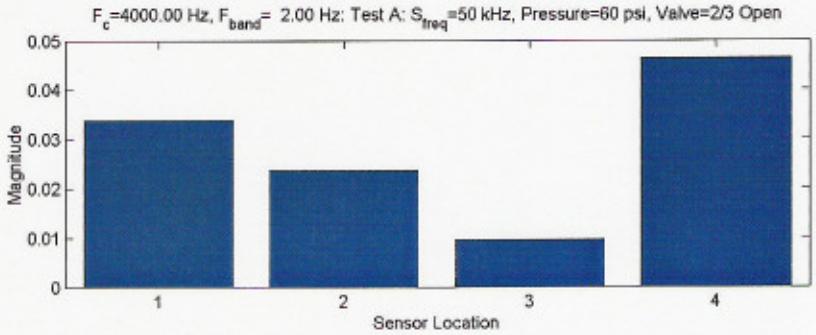
F_c=4000.00 Hz, F_{band}= 2.00 Hz: Test A: S_{freq}=50 kHz, Pressure=60 psi, Valve=2/3 Open
Magnitude
0.05
0.04
0.03
0.02
0.01
0
1
2
3
4
Sensor Location

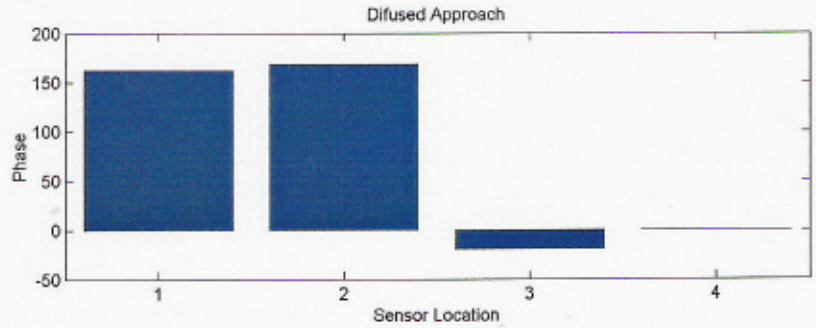
Difused Approach
Phase
200
150
100
50
0
-50
1
2
3
4
Sensor Location

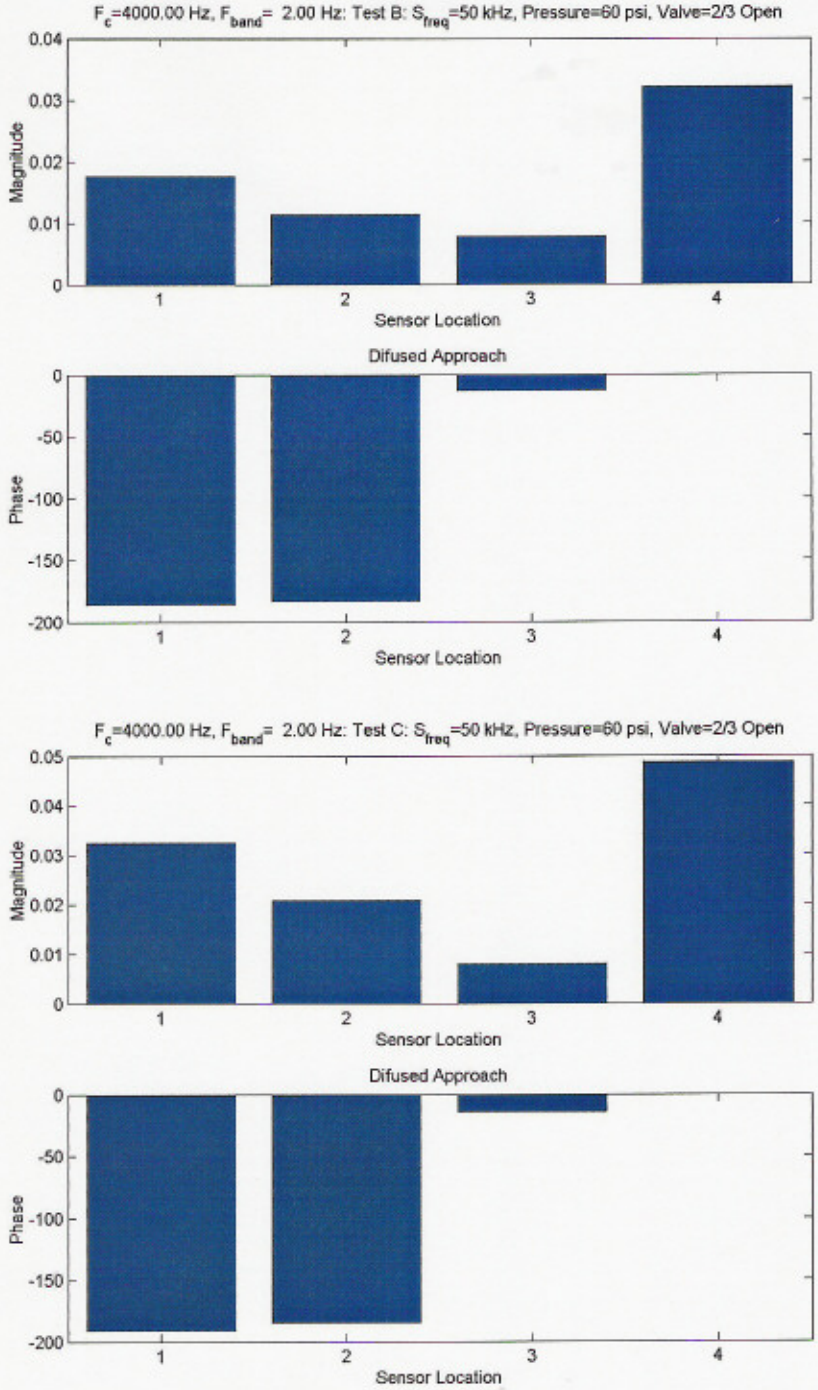
F_c=4000.00 Hz, F_{band}= 2.00 Hz: Test B: S_{freq}=50 kHz, Pressure=60 psi, Valve=2/3 Open
Magnitude
Sensor Location
Difused Approach
Phase
Sensor Location
F_c=4000.00 Hz, F_{band}= 2.00 Hz: Test C: S_{freq}=50 kHz, Pressure=60 psi, Valve=2/3 Open
Magnitude
Sensor Location
Difused Approach
Phase
Sensor Location